CORE LABORATORIES AUSTRALIA PTY LTD

447-449 Belmont Ave, Kewdale, Perth WA 6105
Tel : (61 8) 9353 3944 Fax : (61 8) 9353 1369
Email : corelab.australia@corelab.com

A Special Core Analyses Study Of Selected Samples From The Well : Halladale-1 DW-1 and DW-2

Australia

Prepared for
ORIGIN ENERGY LIMITED

SEPTEMBER 2005

File: PRP-05036A

Rock Properties Group
Core Laboratories Australia Pty. Ltd.
Perth
Australia

CORE LABORATORIES AUSTRALIA PTY LTD

9th September 2005

ORIGIN ENERGY LIMITED
Ground Floor, South Tower
John Oxley Centre
339 Coronation Drive
BRISBANE, QLD 4001

Attention : Dr Andrew Constantine

Subject : Special Core Analysis
Well : Halladale-1 DW-1 and DW-2
File : PRP-05036A

Dear Andrew,

Presented herein is the final report of the Special Core Analyses conducted on the selected core plug samples from the well : Halladale-1 DW-1 and DW-2.

Thank you for the opportunity to have been of service to Origin Energy Limited. If you have any questions regarding these results or if we can be of any further assistance please do not hesitate to contact us.

Yours sincerely,
CORE LABORATORIES AUSTRALIA PTY LTD

Ajit Singh
Supervisor - Rock Properties Group Perth

CONTENTS

SECTION 1
SUMMARY & INTRODUCTION

Summary of Results

- The samples selected for this SCAL study had permeability (Kair) and porosity values, measured at ambient conditions, ranging from 13.7 to greater than 10000 md and 14.4 to 27.4% respectively. Grain density values ranged from 2.625 to 2.677 g/cc.

- Cementation exponent ("m") values range from 1.76 to 1.87 with an average value of 1.79.

- Saturation exponent ("n") values range from 1.66 to 2.06 (average 1.91).

- Qv values from cation exchange capacity tests (wet chemistry method) range from 0.053 to 0.380 (meq/cm^3).

- Centrifuge air-brine (drainage) capillary pressure tests yielded, at the maximum 60 psi capillary pressure, immobile water saturation (Swi) values between 8.4 and 46.0 percent pore volume. Graphical summary of permeability to air versus Swi indicates the expected relationship of increasing Swi with decreasing permeability.

- Specific permeability to brine (Kw at 100% Sw) values indicated Kw/Kair ratios between 59.1 and 91.8%.

- Gas recoveries from the counter-current imbibition tests (representing "true" imbibition) ranged from 28.9 to 59.0 percent pore volume. Residual gas saturations ranged from 29.1 to 36.1 percent pore volume.

- Gas recoveries from the centrifuge water-gas tests (representing a "forced" imbibition scenario where capillary/gravity forces dominate in the reservoir) ranged from 52.0 to 63.6 percent pore volume. Residual gas saturations ranged from 27.2 to 32.3 percent pore volume.

INTRODUCTION

This report contains the final results of the Special Core Analyses study performed on selected core plug samples from the well : Halladale-1 DW-1 and DW-2. This study was initiated by Andrew Constantine of Origin Energy Limited (Origin).

The test programme involved :

- CT-scanning of selected core plugs
- Core plug photographs
- Porosity and permeability measurements at ambient and overburden pressures
- Formation resistivity factor (FRF) at net overburden pressure (NOBP)
- Formation resistivity index (FRI) at NOBP
- Cation exchange capacity (CEC) by wet chemistry method
- Air-brine drainage capillary pressure by centrifuge
- Specific permeability to brine (100% Sw)
- Residual gas saturation by counter-current imbibition (CCI)
- Centrifuge water-displacing–gas relative permeability (end-point data)

SCAL sample selection was carried out by Tim Conroy and Matthew Waugh of Woodside Energy Limited (as partners in this study). All selected samples were submitted for CT-scanning to ensure their suitability for SCAL testing (e.g contain no micro-fractures, differential cementation etc. which can invalidate SCAL data). Substitute samples, selected for those which failed CT-screening, also underwent CT-scanning. A full list of samples which were selected for this SCAL study and the associated base data (permeability, porosity and grain density values) is given on page 1-3. All selected samples had previously undergone routine core analysis measurements with the exception of twelve samples, as indicated with either an “A” or “B” suffix, which were newly drilled for this study.

At Origin’s request, an additional eighteen samples were drilled for mechanical strength tests (Appendix 2). All samples were CT-scanned prior to forwarding to CSIRO for mechanical strength testing.

The simulated formation brine salinity used for this SCAL study was 25,000 ppm (Origin’s email dated 15th June 2005) comprising 80% sodium chloride and 20% potassium chloride as the dissolved constituents.

Preliminary results from the completed analyses were reported on an on-going basis with all preliminary results forwarded by 21st July 2001.

Images of all core plug CT-scans are presented in Appendix 3. White light images of the samples which underwent SCAL testing are also presented in Appendix 4.

SCAL Sample Selection and Base Data

PLUG	Depth (m)	At Ambient (800 psi)			At 3100 psi NOBP			Grain Density (g/cc)	ANALYSIS										
		Kinf (md)	Kair (md)	Porosity (%)	Kinf (md)	Kair (md)	Porosity (%)		CT-SCAN		Clean/ Dry Kphi	FRF FRI NOBP	Off-Cuts CEC	Cent. Air-Brine Pc	CCl	Kw 100% Sw NOBP	USS KwKg NOBP	PLUG PHOTOS	
									Pass	Fail								CT-SCAN	WHITE LIGHT
5A	1792.55	286	302	26.0	271	286	25.6	2.652	√		√			√				√	√
6A	1792.60	450	470	25.0	428	448	24.5	2.661	√		√					√	√	√	√
7	1793.00	937	958	26.6	877	899	26.0	2.648	√			√	√					√	√
28	1808.70	1750	2110	20.9	1590	1960	20.1	2.662	√							√	√	√	√
29	1809.05	654	699	22.9	606	649	22.3	2.670	√			√	√					√	√
40	1812.30	3500	4060	25.0	3230	3690	24.0	2.653	√							√	√	√	√
42	1812.90	3530	3740	26.6	3140	3360	25.6	2.659	√					√	√			√	√
44*	1813.45	2360	3180	22.1	2410	3150	21.1	2.625	√			√	√					√	√
47*	1814.42	439	501	18.6	341	389	17.6	2.651	√					√				√	√
48*	1814.75	269	415	17.3	160	238	15.0	2.652		√								√	
48A*	1814.81	-	-	-	-	-	-	-		√								√	
51A*	1815.73	**	8890	27.4	**	8750	26.3	2.648	√		√					√	√	√	√
55	1816.80	2960	4220	24.3	2410	3490	23.1	2.656	√					√				√	√
56A*	1817.04	2540	3070	22.0	2360	2780	20.9	2.652	√		√			√	√			√	√
56	1817.10	311	385	16.7	271	347	15.9	2.654		√								√	
57A*	1817.50	**	5470	20.6	**	3180	19.2	2.656	√		√	√	√					√	√
59	1818.05	**	>10000	23.8	**	9040	22.6	2.655	√							√	√	√	√
62B*	1818.84	268	416	13.6	262	392	12.7	2.677	√		√	√	√					√	√
62A	1818.95	-	-	-	-	-	-	-		√								√	
64	1819.50	4110	4140	26.7	3640	3680	25.8	2.642	√			√	√					√	√
65	1819.80	2750	2800	26.3	2530	2590	25.5	2.662	√					√				√	√
67A	1820.49	2220	2260	25.7	2050	2090	24.8	2.672	√		√					√	√	√	√
72	1821.90	50.5	55.4	18.6	46.6	51.1	18.0	2.673	√			√	√					√	√
72A	1821.98	11.8	13.7	16.6	10.3	11.9	16.0	2.656	√		√			√	√			√	√
75A	1822.83	685	706	25.7	635	657	25.0	2.656	√		√			√	√			√	√
76	1823.10	588	606	27.3	547	565	26.6	2.665	√							√	√	√	√
77A	1823.36	369	392	24.9	344	366	24.3	2.652	√		√	√	√					√	√
79	1824.03	5860	6430	25.5	5550	6020	24.8	2.646	√					√	√			√	√
82	1824.90	3050	3380	23.4	2780	3090	22.6	2.640	√					√				√	√
84	1825.50	**	>10000	23.7	6490	8230	22.4	2.650	√			√	√					√	√
86	1826.10	**	8140	22.9	**	7260	22.2	2.648	√							√	√	√	√

Notes

1) 'A' and 'B' suffixed samples are newly drilled. The rest are RCA samples.

2) * Sleeved sample.

3) ** Kinf is not available as the permeability (Kair) measurements were done using the steady-state permeameter.

SECTION 2
ELECTRICAL PROPERTIES

Summary of Results from Electrical Properties Measurements

Brine Concentration : 25,000 ppm

Rw : 0.245 ohm-m at 25°C

Sample Number	Depth (m)	Kinf at NOBP (md)	Kair at NOBP (md)	Porosity at NOBP (%)	Grain Density (g/cc)	Qv from CEC (meq/cm3)	At NOBP		
							Formation Factor FRF	Cementation Exponent m	Saturation Exponent n
7	1793.00	877	899	26.0	2.648	0.100	11.53	1.82	2.05
29	1809.05	606	649	22.3	2.670	0.268	14.15	1.77	2.03
44	1813.45	2410	3150	21.1	2.625	0.124	16.86	1.82	1.68
57A	1817.50	**	3180	19.2	2.656	0.053	21.23	1.85	1.86
62B	1818.84	262	392	12.7	2.677	0.380	30.11	1.65	1.66
64	1819.50	3640	3680	25.8	2.642	0.065	10.91	1.76	1.95
72	1821.90	46.6	51.1	18.0	2.673	0.224	21.62	1.79	2.06
77A	1823.36	344	366	24.3	2.652	0.124	14.03	1.87	2.06
84	1825.50	6490	8230	22.4	2.650	0.111	14.95	1.81	1.84
							Average	1.79	1.91

** Kinf is not available as the permeability (Kair) measurements were done using the steady-state permeameter.

Formation Resistivity Factor at 3100 psi NOBP

Brine Concentration : 25,000 ppm Rw : 0.245 ohm-m at 25°C

Sample Number	Depth (m)	Kinf at NOBP (md)	Kair at NOBP (md)	Porosity at NOBP (%)	Grain Density (g/cc)	At NOBP	
						Formation Factor FRF	Cementation Exponent m
7	1793.00	877	899	26.0	2.648	11.53	1.82
29	1809.05	606	649	22.3	2.670	14.15	1.77
44	1813.45	2410	3150	21.1	2.625	16.86	1.82
57A	1817.50	**	3180	19.2	2.656	21.23	1.85
62B	1818.84	262	392	12.7	2.677	30.11	1.65
64	1819.50	3640	3680	25.8	2.642	10.91	1.76
72	1821.90	46.6	51.1	18.0	2.673	21.62	1.79
77A	1823.36	344	366	24.3	2.652	14.03	1.87
84	1825.50	6490	8230	22.4	2.650	14.95	1.81
						Average	1.79

** Kinf is not available as the permeability (Kair) measurements were done using the steady-state permeameter.

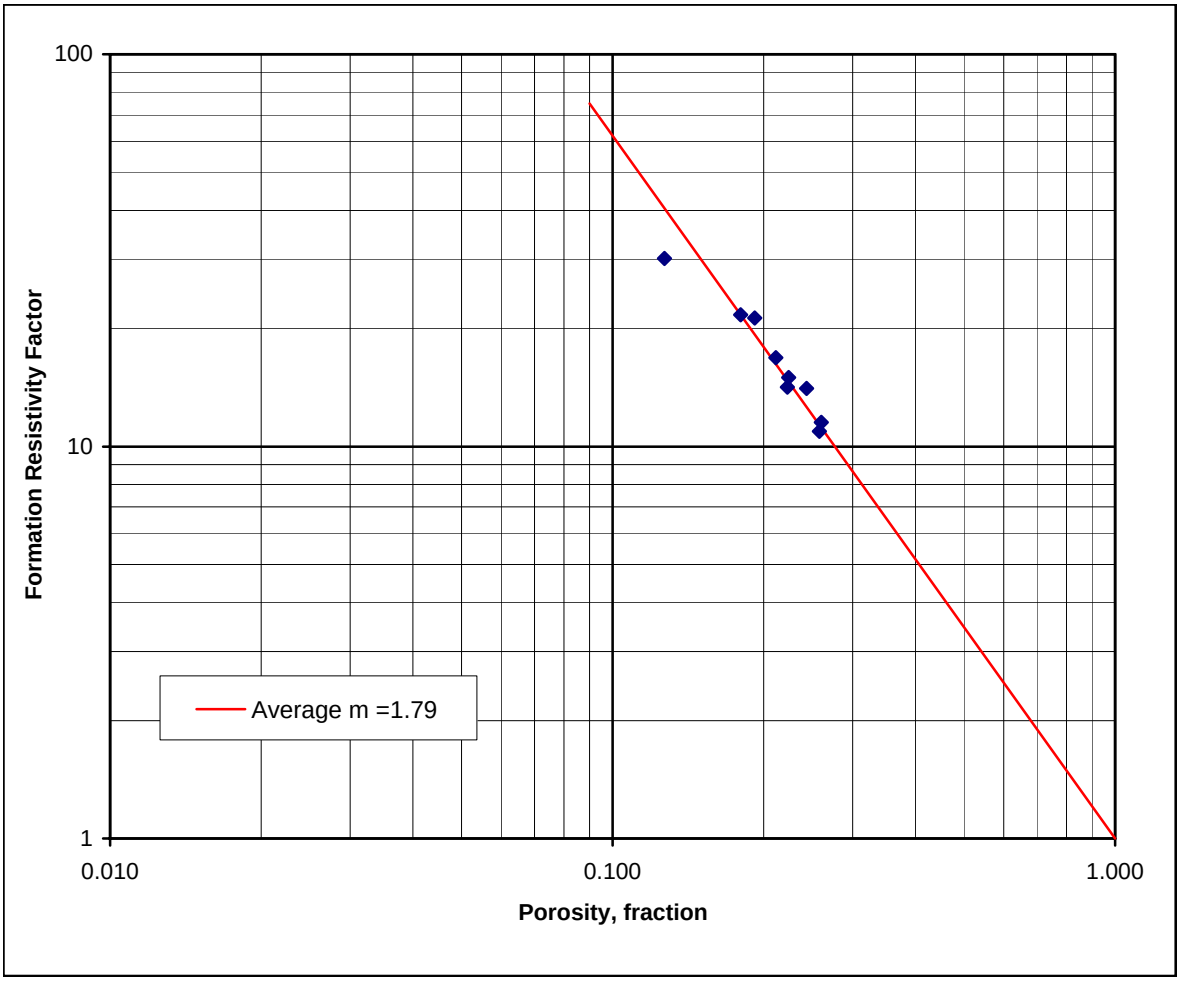

Formation Resistivity Index at 3100 psi NOBP

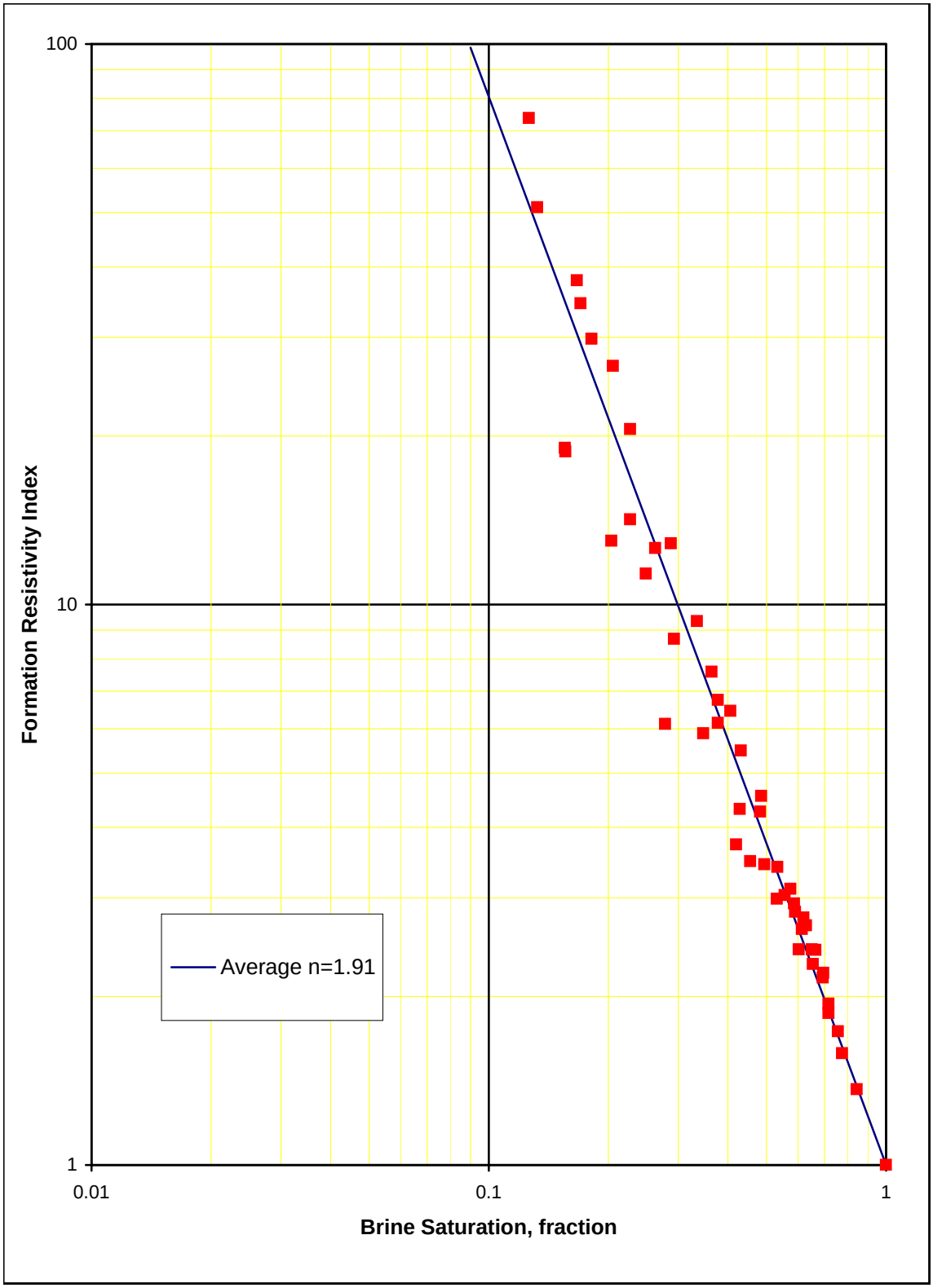

Formation Resistivity Index at 3100 psi NOBP

Sample No.	Depth (metres)	Kair at NOBP (md)	Grain Density (g/cc)	Determined at 3100 psi NOBP			
				Porosity (%)	Brine Saturation (%pv)	Resistivity Index	Sat. Exp. n
7	1793.00	899	2.648	26.0	100.0	1.00	-
					63.0	2.67	2.13
					58.7	2.93	2.02
					37.8	6.76	1.96
					20.5	26.66	2.07
					12.6	73.77	2.08

FRF at NOBP	11.53
Rw at 25°C, ohm-m	0.245

Average Exponent	2.05

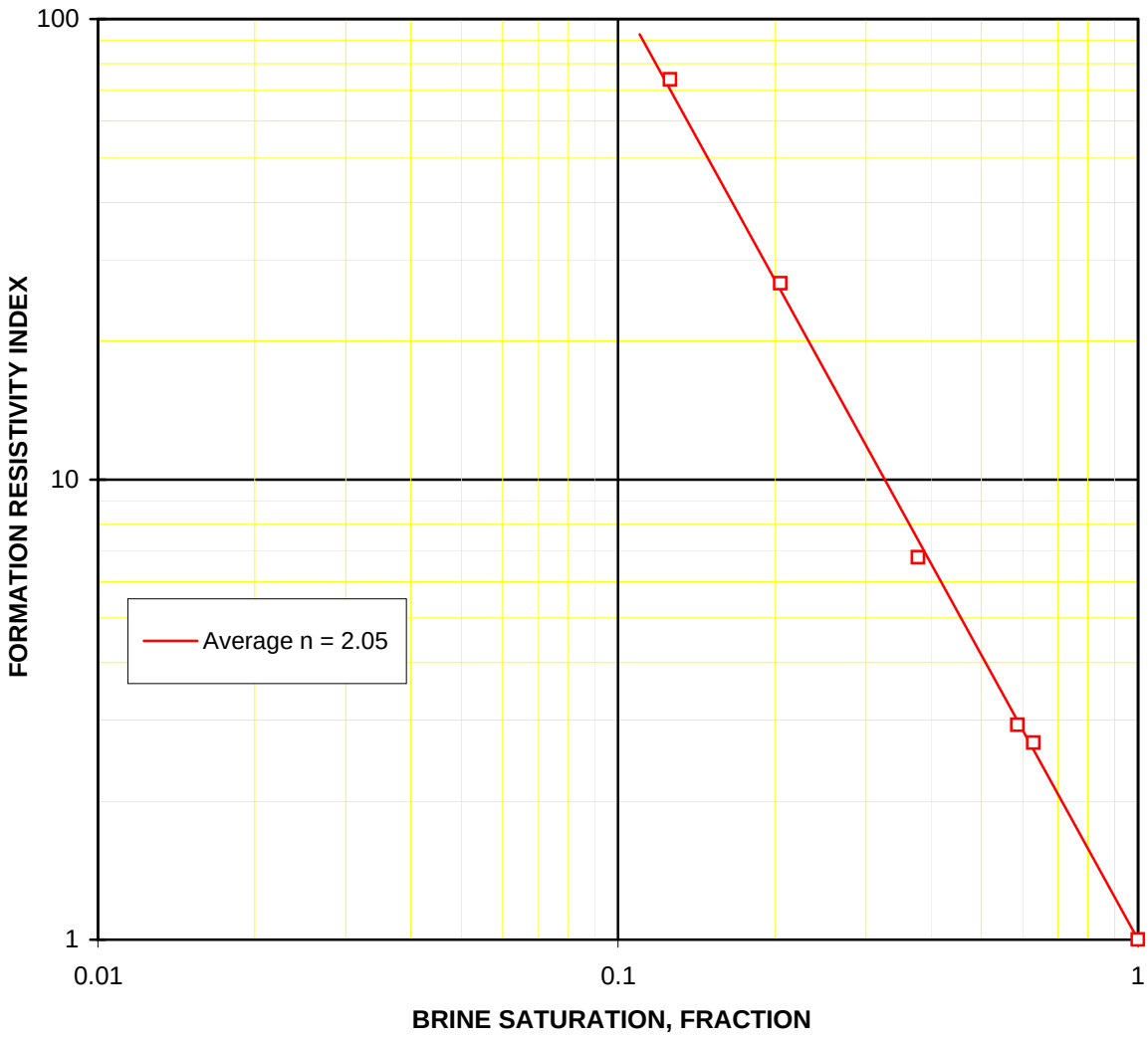

Formation Resistivity Index at 3100 psi NOBP

Sample No.	Depth (metres)	Kair at NOBP (md)	Grain Density (g/cc)	Determined at 3100 psi NOBP			
				Porosity (%)	Brine Saturation (%pv)	Resistivity Index	Sat. Exp. n
29	1809.05	649	2.670	22.3	100.0	1.00	-
					69.4	2.16	2.11
					48.2	4.27	1.99
					43.1	5.49	2.02
					28.7	12.85	2.05
					18.2	29.78	1.99

FRF at NOBP	14.15
Rw at 25°C, ohm-m	0.245

Average Exponent	2.03

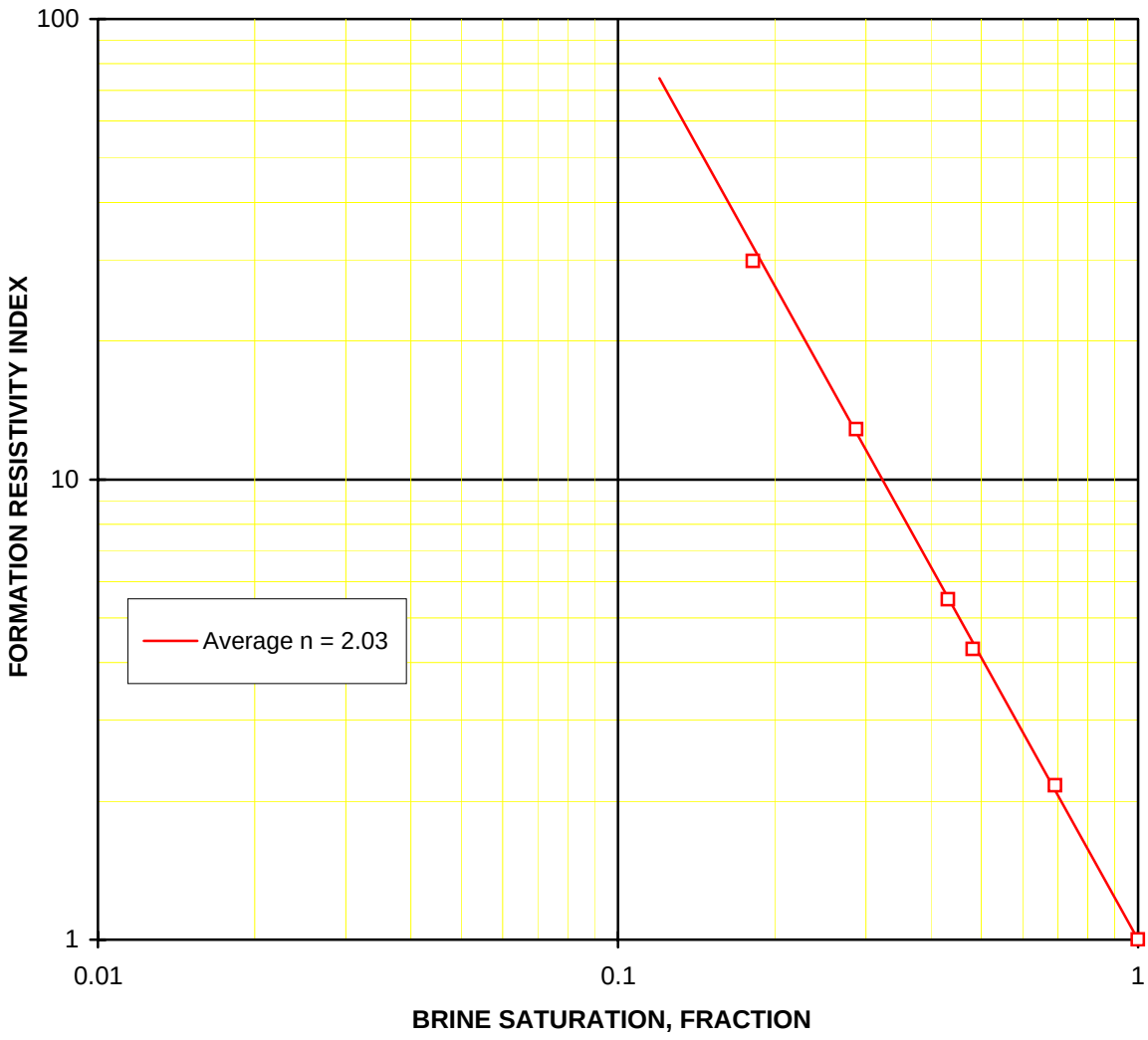

Formation Resistivity Index at 3100 psi NOBP

Sample No.	Depth (metres)	Kair at NOBP (md)	Grain Density (g/cc)	Determined at 3100 psi NOBP			
				Porosity (%)	Brine Saturation (%pv)	Resistivity Index	Sat. Exp. n
44	1813.45	3150	2.625	21.1	100.0	1.00	-
					77.5	1.58	1.80
					53.1	2.98	1.72
					34.7	5.89	1.68
					20.3	12.99	1.61
					15.5	19.02	1.58

FRF at NOBP	16.86
Rw at 25°C, ohm-m	0.245

Average Exponent	1.68

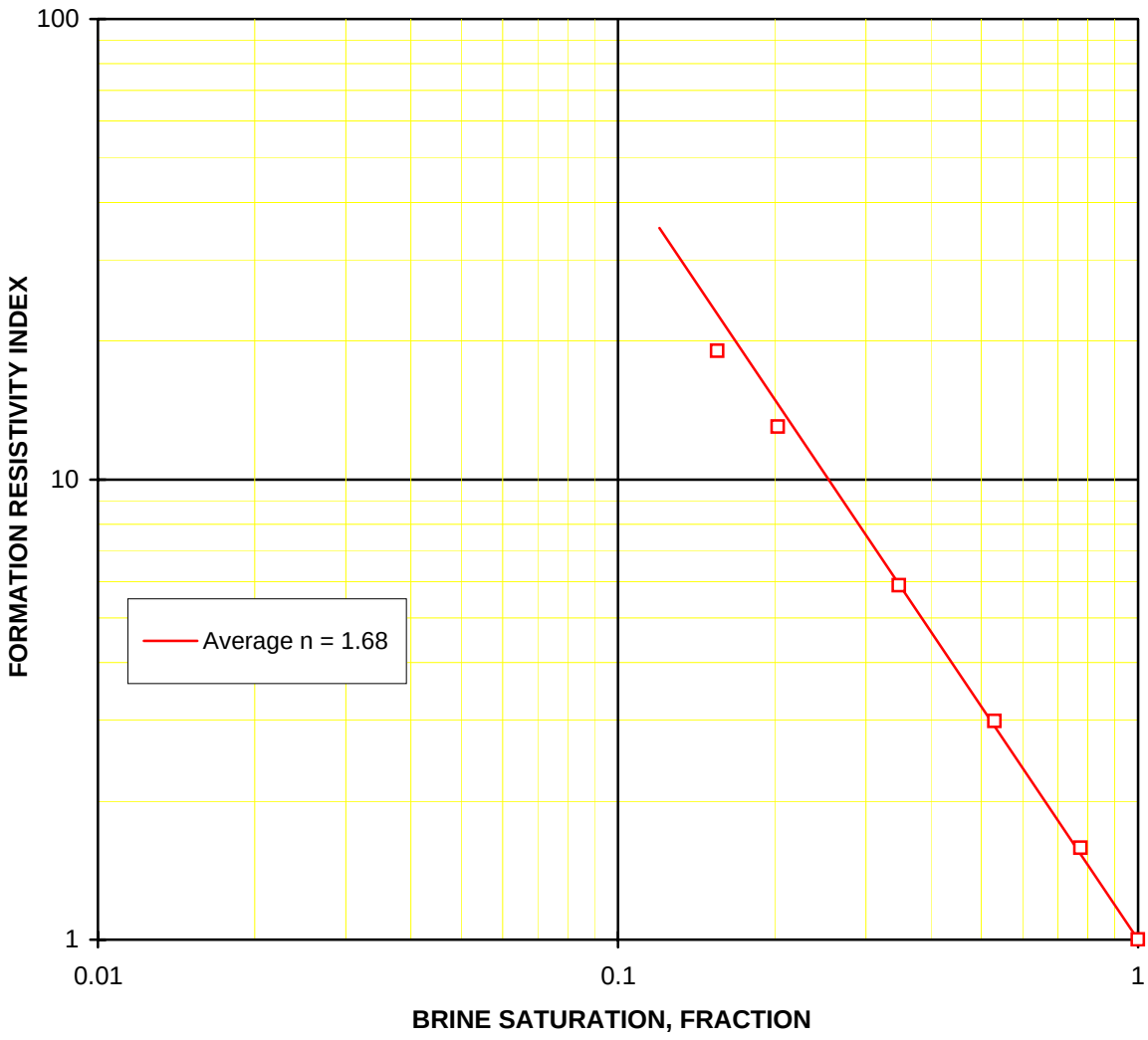

Formation Resistivity Index at 3100 psi NOBP

Sample No.	Depth (metres)	Kair at NOBP (md)	Grain Density (g/cc)	Determined at 3100 psi NOBP			
				Porosity (%)	Brine Saturation (%pv)	Resistivity Index	Sat. Exp. n
57A	1817.50	3180	2.656	19.2	100.0	1.00	-
					75.8	1.73	1.97
					71.6	1.94	1.98
					65.5	2.28	1.95
					55.5	3.03	1.89
					22.7	14.17	1.79
					15.6	18.72	1.58

FRF at NOBP	21.23
Rw at 25°C, ohm-m	0.245

Average Exponent	1.86

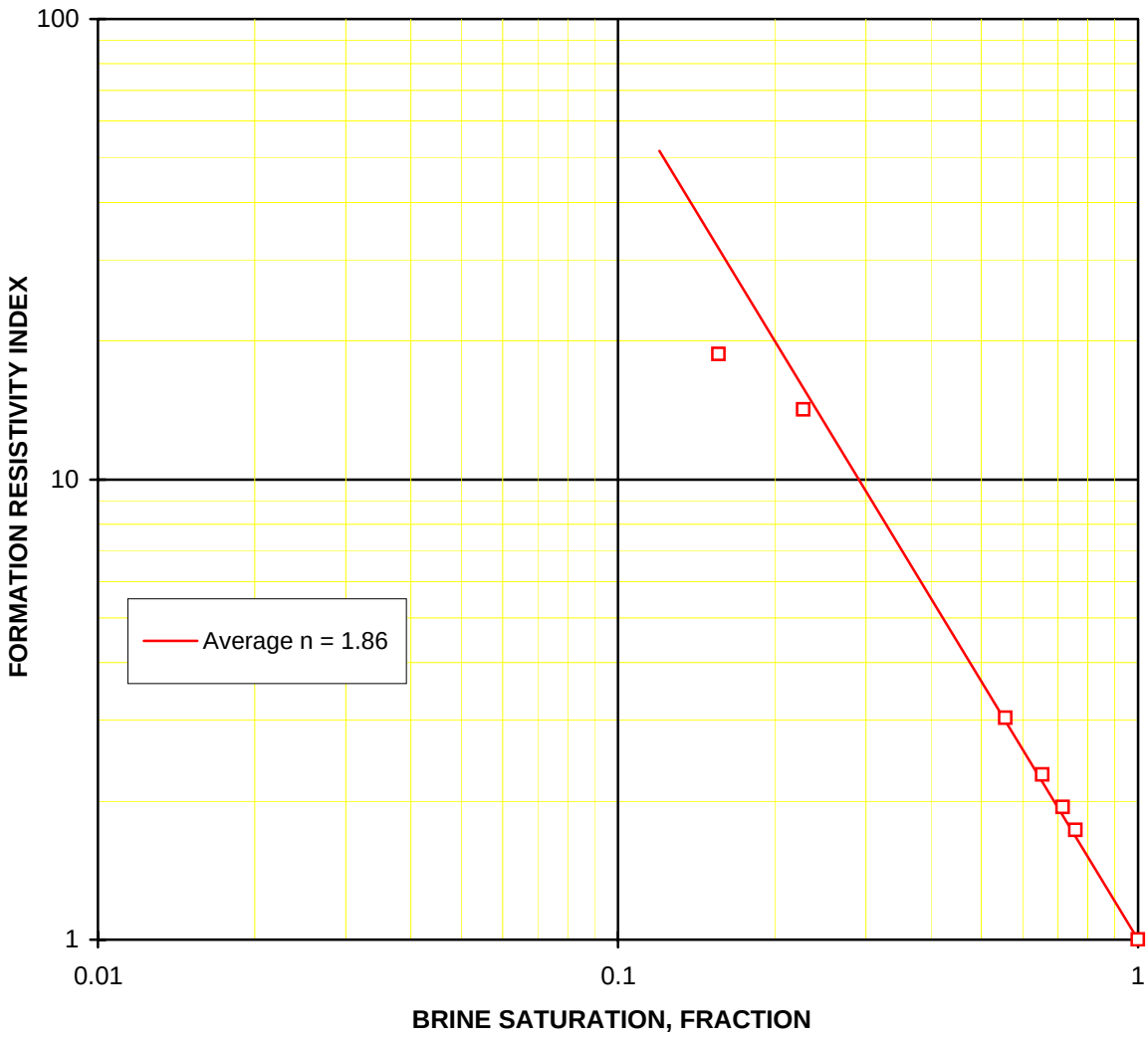

Formation Resistivity Index at 3100 psi NOBP

Sample No.	Depth (metres)	Kair at NOBP (md)	Grain Density (g/cc)	Determined at 3100 psi NOBP			
				Porosity (%)	Brine Saturation (%pv)	Resistivity Index	Sat. Exp. n
62B	1818.84	392	2.677	12.7	100.0	1.00	-
					84.4	1.36	1.83
					71.7	1.87	1.87
					60.4	2.43	1.76
					45.5	3.48	1.58
					41.9	3.73	1.52
					27.8	6.12	1.41

FRF at NOBP	30.11
Rw at 25°C, ohm-m	0.245

Average Exponent	1.66

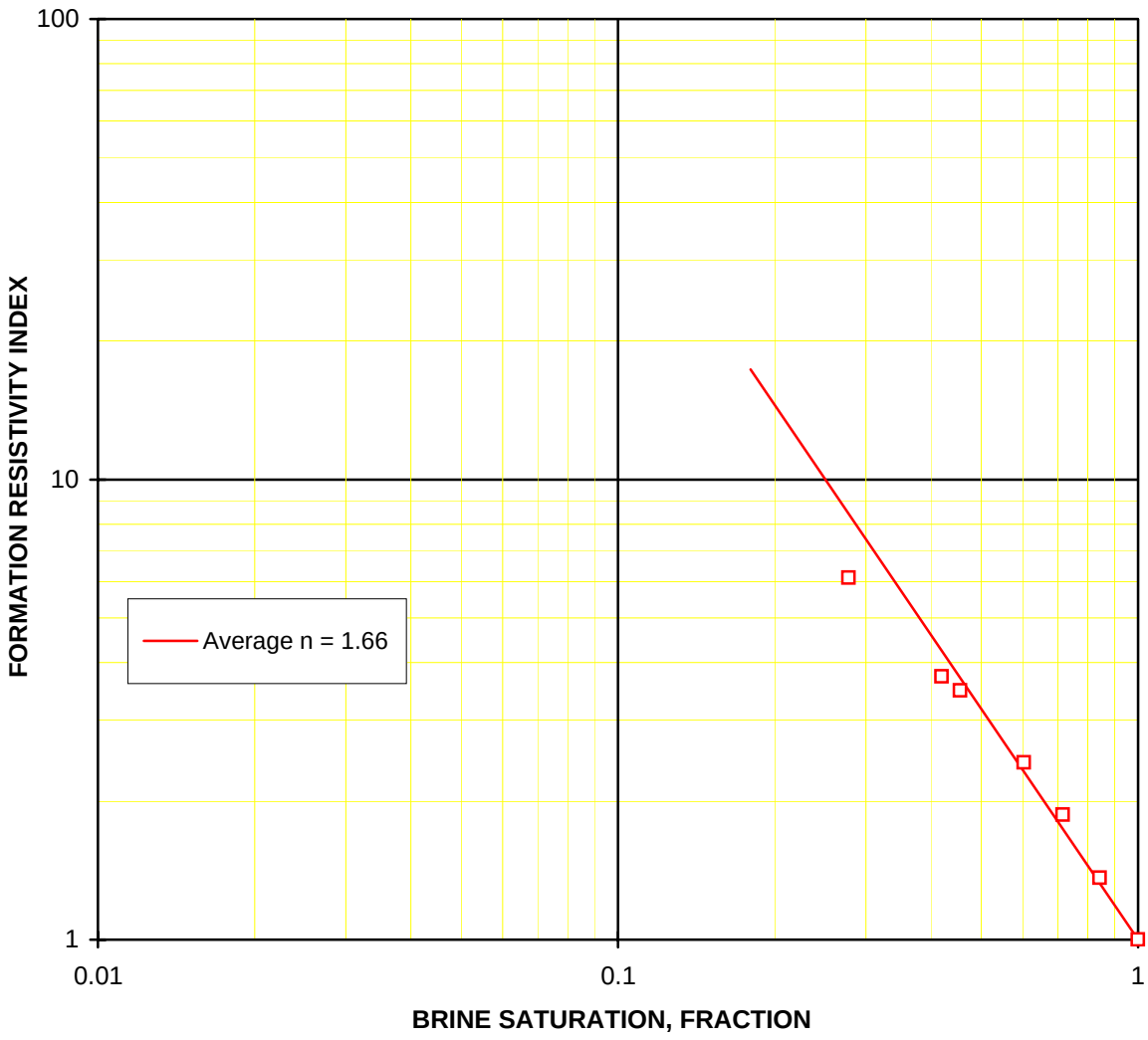

Formation Resistivity Index at 3100 psi NOBP

Sample No.	Depth (metres)	Kair at NOBP (md)	Grain Density (g/cc)	Determined at 3100 psi NOBP			
				Porosity (%)	Brine Saturation (%pv)	Resistivity Index	Sat. Exp. n
64	1819.50	3680	2.642	25.8	100.0	1.00	-
					61.5	2.64	2.00
					53.2	3.40	1.94
					37.8	6.15	1.86
					17.0	34.43	2.00
					13.2	51.16	1.95

FRF at NOBP	10.91
Rw at 25°C, ohm-m	0.245

Average Exponent	1.95

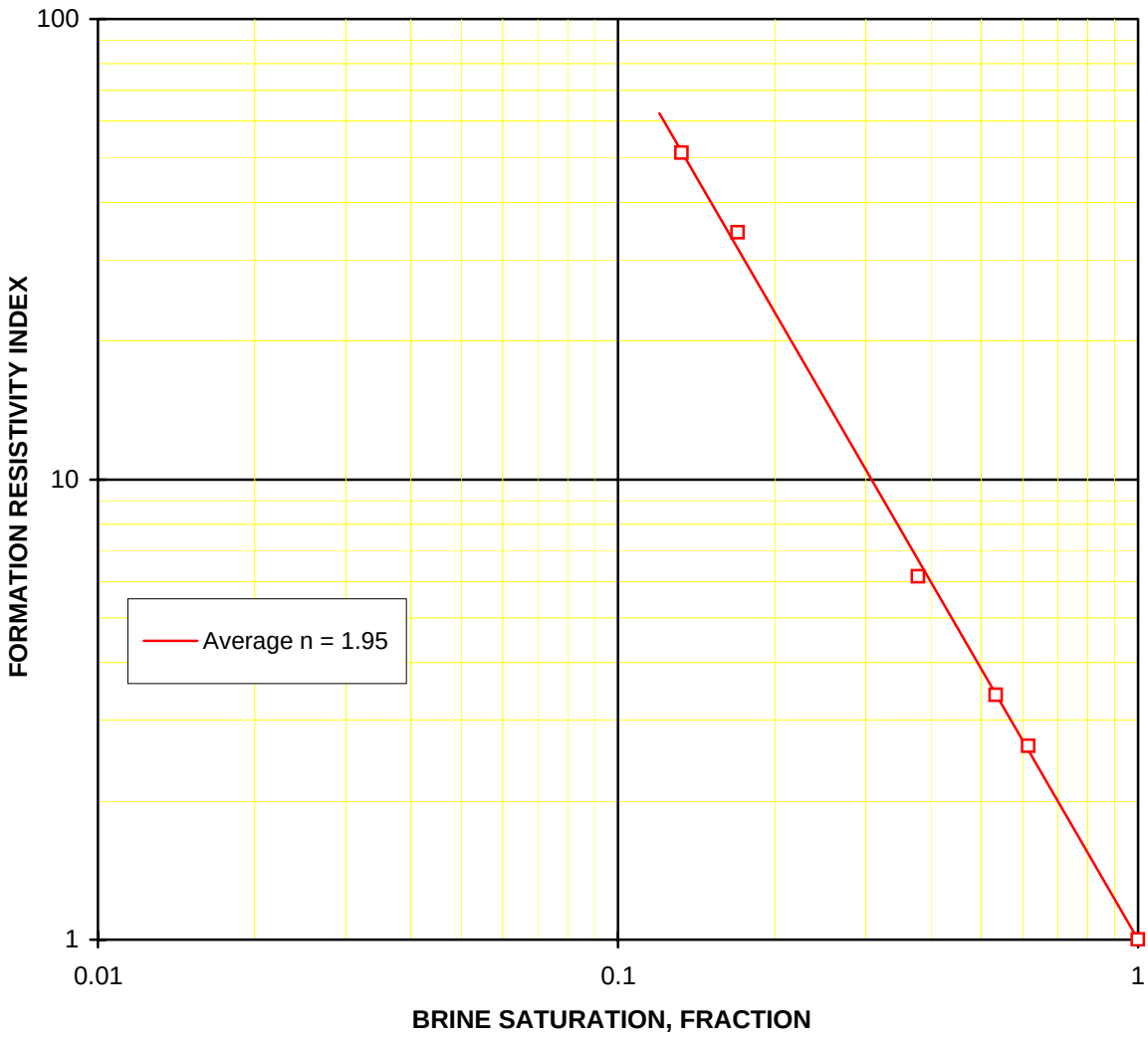

Formation Resistivity Index at 3100 psi NOBP

Sample No.	Depth (metres)	Kair at NOBP (md)	Grain Density (g/cc)	Determined at 3100 psi NOBP			
				Porosity (%)	Brine Saturation (%pv)	Resistivity Index	Sat. Exp. n
72	1821.90	51.1	2.673	18.0	100.0	1.00	-
					66.5	2.42	2.16
					61.9	2.77	2.12
					48.6	4.55	2.10
					40.5	6.46	2.07
					33.4	9.34	2.04
					26.3	12.60	1.90

FRF at NOBP	21.62
Rw at 25°C, ohm-m	0.245

Average Exponent	2.06

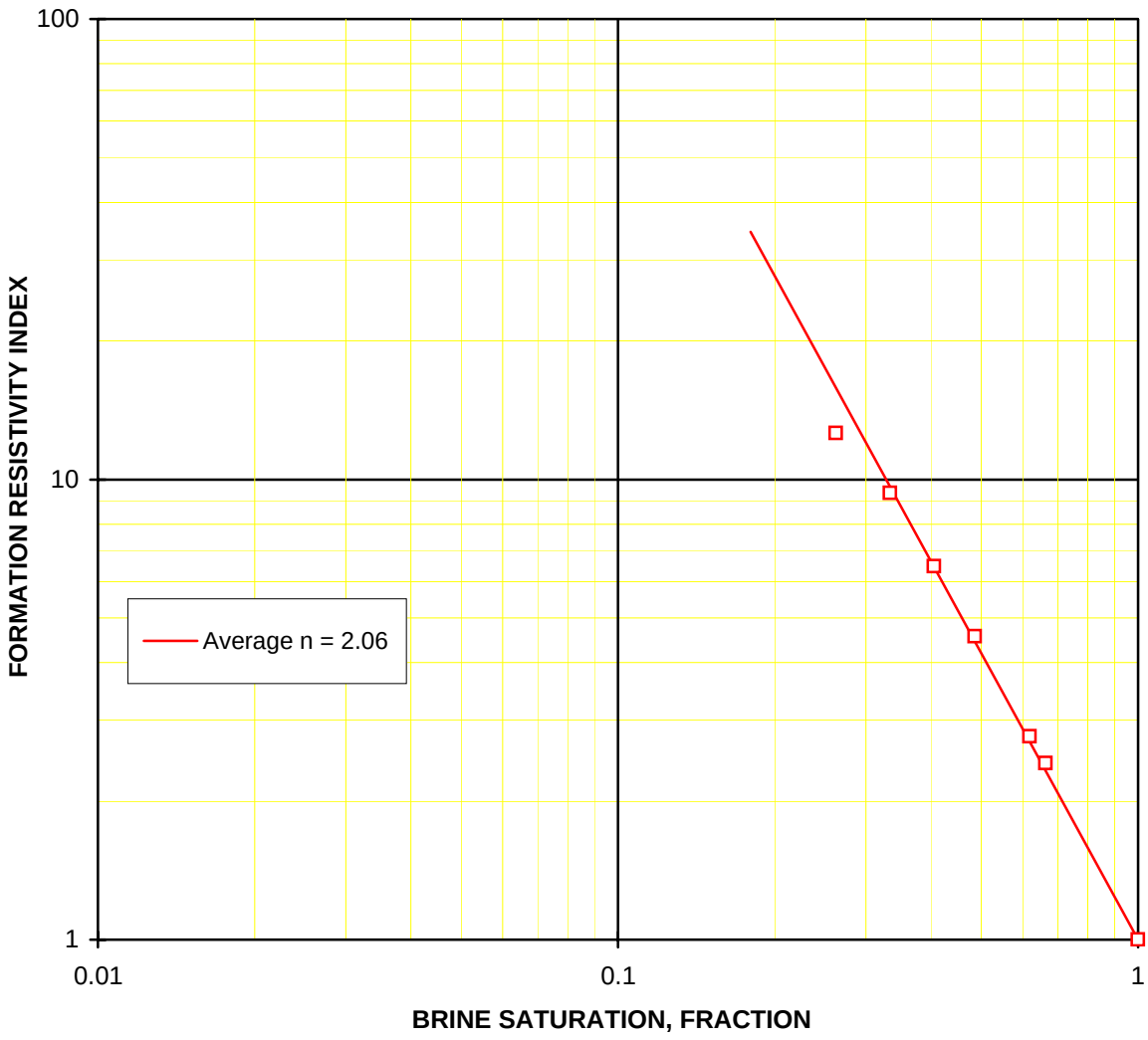

Formation Resistivity Index at 3100 psi NOBP

Sample No.	Depth (metres)	Kair at NOBP (md)	Grain Density (g/cc)	Determined at 3100 psi NOBP			
				Porosity (%)	Brine Saturation (%pv)	Resistivity Index	Sat. Exp. n
77A	1823.36	366	2.652	24.3	100.0	1.00	-
					69.5	2.20	2.17
					57.4	3.11	2.04
					36.4	7.59	2.01
					22.7	20.55	2.04
					16.7	37.84	2.03

FRF at NOBP	14.03
Rw at 25°C, ohm-m	0.245

Average Exponent	2.06

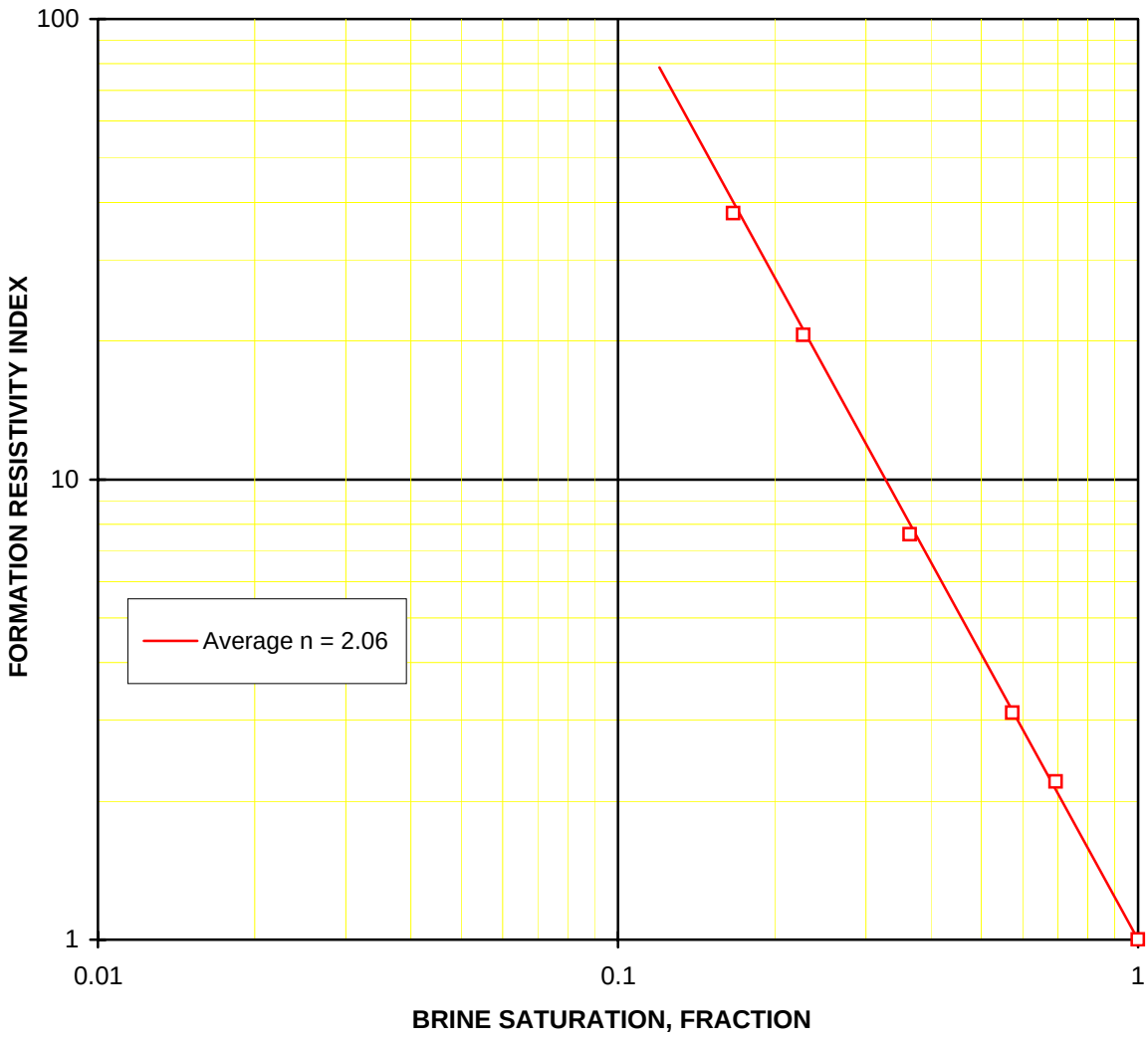

Formation Resistivity Index at 3100 psi NOBP

Sample No.	Depth (metres)	Kair at NOBP (md)	Grain Density (g/cc)	Determined at 3100 psi NOBP			
				Porosity (%)	Brine Saturation (%pv)	Resistivity Index	Sat. Exp. n
84	1825.50	8230	2.650	22.4	100.0	1.00	-
					65.2	2.42	2.07
					59.0	2.83	1.97
					49.4	3.44	1.75
					42.8	4.32	1.72
					29.3	8.68	1.76
					24.9	11.34	1.75

FRF at NOBP	14.95
Rw at 25°C, ohm-m	0.245

Average Exponent	1.84

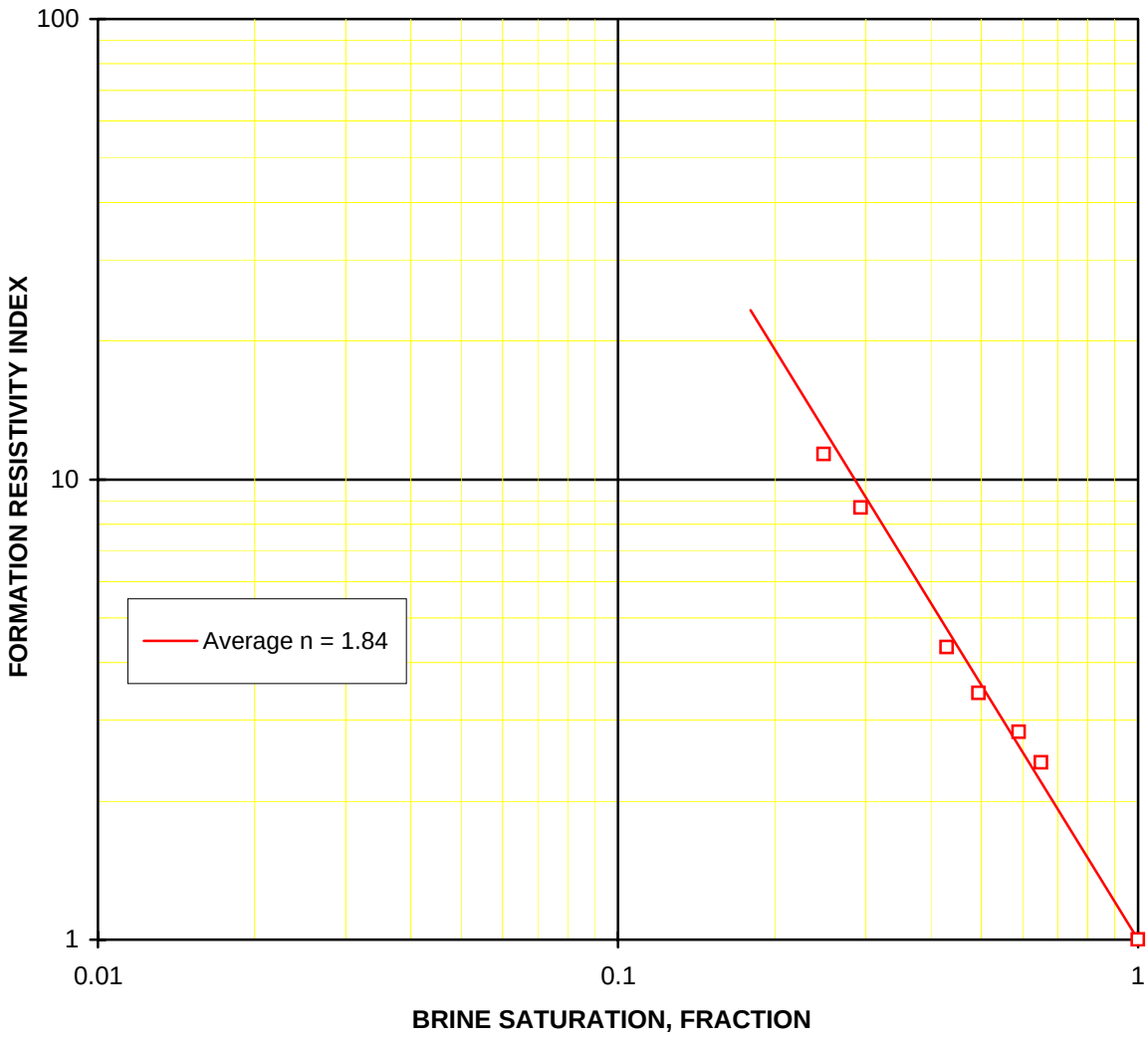

Cation Exchange Capacity by Wet Chemistry Method

Sample no.	Depth (m)	At 3100 psi NOBP		Grain density (g/cc)	CEC (meq/100 g)	Qv from CEC (meq/cm3)
		Kair (md)	Porosity (%)			
7	1793.00	899	26.0	2.648	1.332	0.100
29	1809.05	649	22.3	2.670	2.881	0.268
44	1813.45	3150	21.1	2.625	1.262	0.124
57A	1817.50	3180	19.2	2.656	0.47	0.053
62B	1818.84	392	12.7	2.677	2.063	0.380
64	1819.50	3680	25.8	2.642	0.860	0.065
72	1821.90	51.1	18.0	2.673	1.840	0.224
77A	1823.36	366	24.3	2.652	1.500	0.124
84	1825.50	8230	22.4	2.650	1.21	0.111

CEC analysis conducted on core plug trim-ends.

SECTION 3
CAPILLARY PRESSURE

Summary of the air-brine capillary pressure by centrifuge at ambient

Sample No.	Depth (m)	At Ambient		AIR - BRINE CAPILLARY PRESSURE (psi)							
		Kair (md)	Porosity (%)	0	1	2	5	10	20	40	60
				END-FACE WATER SATURATION Sw (%pv)							
5A	1792.55	302	26.0	100	100	77.4	41.8	32.4	25.9	20.5	18.0
42	1812.90	3740	26.6	100	63.9	46.3	30.5	23.0	16.7	13.3	12.5
47	1814.42	501	18.6	100	76.5	59.1	43.3	35.2	29.4	25.3	23.4
55	1816.80	4220	24.3	100	56.6	45.9	32.7	24.3	17.7	12.8	10.6
56A	1817.04	3070	22.0	100	63.7	45.1	32.4	25.5	18.9	13.5	12.2
65	1819.80	2800	26.3	100	61.3	37.7	29.3	22.0	15.3	12.3	12.0
72A	1821.98	13.7	16.6	100	100	100	80.9	73.6	65.1	54.3	46.0
75A	1822.83	706	25.7	100	80.5	55.7	41.0	30.9	22.9	17.7	15.7
79	1824.03	6430	25.5	100	39.6	27.9	22.3	17.5	13.5	10.1	8.4
82	1824.90	3380	23.4	100	56.0	33.8	20.7	16.5	13.6	11.0	10.4

Water saturation (Swi) vs permeability to air

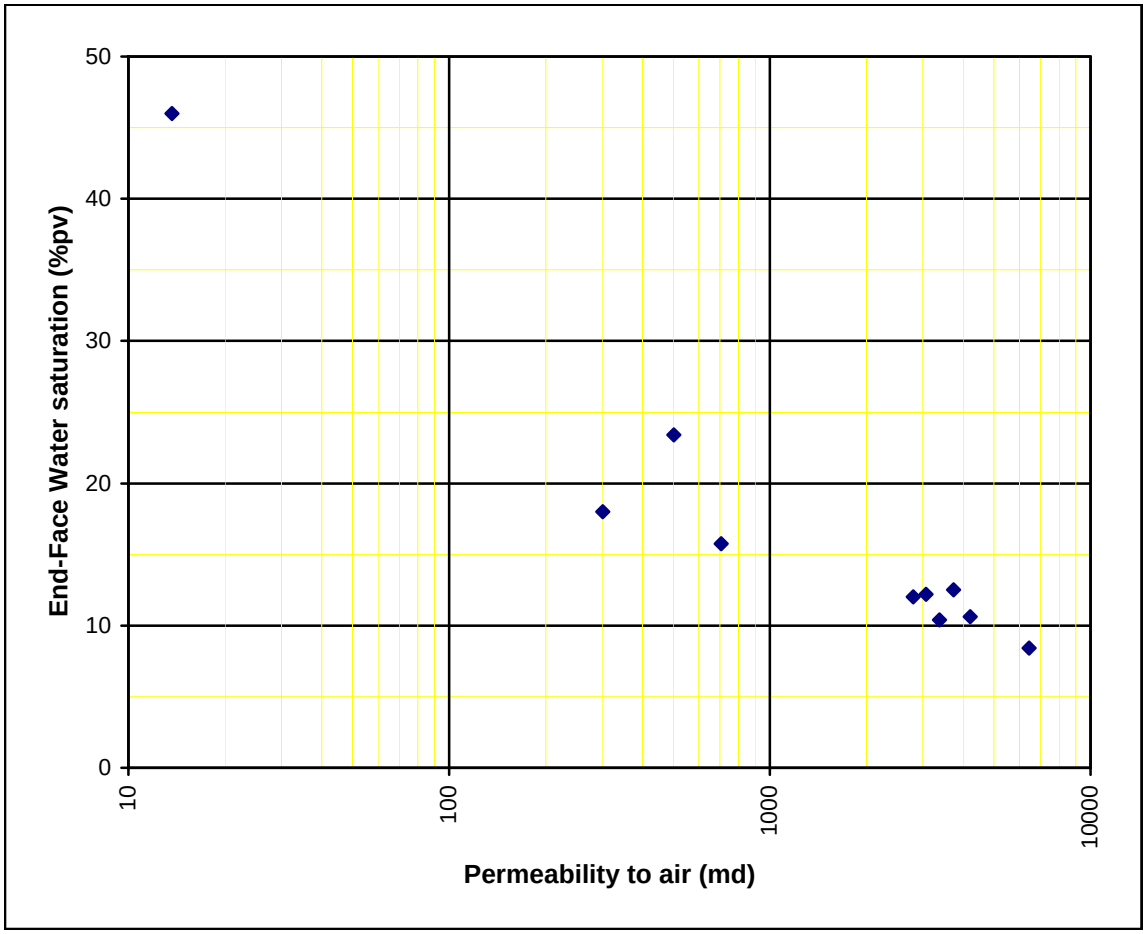

Air-brine Capillary Pressure by Centrifuge at Ambient

Sample no.	Depth (m)	At Ambient		
		Kinf (md)	Kair (md)	Porosity (%)
5A	1792.55	286	302	26.0

Capillary Pressure (psi)	End-Face Water Saturation (%pv)
0	100
1	100
2	77.4
5	41.8
10	32.4
20	25.9
40	20.5
60	18.0

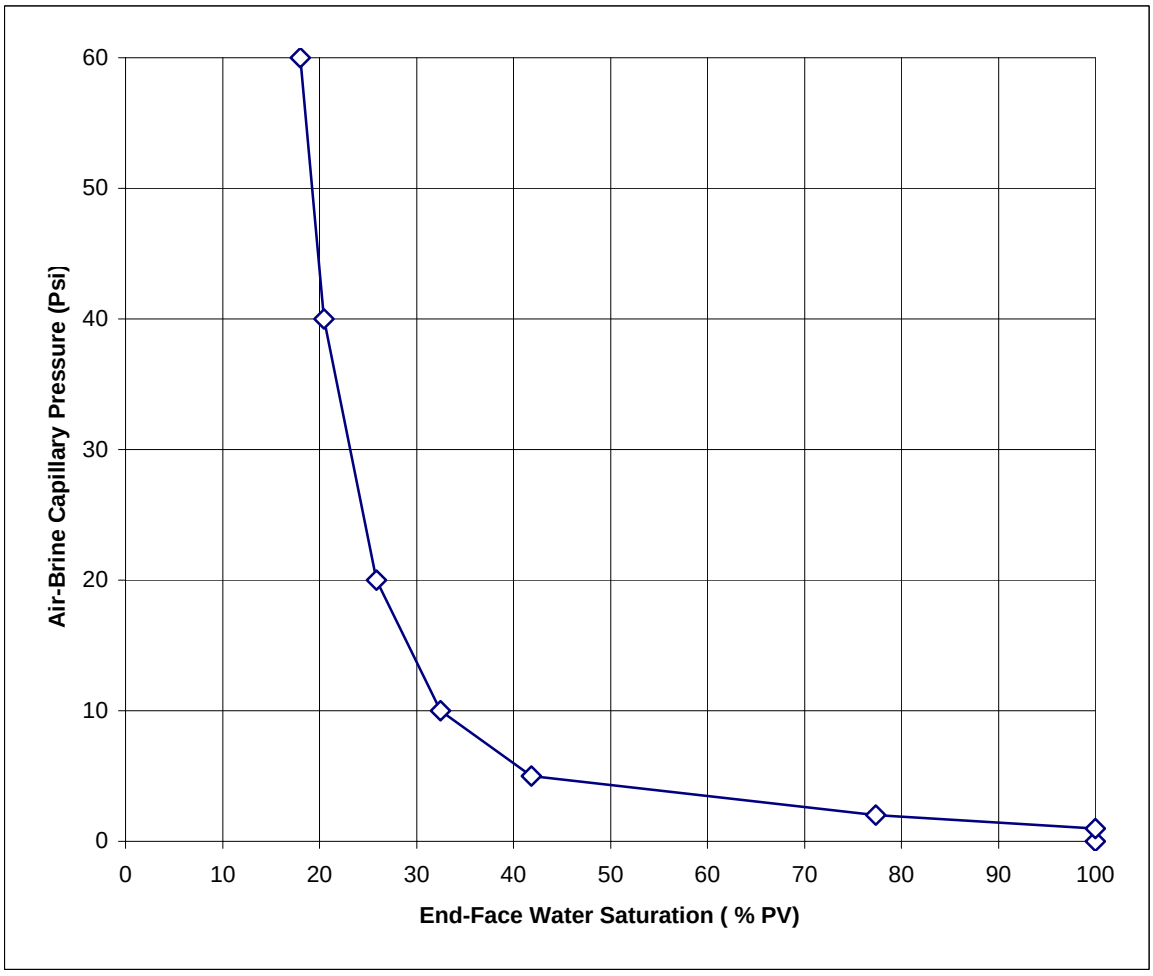

Air-brine Capillary Pressure by Centrifuge at Ambient

Sample no.	Depth (m)	At Ambient		
		Kinf (md)	Kair (md)	Porosity (%)
42	1812.90	3530	3740	26.6

Capillary Pressure (psi)	End-Face Water Saturation (%pv)
0	100
1	63.9
2	46.3
5	30.5
10	23.0
20	16.7
40	13.3
60	12.5

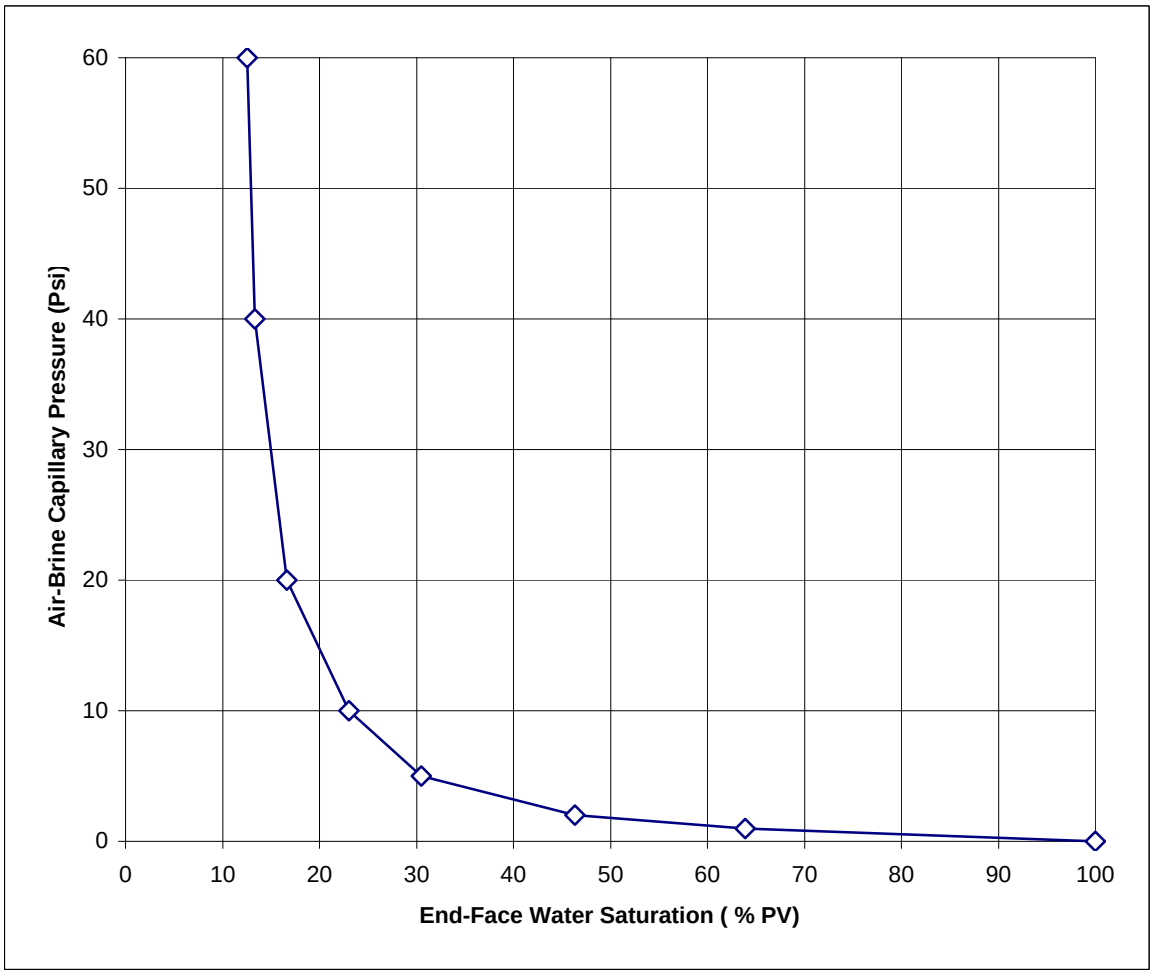

Air-brine Capillary Pressure by Centrifuge at Ambient

Sample no.	Depth (m)	At Ambient		
		Kinf (md)	Kair (md)	Porosity (%)
47	1814.42	439	501	18.6

Capillary Pressure (psi)	End-Face Water Saturation (%pv)
0	100
1	76.5
2	59.1
5	43.3
10	35.2
20	29.4
40	25.3
60	23.4

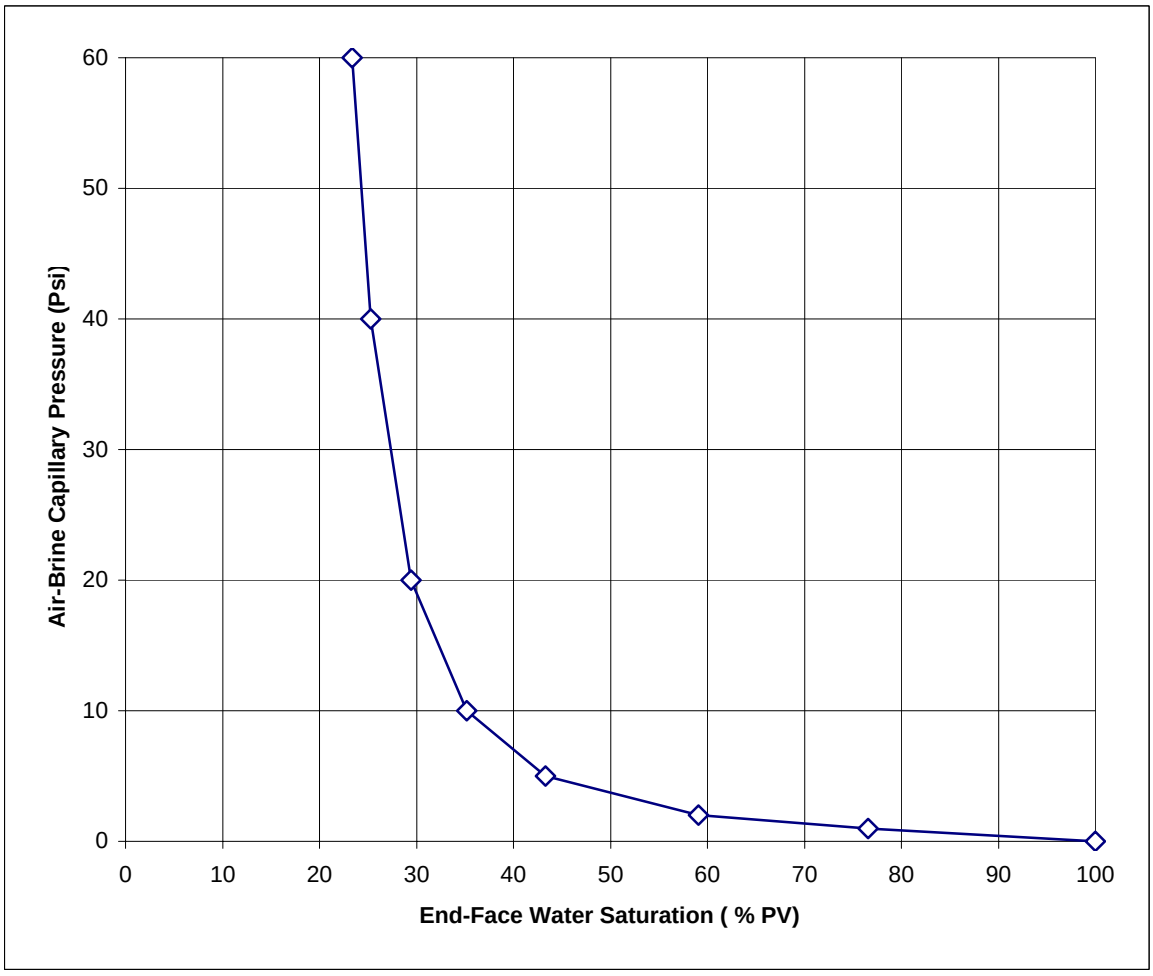

Air-brine Capillary Pressure by Centrifuge at Ambient

Sample no.	Depth (m)	At Ambient		
		Kinf (md)	Kair (md)	Porosity (%)
55	1816.80	2960	4220	24.3

Capillary Pressure (psi)	End-Face Water Saturation (%pv)
0	100
1	56.6
2	45.9
5	32.7
10	24.3
20	17.7
40	12.8
60	10.6

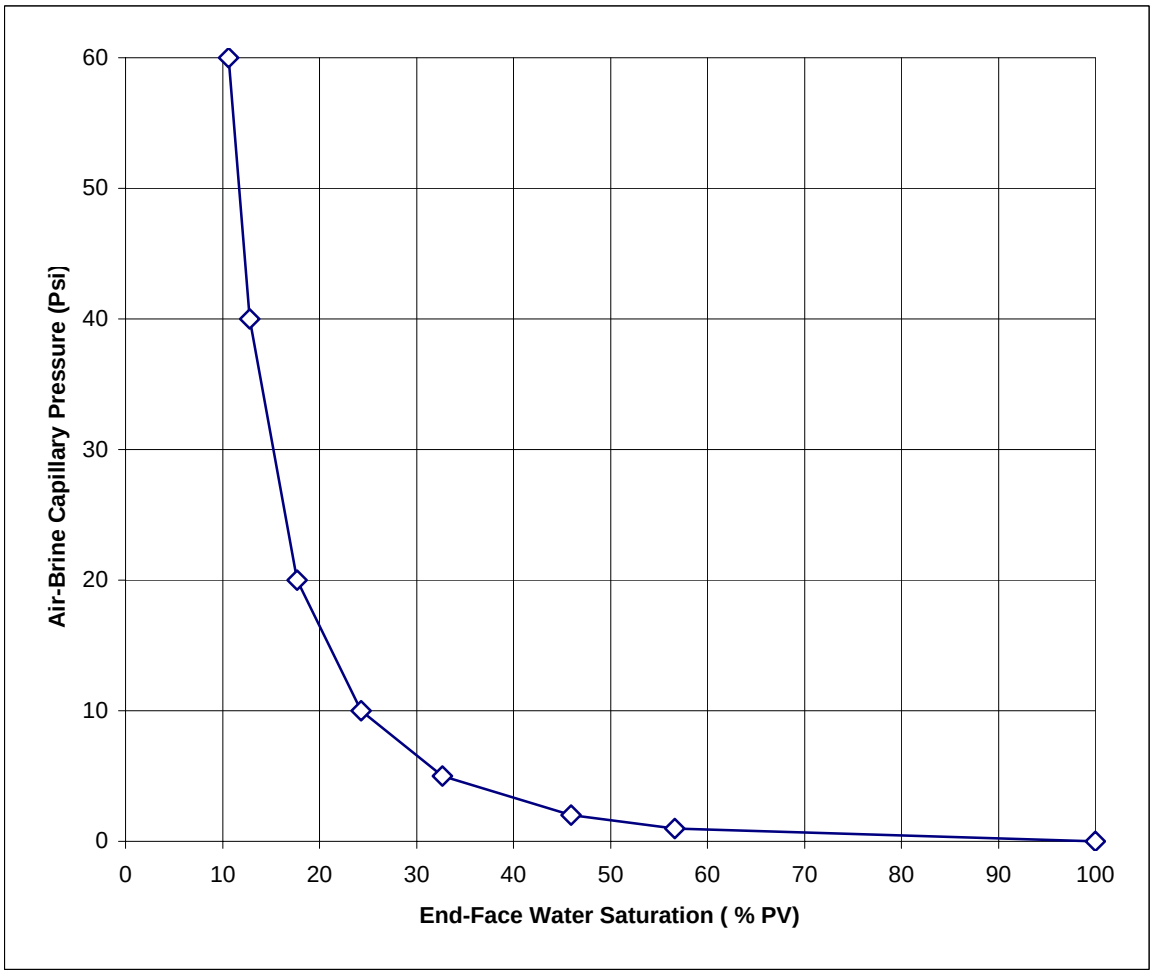

Air-brine Capillary Pressure by Centrifuge at Ambient

Sample no.	Depth (m)	At Ambient		
		Kinf (md)	Kair (md)	Porosity (%)
56A	1817.04	2540	3070	22.0

Capillary Pressure (psi)	End-Face Water Saturation (%pv)
0	100
1	63.7
2	45.1
5	32.4
10	25.5
20	18.9
40	13.5
60	12.2

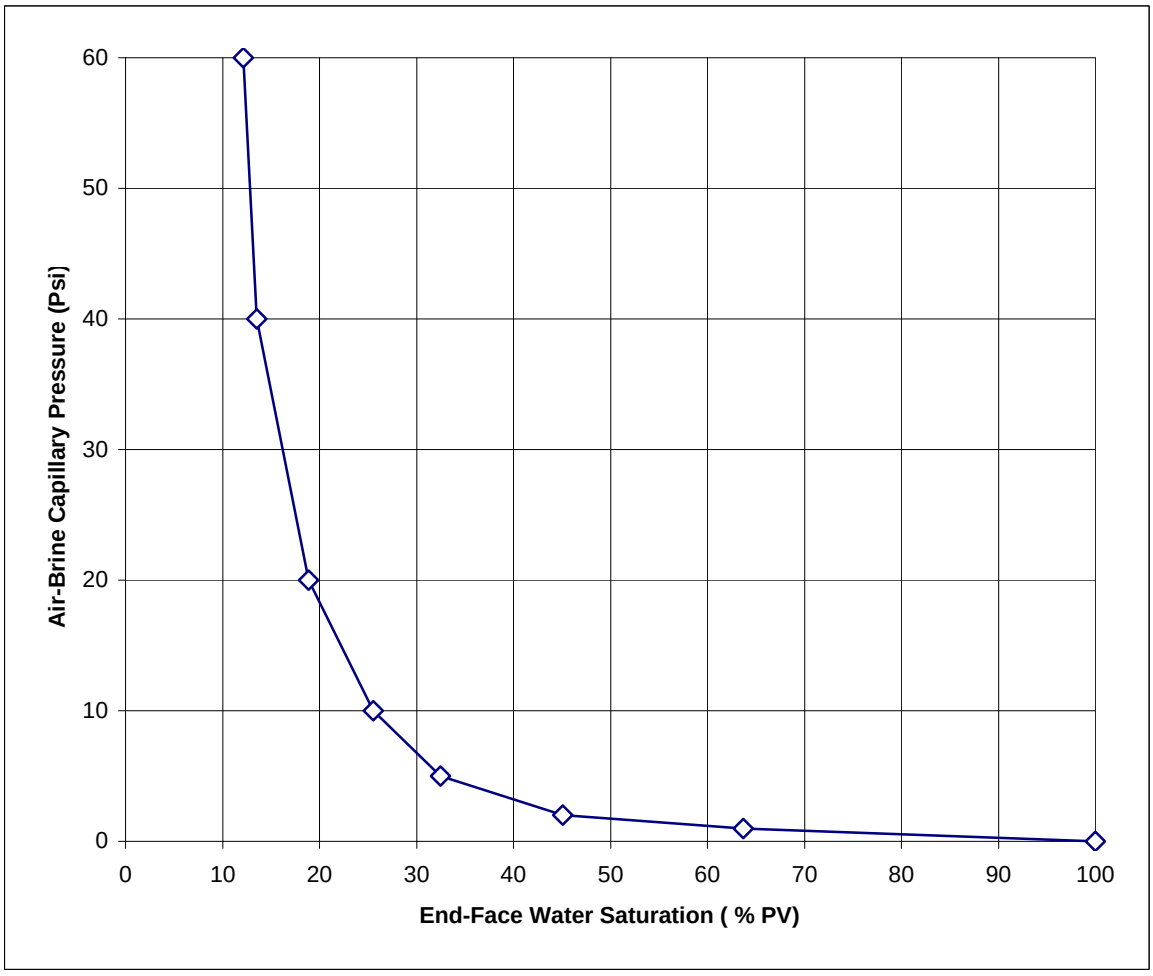

Air-brine Capillary Pressure by Centrifuge at Ambient

Sample no.	Depth (m)	At Ambient		
		Kinf (md)	Kair (md)	Porosity (%)
65	1819.80	2750	2800	26.3

Capillary Pressure (psi)	End-Face Water Saturation (%pv)
0	100
1	61.3
2	37.7
5	29.3
10	22.0
20	15.3
40	12.3
60	12.0

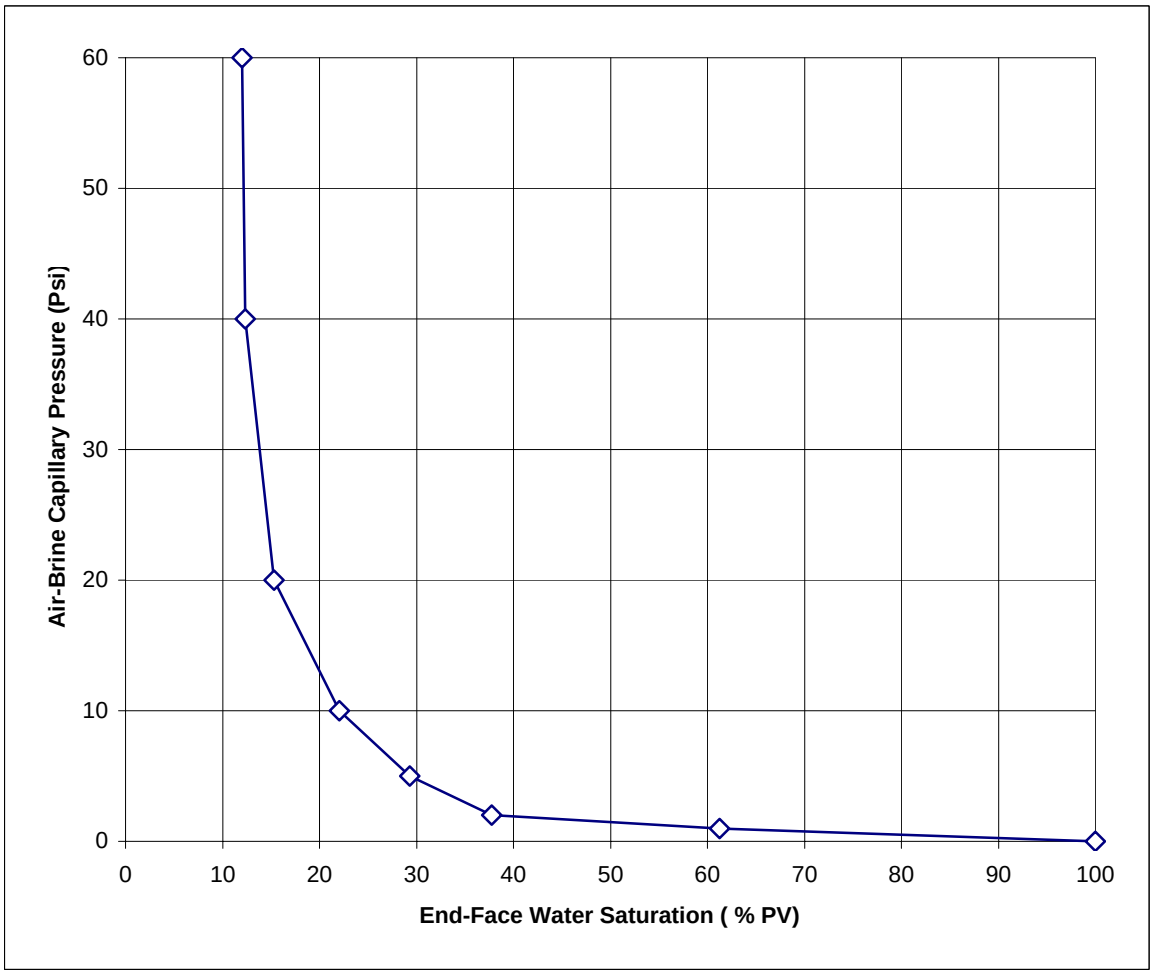

Air-brine Capillary Pressure by Centrifuge at Ambient

Sample no.	Depth (m)	At Ambient		
		Kinf (md)	Kair (md)	Porosity (%)
72A	1821.98	11.8	13.7	16.6

Capillary Pressure (psi)	End-Face Water Saturation (%pv)
0	100
1	100
2	100
5	80.9
10	73.6
20	65.1
40	54.3
60	46.0

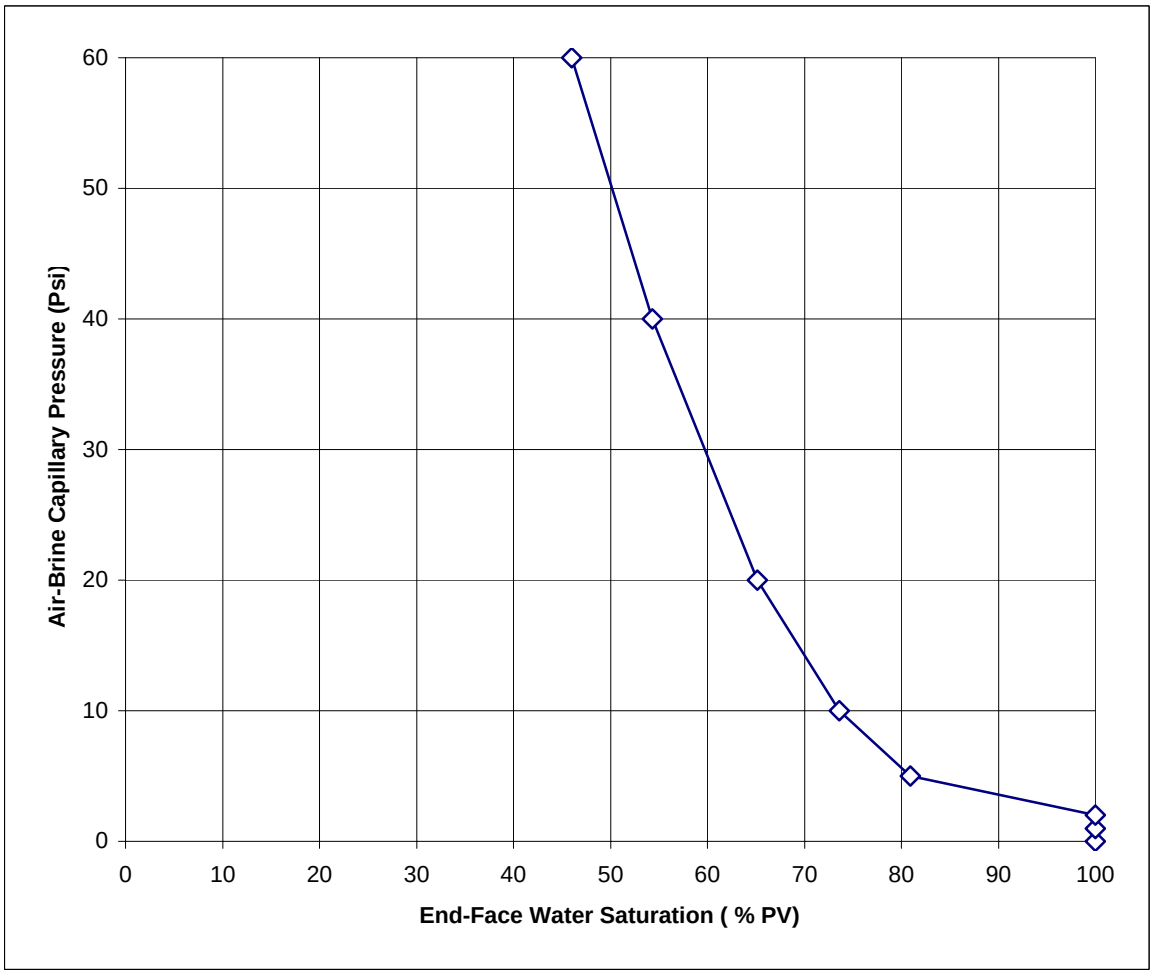

Air-brine Capillary Pressure by Centrifuge at Ambient

Sample no.	Depth (m)	At Ambient		
		Kinf (md)	Kair (md)	Porosity (%)
75A	1822.83	685	706	25.7

Capillary Pressure (psi)	End-Face Water Saturation (%pv)
0	100
1	80.5
2	55.7
5	41.0
10	30.9
20	22.9
40	17.7
60	15.7

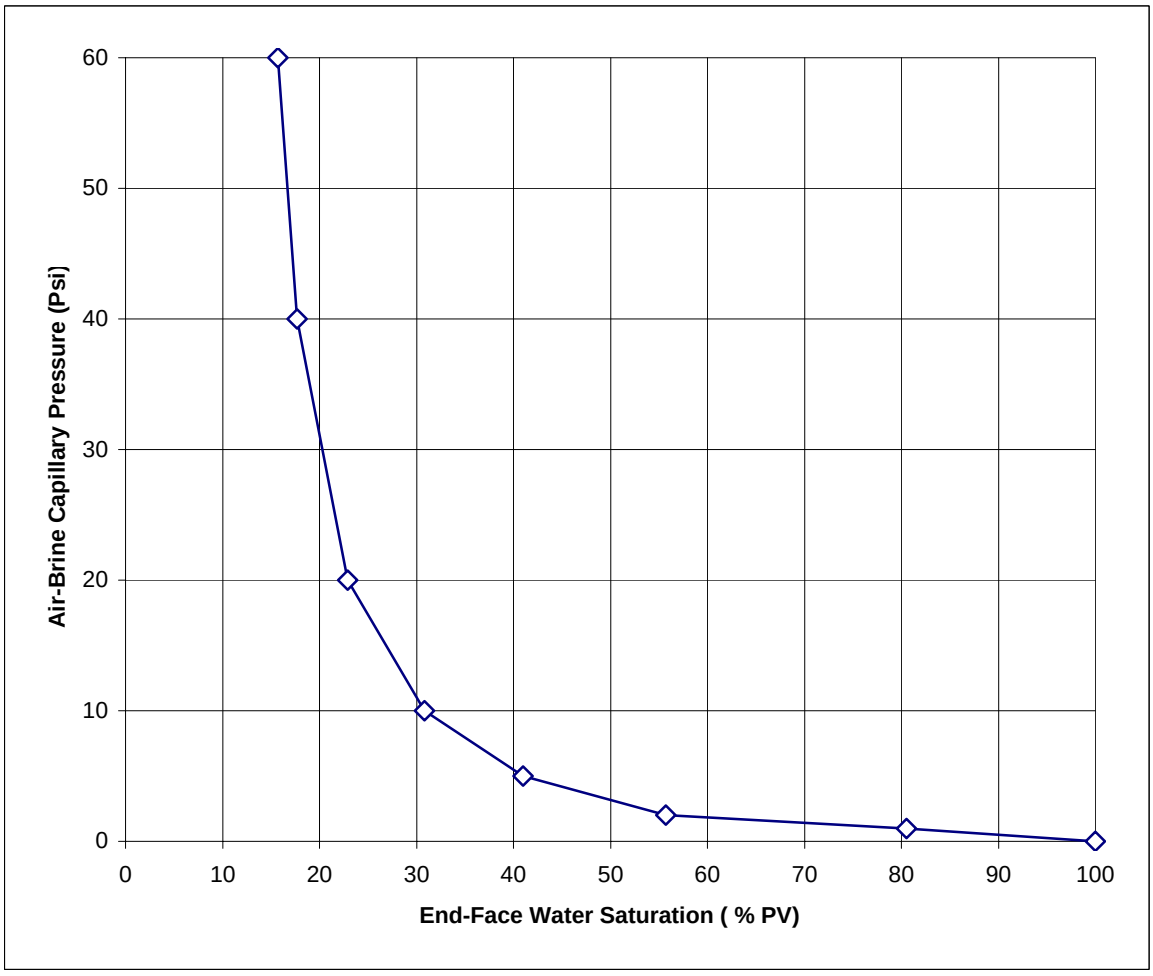

Air-brine Capillary Pressure by Centrifuge at Ambient

Sample no.	Depth (m)	At Ambient		
		Kinf (md)	Kair (md)	Porosity (%)
79	1824.03	5860	6430	25.5

Capillary Pressure (psi)	End-Face Water Saturation (%pv)
0	100
1	39.6
2	27.9
5	22.3
10	17.5
20	13.5
40	10.1
60	8.4

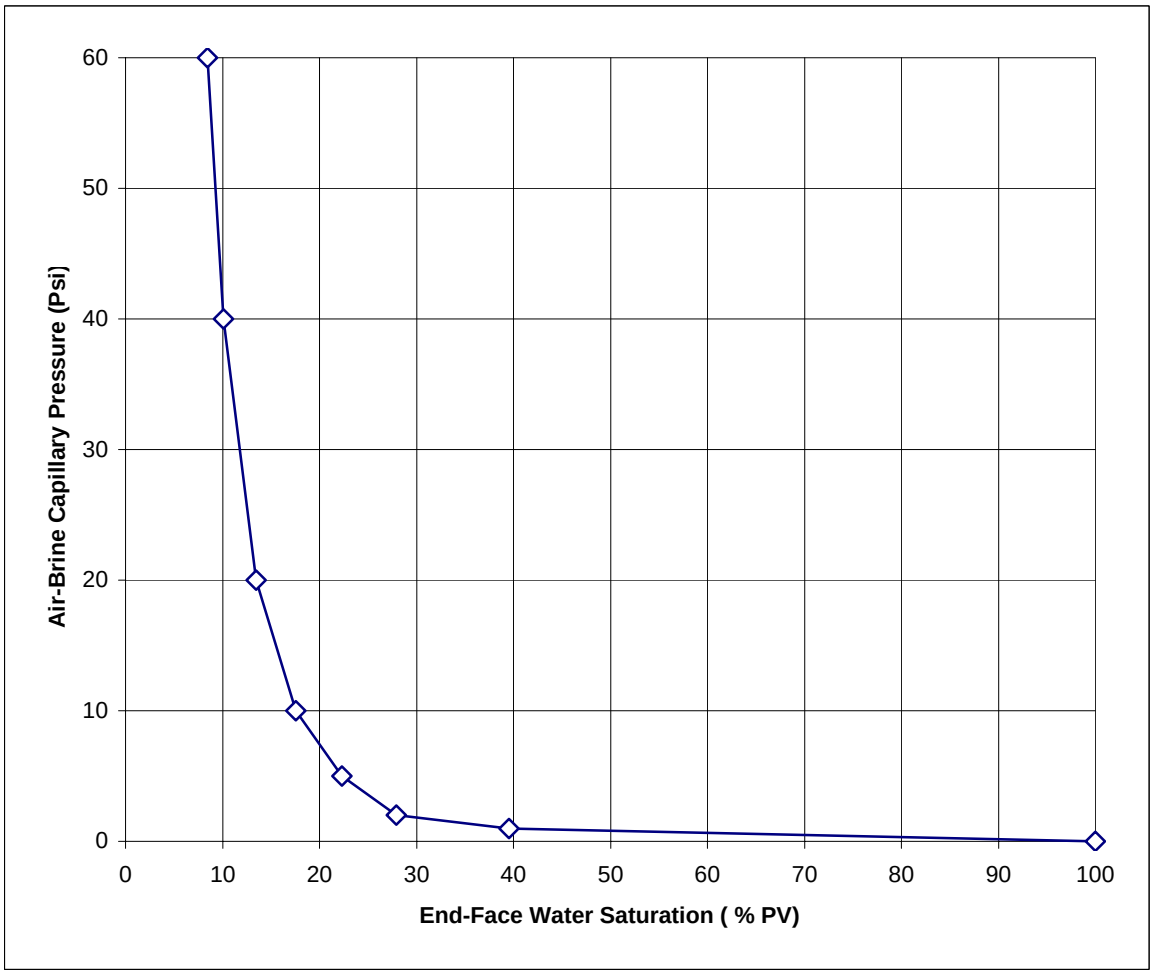

Air-brine Capillary Pressure by Centrifuge at Ambient

Sample no.	Depth (m)	At Ambient		
		Kinf (md)	Kair (md)	Porosity (%)
82	1824.90	3050	3380	23.4

Capillary Pressure (psi)	End-Face Water Saturation (%pv)
0	100
1	56.0
2	33.8
5	20.7
10	16.5
20	13.6
40	11.0
60	10.4

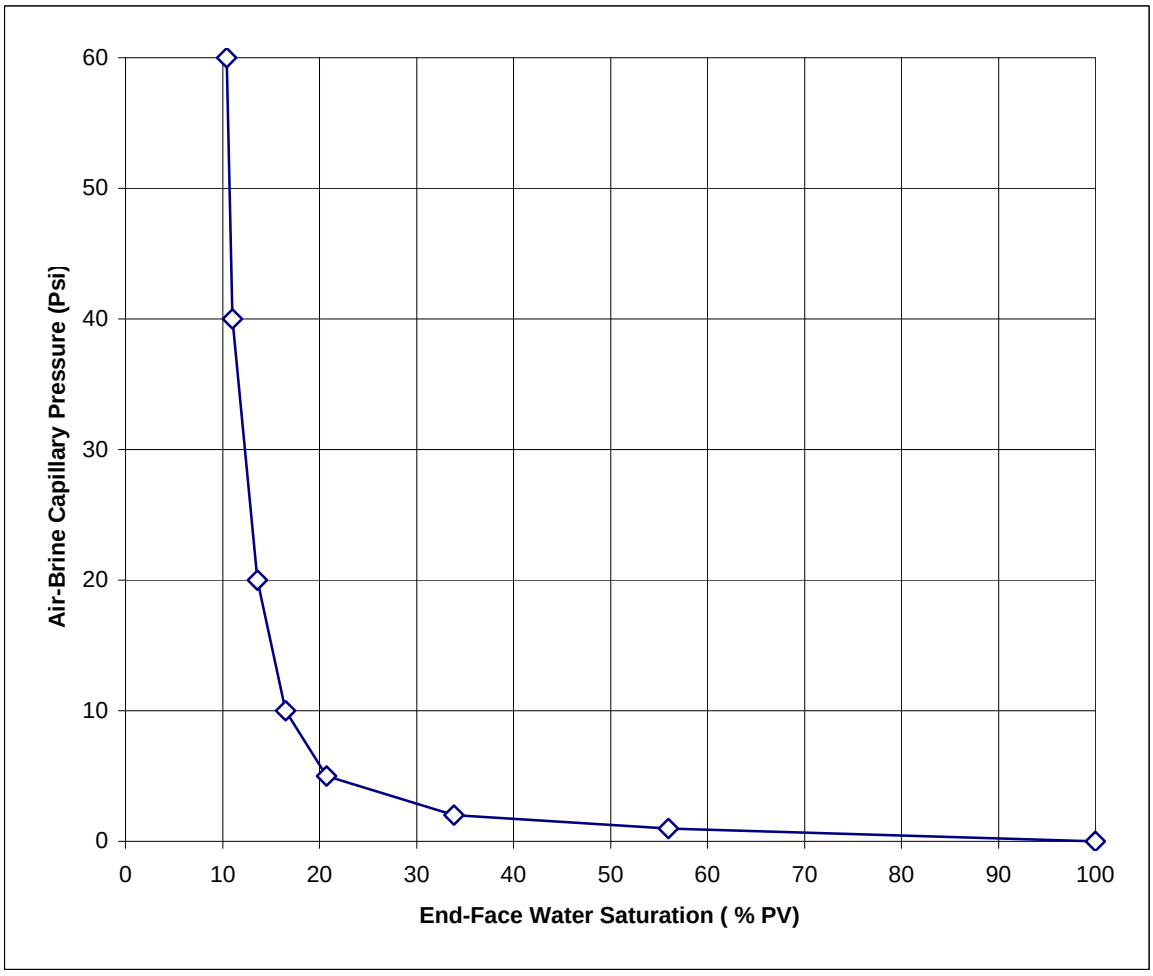

SECTION 4

RESIDUAL GAS SATURATION AND RELATIVE PERMEABILITY

RESIDUAL GAS SATURATION

Counter-Current Imbibition Method

Sample ID	Depth, (m)	Kair (md)	Porosity (%)	Initial Liquid Saturation, % PV	Initial Gas Saturation % PV	Residual Gas Saturation % PV	Gas Displaced	
							% PV	% IGIP
42	1812.90	3740	26.6	15.5	84.5	31.7	52.8	62.5
56A	1817.04	3070	22.0	12.2	87.8	31.5	56.3	64.1
72A	1821.98	13.7	16.6	42.0	58.0	29.1	28.9	49.8
75A	1822.83	706	25.7	19.5	80.5	36.1	44.4	55.2
79	1824.03	6430	25.5	8.7	91.3	32.3	59.0	64.6

Summary of the unsteady-state WATER-GAS relative permeability (end-point) analysis results (determined at 3100 psi NOBP)

Sample No.	Depth (m)	At 3100 psi NOBP				INITIAL CONDITIONS			TERMINAL CONDITIONS			
		Kair (md)	Porosity (%)	Permeability to Brine		Swi (% pv)	Initial gas in place (% pv)	Kgas at Swi (md)	Sgr (% pv)	Gas Recovery		Kw at Sgr (md)
				Kw (md)	Kw/Kair (%)					(% pv)	(% IIGP)	
6A	1792.60	448	24.5	331	73.9	14.9	85.1	421	31.5	53.6	63.0	39.7
28	1808.70	1960	20.1	1530	78.1	16.8	83.2	1739	30.8	52.4	63.0	158
40	1812.30	3690	24.0	2830	76.7	10.3	89.8	3287	31.5	58.2	64.9	251
51A	1815.73	8750	26.3	5170	59.1	9.2	90.8	8500	27.2	63.6	70.1	2429
59	1818.05	9040	22.6	8300	91.8	5.0	95.0	8407	32.3	62.7	66.0	1315
67A	1820.49	2090	24.8	1580	75.6	13.8	86.2	1793	28.8	57.4	66.6	205
76	1823.10	565	26.6	342	60.5	20.6	79.4	470	27.5	52.0	65.4	37.6
86	1826.10	7260	22.2	5200	71.6	11.4	88.6	6405	31.6	56.9	64.3	690

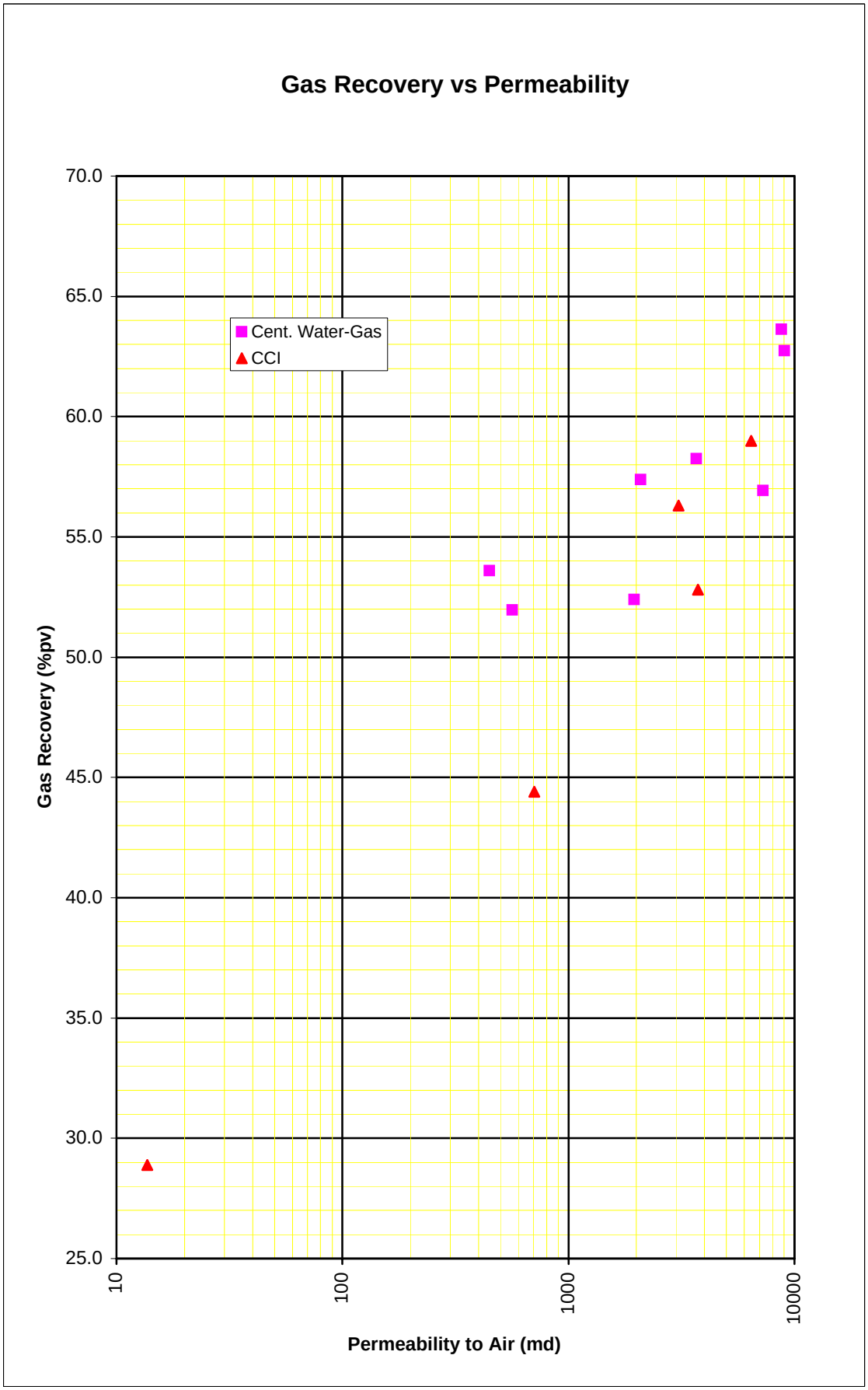
Gas Recovery vs Permeability
70.0
65.0
60.0
55.0
50.0
45.0
40.0
35.0
30.0
25.0
Gas Recovery (%pv)
Cent. Water-Gas
CCI
10
100
1000
10000
Permeability to Air (md)

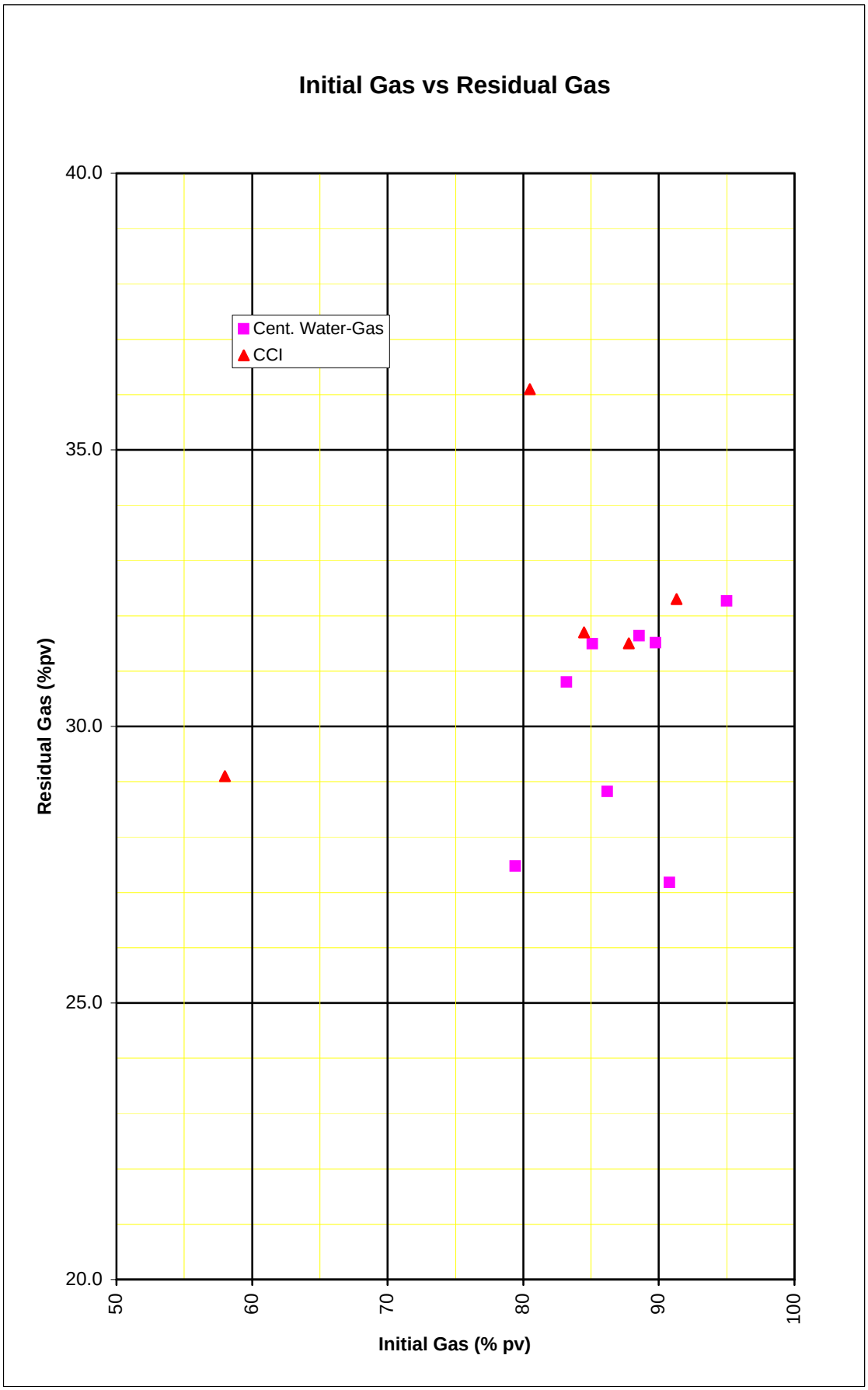
Initial Gas vs Residual Gas
Cent. Water-Gas
CCI
Residual Gas (%pv)
40.0
35.0
30.0
25.0
20.0
50
60
70
80
90
100
Initial Gas (% pv)

APPENDICES

APPENDIX 1
SUMMARY OF LABORATORY PROCEDURES

Summary of Laboratory Procedures

Sample Preparation

The core plugs tested comprised a combination of samples that had either undergone routine core analysis (RCA) or were newly drilled for this SCAL study (samples labelled with “A” or “B” suffices).

All samples selected for the study underwent visual and CT-screening to determine their suitability for SCAL. Samples which failed the screening stage were replaced with substitute samples. All replacement plugs also underwent visual and CT-screening.

The twelve newly drilled samples were cleaned in hot refluxing methanol prior to oven drying (at 90^{o}C) for porosity, permeability and grain density measurements.

Grain Volume and Grain Density

The weight, diameter and length of all samples were measured before they were processed through the Ultrapore^{TM} porosimeter to determine grain volume. As a standard quality control measure, a calibration check plug was run after every ten samples. Grain density data was calculated from grain volume and sample weight data.

Permeability and Porosity

Permeability and pore volume measurements were made on all twelve core plug samples at 800 and 3100 psi confining pressure in the CMS^{TM}300 automated core measurement system. A standard check plug was run with every five plug samples. Klinkenberg permeability (Kinf) values are obtained directly from the CMS-300, since it operates by unsteady-state principles. Porosity data was obtained by combining pore volumes from the CMS-300 with grain volumes from the Ultrapore^{TM} porosimeter.

The complete routine core analysis results are presented on 1-3.

Saturation

All samples undergoing SCAL analyses were evacuated and pressure saturated with a simulated formation brine of 25,000 ppm concentration comprising 80% NaCl and 20% KCl. All samples were weighed after saturation to check measured pore volumes.

Formation Resistivity

Nine samples were selected to undergo electrical properties measurements.

Each fully saturated sample was loaded into a coreholder at the reservoir equivalent NOBP (3100 psi) and the electrical resistivities measured on consecutive days until they were stable, indicating ionic equilibrium in the pore spaces. Formation resistivity factor (FRF) and cementation exponent (“m”) values were then calculated.

Each sample was then desaturated at incrementally increasing pressures using humidified air as the displacing medium. Electrical resistivity of the sample was measured at the incrementally decreasing partial saturations. When the sample had attained electrical equilibrium at each incremental desaturation stage, values of resistivity index (FRI) and saturation exponent (“n”) were calculated.

The trimmed ends of the plugs which underwent FRF and FRI measurements were cleaned in methanol, dried at 60^{o}C in a conventional oven then crushed and subjected to determinations of cation exchange capacity (CEC) using the ammonium acetate wet chemistry technique. These CEC values are used to calculate idealised “m*” and “n*” values using Waxman-Smits-Thomas equations.

Results from the electrical analysis are presented within SECTION 2 of this report.

Air-Brine Capillary Pressure by Centrifuge

The ten selected samples were initially pressure saturated with the simulated formation brine. All samples were weighed after saturation to check measured pore volumes.

The fully saturated samples were each loaded into individual centrifuge cups and loaded into the centrifuge. The samples were then subjected to non-stop centrifugation at rotational rates that were increased incrementally to generate equivalent pressures ranging from 1 to 60 psi in an air-brine system. Effluent brine volumes were monitored as the samples achieved capillary equilibrium at each incremental pressure.

Capillary pressure and end-face saturation data were then calculated from the raw data using data reduction techniques developed by Hassler-Brunner and later modified by other workers (e.g Rajan, Forbes). These results are presented within SECTION 3 of this report.

Residual Gas by Counter-Current-Imbibition (CCI)

On completion of the air-brine capillary pressure tests, a sub-set of five samples was selected to undergo residual gas saturation by CCI method.

The selected samples were re-cleaned, dried and the base data (permeability, porosity and grain density values) re-confirmed. Next the samples were saturated with toluene and their saturated weights checked to confirm helium injection pore volume data.

Each sample was then evaporated to a gravimetrically-determined initial “liquid” saturation with the remaining void pore space being air (“gas”) filled. Initial liquid saturations were estimated from Swi values established during capillary pressure measurements.

The samples were suspended, in turn, in a tared cradle below a weigh balance in a container of toluene. As the toluene imbibed into the samples, gas displacement was recorded by increasing weight versus time. Equilibrium residual gas saturations were then calculated and these data are presented in SECTION 4 of this report.

Specific Permeability to Brine

The eight selected samples were initially pressure saturated with the simulated formation brine. All samples were weighed after saturation to check measured pore volumes.

The brine saturated (100% Sw) samples were loaded into individual hydrostatic core holders and the confining pressure gradually increased to 3100 psi NOBP. Simulated formation brine was flowed through each sample at a slow constant rate. At equilibrium, when constant flow pressure was attained, permeability to brine (Kw at 100% Sw) measurements were recorded.

Unsteady-State Water-Displacing-Gas Relative Permeability (End-Point)

Unsteady-state water-displacing-gas tests were conducted on the same eight samples which underwent specific permeability to brine measurements.

The fully saturated (100% Sw) samples were reduced to immobile water saturation using the centrifuge. The samples were then removed from the centrifuge, weighed, and loaded into individual hydrostatic core holders. The confining stress was gradually increased to 3100 psi. Humidified gas (nitrogen) was then flowed through each sample and Krg at Swi determined.

Next, the sample was flooded at constant rate with simulated formation brine and gas production monitored until residual gas saturation was achieved (based on stable effluent gas volumes and differential pressures). At this stage, an effective permeability to brine at residual gas saturation (Kw at Sgr) was measured.

Utilising data from the unsteady-state water-gas (end-point) analysis, full relative permeability water-displacing-gas curves can be derived using suitable correlations (e.g Corey, MAK and other).

Results from the unsteady-state water-gas relative permeability (end-point) by centrifuge are presented in SECTION 4 of this report.

APPENDIX 2
SAMPLES DRILLED FOR MECHANICAL STRENGTH TESTS

Samples Drilled for Mechanical Strength Tests

Sample ID	Depth (m)

1.5" diameter horizontal plugs drilled with brine

A	1809.45
B	1809.50
C	1812.40
D	1812.45
E	1812.50
F	1817.77
G	1817.83
H	1817.88
I	1819.62
J	1819.67
K	1822.91
L	1822.95
M	1826.27
N	1826.33

1.0" diameter vertical plugs drilled with oil

W	1831.21
X	1831.21
Y	1831.21
Z	1831.21

APPENDIX 3
CT-SCAN DESCRIPTIONS

CT-Scan Descriptions (SCAL Plugs)

Sample 5A : (1792.55 m)

Predominantly fine quartz sandstone containing a few scattered framework grains to medium sand size. Rare greenish grains of possible glauconite are noted and other accessory components include mica and pyrite. Layering of mm-scale is a feature of the attenuation fabric; it trends more or less with the plug axis. Diffuse higher attenuation is related to finer grain size and associated pyrite dust. Rare spots of very high attenuation are almost certainly localised pyrite or possibly pyritised organic matter. The sample is moderately homogeneous and no defects are evident.

Sample 6A : (1792.60 m)

Fine quartz sandstone containing rare greenish grains of possible glauconite. Layering of mm-scale is apparent and this is the main feature of the attenuation fabric. Layers trend lengthwise with the plug axis but crossbedding is noted. Relatively higher attenuation highlighting some layers is attributable to traces of pyrite cement. Pyritised organic matter and glauconite also contributes to localised higher attenuation. More diffuse variations in attenuation relate to pore development; lower attenuation domains are inferred as more porous. The sample is moderately homogeneous and no defects are evident.

Sample 7 : (1793.00 m)

Mainly fine, rarely medium quartz sandstone; it shows layering trending more or less lengthwise with the plug axis. Accessory components include coaly organic matter with associated specks of siderite, greenish grains of possible glauconite and pyrite. The dominant feature of the attenuation fabric is localised very low attenuation (around 50 to 300 HU) inferred as organic matter. Layering of mm-scale is apparent and crossbedding is inferred. Scattered spots of highest attenuation are mainly related to localised pyrite but there also is some contribution from traces of siderite. The sample is moderately homogeneous and no defects are apparent.

CT-Scan Descriptions (SCAL Plugs) … cont'd

Sample 28 : (1808.70 m)

Poorly sorted somewhat bimodal quartz sandstone; it comprises layers that are fine to medium interspersed with coarser layers that are granular to pebbly in places. The layering is mm-scale, somewhat disturbed and trends generally lengthwise with the plug axis. Feldspars are noted amongst the coarser framework grains and accessory components include clays, pyrite and specks of 'coaly' organic matter. The poor layering and localised concentrations of coarser grains are revealed in the attenuation fabric. For the most part these grains float in a finer matrix but in places very low attenuation spots indicate the presence of larger pores. However a few of these are possibly attributable to organic matter. Disseminated spots and specks of very high attenuation are inferred as pyrite cement. The sample is overall moderately homogeneous and no defects are evident.

Sample 29 : (1809.05 m)

Mainly fine to medium, rarely coarse to granular quartz sandstone; it is layered on mm-scale. Accessory components include traces of pyrite, organic matter commonly pyritised, clays and mica. The attenuation fabric shows subplanar layers with a slight lengthwise dip; minor crossbedding is noted. Individual coarsest grains show moderately high attenuation. Several of the laminations also show moderately high attenuation but this is related to finer grain size and in particular the presence of clays. Localised very high attenuation is attributable to pyrite and pyritised organic matter. Lower attenuation speckling and spots point to relatively more porous domains. The sample is moderately homogeneous and no defects are evident.

Sample 40 : (1812.30 m)

Quartz sandstone, it comprises disturbed layers that are alternatively fine to medium and coarse to rarely granular; these are in subequal abundance. Accessory components include traces of organic matter and pyrite. Irregularly disseminated, low attenuation spots and speckles dominate the attenuation fabric. These are open pores. Rare spots of very high attenuation are localised pyrite cement. The disturbed layering is set slightly oblique to the plug axis and trends more or less lengthwise with the plug axis. The sample is moderately homogeneous and no defects are apparent.

CT-Scan Descriptions (SCAL Plugs) … cont'd

Sample 42 : (1812.90 m)

Fine to rarely granular quartz sandstone; it comprises layers that are alternately mainly fine to medium and medium to coarse. Accessory components include traces of pyrite and possible glauconite. The attenuation fabric reveals subplanar mm-scale layers that trend lengthwise with the plug axis. Disseminated very low attenuation spots and speckles and the generally low average attenuation point to a well-developed pore network. Rare very high attenuation is attributable to localised pyrite cement. The sample is moderately homogeneous and no defects are inferred.

Sample 44: (1813.45 m)

The sample is a probable coarse to granular quartz sandstone. The attenuation fabric reveals planar layering set slightly oblique to the plug axis. Disseminated very low attenuation spots and speckles point to a well-developed pore network in some of the layers. A minor streak of very high attenuation is possibly pyritised organic matter and other spots of very high attenuation are almost certainly attributable to traces of localised pyrite. The sample is moderately homogeneous and no defects are inferred.

Sample 47 : (1814.42 m)

The sample is a probable coarse to at least granular quartz sandstone. The fabric is quite chaotic with patchy concentrations of finer and coarser grains. Nevertheless, layering trending more or less lengthwise with the plug axis is apparent. Scattered spots and specks of very low attenuation are mainly attributable larger open pores although traces of organic matter cannot be discounted. Rare spots of very high attenuation are almost certainly localised pyrite cement. The sample is moderately homogeneous and no defects are evident.

CT-Scan Descriptions (SCAL Plugs) … cont'd

Sample 48 : (1814.75 m)

The sample is a probable medium to at least granular quartz sandstone. Disturbed layering trends lengthwise with the plug axis with high attenuation streaks inferred as pyritised organic matter along the layering trend. Other spots of very high attenuation are almost certainly localised pyrite cement. Sporadic very low attenuation spots are open pores, however irregular traces of low attenuation point to an open defect. The homogeneity of the sample is poor to moderate and it is probably defected.

Sample 48A : (1814.81 m)

The sample is a probable fine to medium, rarely coarse quartz sandstone containing minor 'coaly' organic matter and traces of pyrite. Two irregular very low attenuation features dominate the attenuation fabric; one of these is inferred as concentrated organic matter (around 150 to 350 HU) whereas the other is inferred as a possible open defect.

Sample 51A : (1815.73 m)

The sample is a probable coarse to very coarse quartz sandstone. The attenuation fabric reveals poorly defined layering trending more or less lengthwise with the plug axis. Most apparent however are disseminated spots of very low attenuation that point to a well-developed pore network. Overall the sample is essentially homogeneous and no defects are evident.

Sample 55 : (1816.80 m)

Fine to coarse, rarely granular quartz sandstone; it is moderately indurated and shows significant surficial spalling of grains. The attenuation fabric reveals mm-scale planar layers, trending more or less lengthwise with the plug axis. All layers and some more than others show disseminated spots of very low attenuation pointing to a well-developed pore network. The sample is moderately homogeneous and no defects are inferred.

CT-Scan Descriptions (SCAL Plugs) … cont'd

Sample 56 : (1817.00 m)

Fine to granular, rarely pebbly quartz sandstone; it shows disturbed subplanar layering trends at a somewhat oblique angle to the plug axis. Accessory components include traces of 'coaly' organic matter, 'golden' nodular pyrite and clays. The attenuation fabric reveals the layering but also two domains with significantly different average attenuation. The domain showing lower overall attenuation (around 1300 HU) is considered more porous. In contrast, the other domain averages around 1650 HU: it almost certainly contains a greater finer grained component. Several irregular shaped specks of very low attenuation are almost certainly organic matter. Scattered spots of very high attenuation are localised pyrite cement. The sample shows moderately poor homogeneity and no defects are inferred.

Sample 56A : (1817.04 m)

The sample is a probable fine to medium, rarely granular to pebbly quartz sandstone containing accessory traces of 'coaly' organic matter and pyrite. The attenuation fabric shows poorly defined disturbed layering trending lengthwise with the plug axis. Very low attenuation spots are for the most part pores, however larger patches are almost certainly concentrations of organic matter. Rare spots of very high attenuation are almost certainly pyrite cement. The sample is moderately homogeneous and no defects are inferred.

Sample 57A : (1817.50 m)

The sample is a probable medium to at least lower pebbly quartz sandstone. The attenuation fabric reveals mm-scale layering trending more or less lengthwise with the plug axis. Also apparent is cross bedding with layers in this domain set more oblique to the plug axis. Irregularly disseminated spots of very low attenuation are larger open pores although traces of organic matter cannot be discounted. The sample is moderately homogeneous and no defects are inferred.

CT-Scan Descriptions (SCAL Plugs) … cont'd

Sample 59 : (1818.05 m)

Medium to coarse, rarely granular to pebbly quartz sandstone; it is moderately indurated and shows significant surficial spalling of grains. Accessory components include pyrite in the form of 'dust' and 'golden' nodules. The attenuation fabric reveals mm-scale planar layers, trending more or less lengthwise with the plug axis. All layers and some more than others show disseminated spots of very low attenuation pointing to a well-developed pore network. Rare spots of very high attenuation are localised pyrite cement. The sample is moderately homogeneous and no defects are inferred.

Sample 62B : (1818.84 m)

A probable quartz sandstone; it is bimodal with layers that are fine to medium juxtaposed with coarser domains that are dominantly granular to pebbly. The attenuation fabric reveals the layering as well as individual coarser grains. Layering is set somewhat oblique to the plug axis. Irregular very high attenuation streaks and spots are a feature of on finer domain; these are attributable to pyrite, possibly pyritised organic matter. Spots of very low attenuation within the coarser domain are inferred as intergranular pores. The sample shows moderately poor homogeneity and no defects are apparent.

Sample 62A : (1818.95 m)

Mainly very fine, rarely medium silty quartz sandstone; it contains a significant clay component that is in places is associated with pyrite 'dust' as well as traces of 'coaly' organic matter. The speckled somewhat compartmental attenuation fabric is reminiscent of bioturbation. Highest attenuation spots and streaks are attributable to the presence of pyrite. Patchy moderately lower attenuation domains are indicative of cleaner sand. The sample shows poor to moderate homogeneity overall and no defects are inferred.

CT-Scan Descriptions (SCAL Plugs) … cont'd

Sample 64 : (1819.50 m)

Mainly fine to coarse, minor granular quartz sandstone; it is moderately indurated and shows significant surficial spalling of grains. Accessory components include pyrite in the form of 'dust' and 'golden' nodules as well as traces of organic matter. The attenuation fabric reveals poorly defined planar layers, trending more or less lengthwise with the plug axis. Disseminated spots of very low attenuation point to a well-developed pore network. Rare spots of very high attenuation are localised pyrite cement. Several diffuse patches of moderate attenuation are probably finer grained. The sample is moderately homogeneous and no defects are inferred.

Sample 65 : (1819.80 m)

Mainly fine to coarse, minor granular quartz sandstone; it shows layering of mm-scale trending more or less lengthwise with the plug axis. Accessory components include 'coaly' organic matter and pyrite in the form of 'dust' and 'golden' nodules. The attenuation fabric reveals the layering as subplanar; a distinctive lamination showing moderately high attenuation is finer grained with accessory organic matter and clays. Disseminated spots of very low attenuation are indicative of a well-developed pore network. Rare spots of very high attenuation are localised pyrite cement. The sample is moderately homogeneous and no defects are inferred.

Sample 67A : (1820.49 m)

Mainly fine to medium, rarely coarse quartz sandstone with accessory pyrite and traces of organic matter. The attenuation fabric shows evidence of mm-scale planar layering trending lengthwise with the plug axis. Disseminated spots of lower attenuation are predominantly larges pores. Sporadic spots and clumps of very high attenuation are localised pyrite cement. The sample is moderately homogeneous and no defects are inferred.

CT-Scan Descriptions (SCAL Plugs) … cont'd

Sample 72 : (1821.90 m)

Mainly very fine, rarely medium silty quartz sandstone; it contains a significant clay component that is in places is associated with pyrite 'dust' as well as traces of 'coaly' organic matter. Some of the organic matter is pyritised. The attenuation fabric is reminiscent of bioturbation and probable burrows are noted. Highly disturbed layering trends generally lengthwise with the plug axis. Highest attenuation spots and streaks are attributable to relatively finer grainsize and the presence of pyrite cement. Moderately higher attenuation is suggestive of finer grainsize with a somewhat lesser pyrite component. Patchy moderately lower attenuation domains are indicative of cleaner sand. In these domains some relict cross ripples are inferred. The sample shows poor to moderate homogeneity overall and no defects are evident.

Sample 72A : (1821.98 m)

Mainly very fine, rarely medium silty quartz sandstone; it contains a significant clay component, localised pyrite and traces of 'coaly' organic matter. The attenuation fabric is reminiscent of bioturbation and burrow structures are noted. Highest attenuation spots and streaks are attributable to the presence of pyrite. Very low and high attenuation juxtaposed points to pyritised organic matter. Patchy moderately lower attenuation domains are indicative of cleaner sand. The sample shows poor to moderate homogeneity overall and no defects are inferred.

Sample 75A : (1822.83 m)

Mainly fine to medium, rarely pebbly quartz sandstone. Accessory components include traces of pyrite and 'coaly' organic matter. The attenuation fabric shows somewhat disturbed mm-scale layering set at an oblique angle to the plug axis. Minor finer grained laminations are indicated by diffuse slightly higher attenuation. Isolated irregular patches of moderately high attenuation are individual larger grains. Lower attenuation spots are predominantly larger pores although organic matter cannot be discounted. Rare spots of very high attenuation are localised pyrite. The sample is moderately homogeneous and no defects are inferred.

CT-Scan Descriptions (SCAL Plugs) … cont'd

Sample 76 : (1823.10 m)

Mainly fine to medium, rarely granular quartz sandstone; it contains accessory traces of pyrite and 'coaly' organic matter. The attenuation fabric shows possible layering set lengthwise with the plug axis. Lower attenuation spots are predominantly larger pores although organic matter cannot be discounted. A distinctive very high attenuation streak is inferred as a pyritised flake of organic matter. The sample is essentially homogeneous and no defects are inferred.

Sample 77A : (1823.36 m)

Mainly fine to medium quartz sandstone, it contains a minor component of coarser framework grains to at least upper granule-size. The attenuation fabric shows somewhat disturbed mm-scale layering set at an oblique angle to the plug axis. Minor finer grained laminations are indicated by diffuse slightly higher attenuation. Isolated irregular patches of moderately high attenuation are individual larger grains. Lower attenuation spots are predominantly larger pores although organic matter cannot be discounted. Rare spots of very high attenuation are localised pyrite. The sample is moderately homogeneous and no defects are evident.

Sample 79 : (1824.03 m)

Mainly medium, rarely granular quartz sandstone; it contains accessory traces of 'coaly' organic matter and pyrite. A distinctive patch of 'coal' several mm thick is noted at the plug margin. Disseminated very low attenuation spots that for the most part are inferred as larger intergranular pores, dominate the attenuation fabric. More rarely this very low attenuation points to organic matter, as is the case for the largest of these domains. The organic matter noted at the plug margin is not significantly penetrative. The sample is essentially homogeneous and no defects are inferred.

CT-Scan Descriptions (SCAL Plugs) … cont'd

Sample 82 : (1824.90 m)

Mainly medium, rarely granular to pebbly quartz sandstone; it contains accessory traces of pyrite and 'coaly' organic matter. The attenuation fabric reveals mm-scale planar layering set somewhat oblique to the plug axis. However, disseminated very low attenuation spots inferred for the most part as larger intergranular pores dominate the fabric. Largest patches of very low attenuation (around 30 to 300 HU) are inferred as organic matter. Rare spots of very high attenuation are localised pyrite cement. The sample is moderately homogeneous and no defects are evident.

Sample 84 : (1825.50 m)

Mainly medium to coarse, rarely granular to pebbly quartz sandstone; it contains accessory traces of 'coaly' organic matter and pyrite. The attenuation fabric reveals disturbed layering set at an oblique angle to the plug axis. However, dominant disseminated spots of very low attenuation point to a well-developed pore network. The sample is moderately homogeneous and no defects are inferred.

Sample 86 : (1826.10 m)

Mainly fine to coarse, rarely granular quartz sandstone; it contains accessory traces of 'coaly' organic matter and pyrite. The attenuation fabric reveals mm-scale planar layers, these are set oblique to the plug axis. All layers and some more than others show disseminated spots of very low attenuation pointing to a well-developed pore network. The sample is moderately homogeneous and no defects are inferred.

CT-Scan Descriptions (Horizontal Plugs Drilled for Mechanical Strength Tests)

Sample A : (1809.45 m)

Moderately well sorted, fine to coarse, mainly upper fine, quartz sandstone; the minor coarser component (~5%) occurs as rare 'floating' grains as well as in localised patches and as millimetre scale subplanar layers. Accessory components include traces of 'coaly' organic matter, both disseminated and rarely layer-dominant, pyrite, mica and greenish micaceous grains of possible glauconite. The attenuation fabric shows millimetre to centimetre scale subplanar layering set at an oblique angle to the plug axis. Higher attenuation defining some layers is attributable to relatively finer grain size and associated traces of pyrite 'dust'. Lowest attenuation is for the most part attributable to open pore abundance although rare local contribution from organic matter cannot be discounted. The sample shows non-parallel bedding, is moderately homogeneous overall and no defects are evident.

Sample B : (1809.50 m)

Moderately sorted, fine to granular, mainly upper fine, quartz sandstone; the lesser (~10 %) coarser component is predominantly localised in millimetre scale subplanar layers. Accessories include traces of 'coaly' organic matter (~1%), both disseminated and in millimetre scale layers, pyrite as 'dust' and intergranular nodules, and mica. Layering is the dominant feature of the attenuation fabric; it is millimetre scale and set at an oblique angle to the plug axis. Low angle crossbedding is inferred. Higher attenuation defining many of the layers is attributable to relatively finer grain size and the presence of pyrite 'dust'. Streaks of highest attenuation are domains that are pyrite-dominated (possibly pyritised organics). Isolated spots showing highest attenuation are almost certainly attributable to intergranular pyrite. Lowest attenuation is for the most part attributable to open pore abundance although rare local contribution from organic matter cannot be discounted. The sample shows non-parallel bedding, is moderately homogeneous overall and no defects are evident.

CT-Scan Descriptions (Horizontal Plugs Drilled for Mechanical Strength Tests) … cont'd

Sample C : (1812.40 m)

Moderately sorted, very fine to very coarse, mainly medium, quartz sandstone; the minor coarser component (~20%) is localised in millimetre scale subplanar layers. Grain spalling is noted. Accessory components include 'coaly' organic matter, concentrated for the most part in millimetre scale layers, pyrite and mica. The attenuation fabric reveals low angle crossbedding but overall layering is lengthwise with the plug axis. Concentrations of lowest attenuation spots are for the most part attributable to larger pores, and lower attenuation generally is indicative of pore abundance. However, rare spots and specks of low attenuation are due to the presence of organic matter. Highest attenuation specks particularly associated with one layer are probably pyrite concentrations either as pyritised organics or intergranular cement. However, siderite cannot be discounted. The sample is moderately homogeneous overall and no defects are evident.

Sample D : (1812.45 m)

Moderately poorly sorted, fine to pebbly, mainly medium, quartz sandstone; the lesser coarser component (~10%) occurs as localised patches and in millimetre scale subplanar layers. Accessory components include 'coaly' organic matter (~1%), both disseminated and in millimetre scale layers, and traces of pyrite and mica. The attenuation fabric reflects the layering that trends generally lengthwise with the plug axis; low angle crossbedding is apparent. Individual coarsest framework grains are evident and show typical uniform moderately high attenuation. Lower attenuation generally is associated with pore abundance, but in places larger low attenuation specks are almost certainly attributable to organic matter. Rare highest attenuation specks are inferred as pyrite cement. The sample shows poor to moderate homogeneity and no defects are apparent.

Sample E : (1812.50 m)

Moderately well sorted, very fine to granular, predominantly medium, quartz sandstone; the minor coarser component (~10%) is localised in millimetre scale subplanar layers. Grain spalling is noted. Accessory components include 'coaly' organic matter concentrated for the most part in millimetre scale layers, pyrite and mica. The main feature of the attenuation fabric is layering trending generally lengthwise with the plug axis; very low angle crossbedding is apparent. Lower attenuation generally is associated with pore abundance, but in places there is very minor contribution from organic matter. Rare spots of highest attenuation are almost certainly attributable to pyrite cement, however traces of siderite may also contribute in places. The sample is moderately homogeneous and no defects are evident.

CT-Scan Descriptions (Horizontal Plugs Drilled for Mechanical Strength Tests) … cont'd

Sample F : (1817.77 m)

Moderately poorly sorted, medium to lower pebbly, mainly coarse to very coarse, quartz sandstone; significant grain spalling is noted. A trace of pyrite occurs as 'dust' and rare 'golden' nodules. Coarsest individual framework grains and low attenuation macropores are the features most apparent in the fabric; less apparent is layering set parallel to and variably oblique to the plug axis; crossbedding is inferred. Rare specks of highest attenuation (>3000 HU) are almost certainly attributable to localised intergranular pyrite cement. The sample is moderately homogeneous overall and no defects are evident.

Sample G : (1817.83 m)

Moderately poorly sorted, medium to lower pebbly, mainly very coarse to granular, quartz sandstone; significant grain spalling is noted. A trace of pyrite occurs as 'dust' and rare 'golden' nodules. Coarsest individual framework grains and low attenuation macropores are the features most apparent in the fabric. Layering also is evident; it dips at a low angle to the plug axis. Rare specks of highest attenuation (>3000 HU) are almost certainly attributable to localised intergranular pyrite cement. The sample may be more bimodal than is visually apparent but overall it is moderately homogeneous and no defects are evident.

Sample H : (1817.88 m)

Moderately poorly sorted, medium to granular, mainly coarse to very coarse, quartz sandstone; it is a relatively short sample and significant grain spalling is noted. A trace of pyrite occurs as 'dust' and rare 'golden' nodules. Disseminated spots of low attenuation, inferred as open macropores, are the main feature of the attenuation fabric. Poorly developed layering is inferred; it trends more or less lengthwise with the plug axis. Rare spots of very high attenuation are almost certainly attributable to intergranular pyrite cement. The sample is moderately homogeneous and no defects are apparent.

CT-Scan Descriptions (Horizontal Plugs Drilled for Mechanical Strength Tests) … cont'd

Sample I : (1819.62 m)

Moderately well sorted, fine to coarse, mainly medium, quartz sandstone; the minor coarser component (~5%) occurs as rare 'floating' grains as well as concentrated in millimetre scale subplanar layers. Spalling of grains is noted. Accessory components include clay clasts and trails (~1%), traces of 'coaly' organic matter, both disseminated granular and as flecks in millimetre scale layers, pyrite and mica. The attenuation fabric shows disturbed layering trending slightly oblique to the plug axis. Diffuse moderately higher attenuation defining several layers and patches is suggestive of finer grain size, possibly clay concentrations. Rare very high attenuation spots are almost certainly attributable to pyrite cement. Although lower attenuation generally is associated with pore abundance, rarely in places there is a contribution from organic matter; this is the case for several of the larger low attenuation specks. The sample is moderately homogeneous overall and no defects are evident.

Sample J : (1819.67 m)

Moderately sorted, fine to granular, mainly medium quartz sandstone; the minor coarser component (~5%) occurs as rare 'floating' grains as well as concentrated in millimetre scale layers. Accessories include traces of 'coaly' organic matter, both disseminated granular and as flecks in trails associated with clays, pyrite and mica. It is a relatively short sample and grain spalling is noted. The attenuation fabric reveals poorly developed layering set at a low angle to the plug axis; slightly higher attenuation in a marginal layer is attributable to finer grain size, possibly clays. Disseminated low attenuation spots and specks are for the most part attributable to larger pores but there also is a very minor contribution from organic matter. Individual larger framework grains show moderately high attenuation. Rare spots of very high attenuation are almost certainly attributable to pyrite cement. The sample is moderately homogeneous overall and no defects are evident.

CT-Scan Descriptions (Horizontal Plugs Drilled for Mechanical Strength Tests) … cont'd

Sample K : (1822.91 m)

Moderately poorly sorted, fine to very coarse, mainly lower medium silty quartz sandstone. The minor coarser component (~5%) is localised in patches and concentrated in millimetre scale layers. Grain spalling is noted. Accessory components include organic matter in wispy trails (1%), clays (tr-1%) with associated traces of pyrite 'dust', nodular pyrite and mica. The ragged attenuation fabric is reminiscent of bioturbation; disturbed bedding is set at an oblique angle to the plug axis. Moderately higher attenuation in the fabric reflects finer grain size, silt and in particular clays. Highest attenuation (>3000 HU) is almost certainly attributable to pyrite cement. Generally, lower attenuation is associated with pore abundance, however isolated spots of very low attenuation may well be attributable to traces of organic matter. The sample shows poor to moderate homogeneity and no defects are evident.

Sample L : (1822.95 m)

Moderately poorly sorted, fine to granular, mainly lower medium silty quartz sandstone. The minor coarser component (~7%) is localised in patches and concentrated in millimetre scale layers. Grain spalling is noted. Accessory components include traces of organic matter both disseminated and concentrated in millimetre scale layers, clays with associated traces of pyrite 'dust', nodular pyrite, and pale as well as greenish mica. The ragged attenuation fabric is reminiscent of bioturbation; disturbed bedding is set at an oblique angle to the plug axis. Moderately higher attenuation in the fabric reflects finer grain size, silt and in particular clays. Highest attenuation (>3000 HU) is almost certainly attributable to localised pyrite cement. Generally lower attenuation is associated with pore abundance, however isolated spots of very low attenuation may well be attributable to traces of organic matter. The sample shows poor to moderate homogeneity and no defects are apparent.

Sample M : 1826.27 m

Poorly sorted, bimodal quartz sandstone; it is mainly coarse to very coarse with lesser domains (~30%) more of medium sand size. Grain spalling is noted. In places there are rare trails of organic-charged clays, several feldspar grains show evidence of degradation. Irregularly disseminated low attenuation macropores are the most dominant feature of the fabric, layering also is evident; it dips at a low angle to the plug axis and may show very low angle crossbedding. Very rare specks of highest attenuation (>3000 HU) are almost certainly attributable to localised intergranular pyrite cement. The sample is poorly to moderately homogeneous and no defects are evident.

CT-Scan Descriptions (Horizontal Plugs Drilled for Mechanical Strength Tests) … cont'd

Sample N : (1826.33 m)

Poorly sorted, bimodal quartz sandstone; it is mainly medium to coarse with a lesser component (~20%) coarse to very coarse and rarely pebbly. Grain spalling is noted. Accessory components include traces of 'coaly' granular organic matter, localised clays with associated pyrite 'dust', mica and partially degraded feldspars. Low attenuation spots and specks in the fabric are inferred as macropores for the most part but rarely these may also be attributable to organic matter. Layering also is evident; it is subplanar and dips at a low angle to the plug axis. Rare specks of highest attenuation (>3000 HU) are almost certainly attributable to localised intergranular pyrite cement. The sample is poorly to moderately homogeneous and no defects are evident.

CT-Scan Descriptions (Vertical Plugs Drilled for Mechanical Strength Tests)

Sample W : (1831.21 m)

Shale with accessory traces of 'coaly' organic matter in the form of disseminated flecks. Minor patches of silt gradational in part to very fine sand are noted. Minor pyrite cement (~5%) forms elongate intergranular nodules to at least 15 mm; these very high attenuation domains are the most dominant feature of the attenuation fabric. Layering set at a high oblique angle to the plug axis is inferred. No significant fracture defects are apparent but a very minor open defect is inferred; it is partially penetrative lengthwise from one of the plug faces. This defect can be removed by trimming. The sample shows very poor homogeneity.

Sample X: (1831.21 m)

Slightly silty shale with accessory traces of disseminated 'coaly' organic matter; it contains minor nodular pyrite cement (~3%). More diffuse traces of pyrite follow the inferred trend of layering that is set highly oblique to the plug axis. Along this trend is a low attenuation trace inferred as a possible fine open defect. The sample shows poor to moderate homogeneity. The defect can be removed and subsequent homogeneity improved by trimming.

Sample Y : (1831.21 m)

Slightly silty shale with accessory traces of disseminated 'coaly' organic matter; it contains minor nodular pyrite cement (~3%). Apparent layering is set at high oblique angle to the plug axis. No defects are inferred and the sample shows poor to moderate homogeneity.

Sample Z : (1831.21 m)

Slightly silty shale with accessory traces of disseminated 'coaly' organic matter; it contains minor nodular pyrite cement (~3%). Apparent layering is set at high oblique angle to the plug axis. No defects are inferred and the sample shows poor to moderate homogeneity.

APPENDIX 4
CT-SCAN AND CORE PLUG PHOTOGRAPHS

Origin Energy Limited
Halladale - 1
X-ray CT Images and Base Data

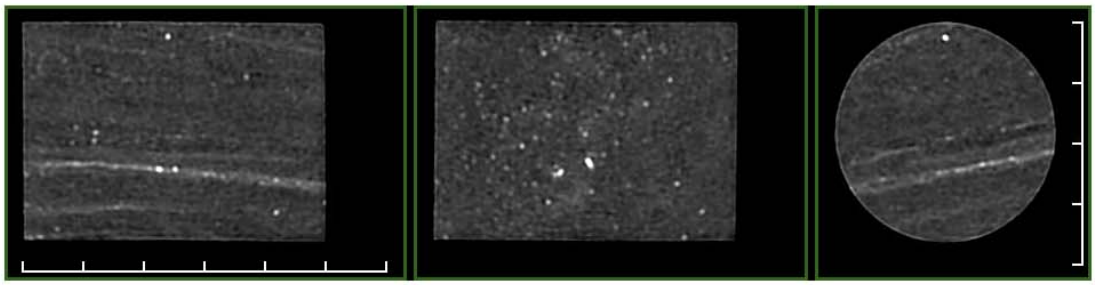

SAMPLE : 5A
DEPTH (m): 1792.55

Ka (mD): 302
Por (%): 26.0
GD (g/cc): 2.652

CT No.(HU): 1292

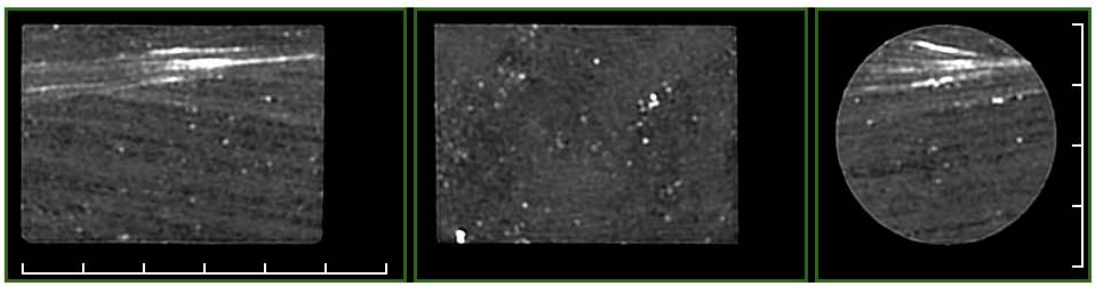

SAMPLE : 6A
DEPTH (m): 1792.60

Ka (mD): 470
Por (%): 25.0
GD (g/cc): 2.661

CT No.(HU): 1379

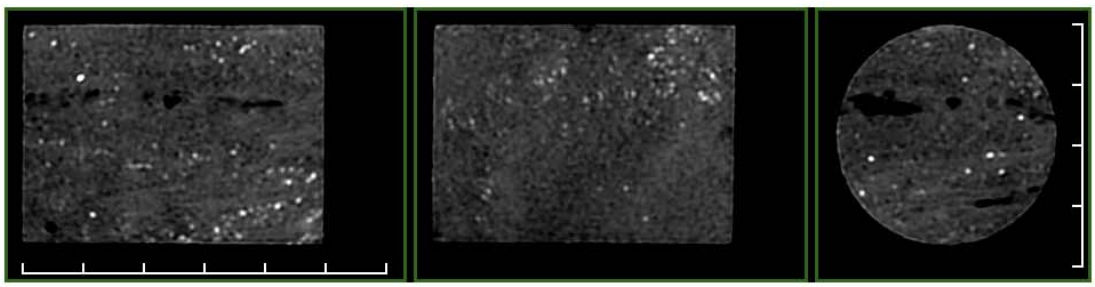

SAMPLE : 7
DEPTH (m): 1793.00

Ka (mD): 958
Por (%): 26.6
GD (g/cc): 2.648

CT No.(HU): 1200

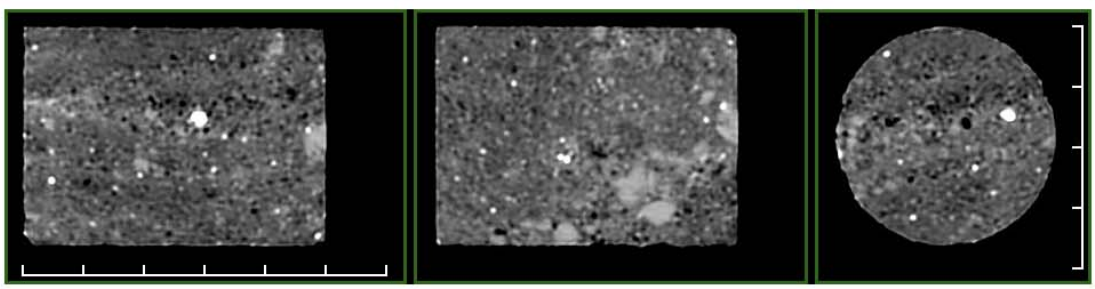

SAMPLE : 28
DEPTH (m): 1808.70

Ka (mD): 2110
Por (%): 20.9
GD (g/cc): 2.662

CT No.(HU): 1445

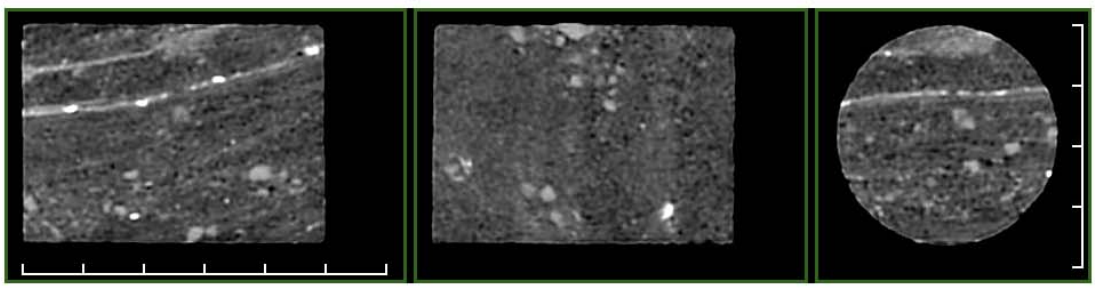

SAMPLE : 29
DEPTH (m): 1809.05

Ka (mD): 699
Por (%): 22.9
GD (g/cc): 2.670

CT No.(HU): 1410

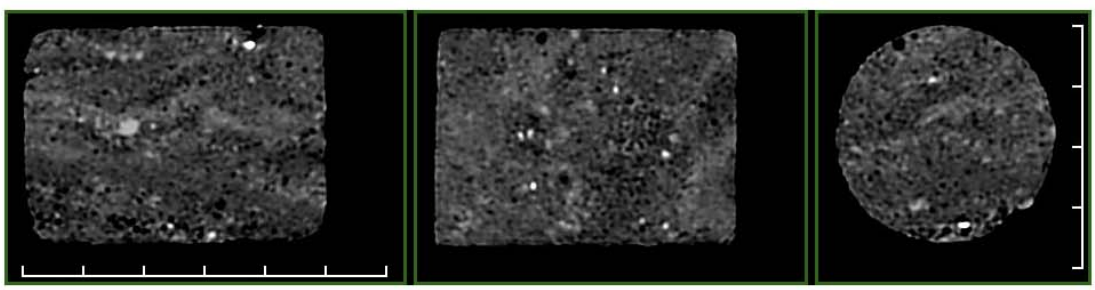

SAMPLE : 40
DEPTH (m): 1812.30

Ka (mD): 4060
Por (%): 25.0
GD (g/cc): 2.653

CT No.(HU): 1289

scale in centimetres

Origin Energy Limited
Halladale - 1
X-ray CT Images and Base Data

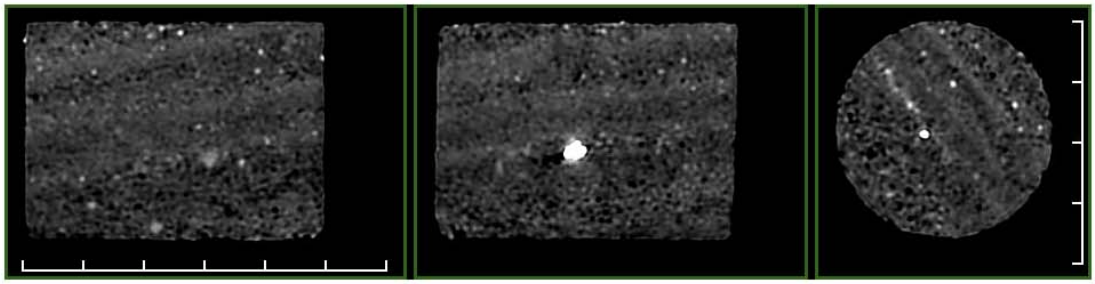

SAMPLE : 42
DEPTH (m): 1812.90

Ka (mD): 3740
Por (%): 26.6
GD (g/cc): 2.659

CT No.(HU): 1264

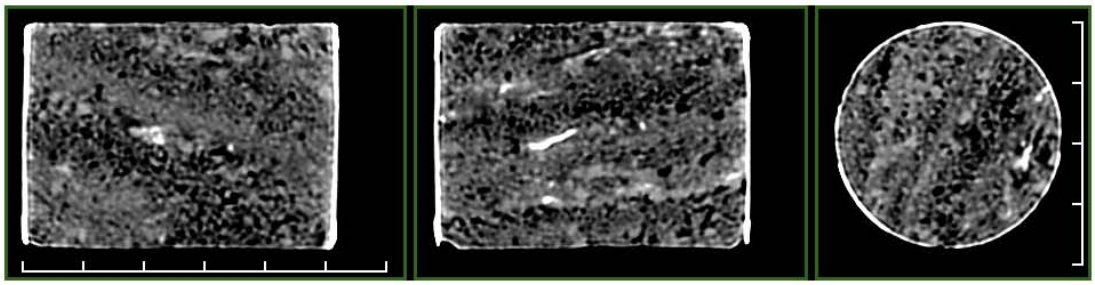

SAMPLE : 44
DEPTH (m): 1813.45

Ka (mD): 3180
Por (%): 22.1
GD (g/cc): 2.625

CT No.(HU): 1377

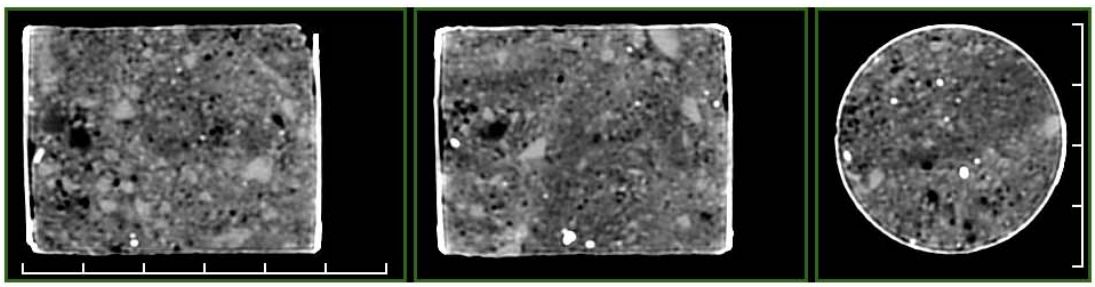

SAMPLE : 47
DEPTH (m): 1814.42

Ka (mD): 501
Por (%): 18.6
GD (g/cc): 2.651

CT No.(HU): 1474

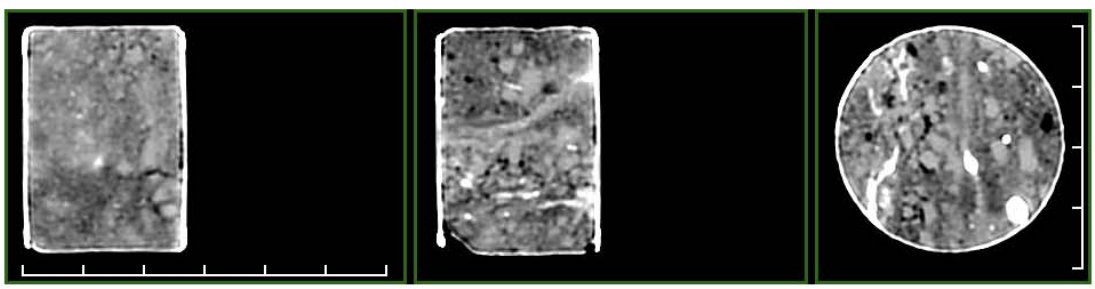

SAMPLE : 48
DEPTH (m): 1814.75

Ka (mD): 415
Por (%): 17.3
GD (g/cc): 2.652

CT No.(HU): 1697

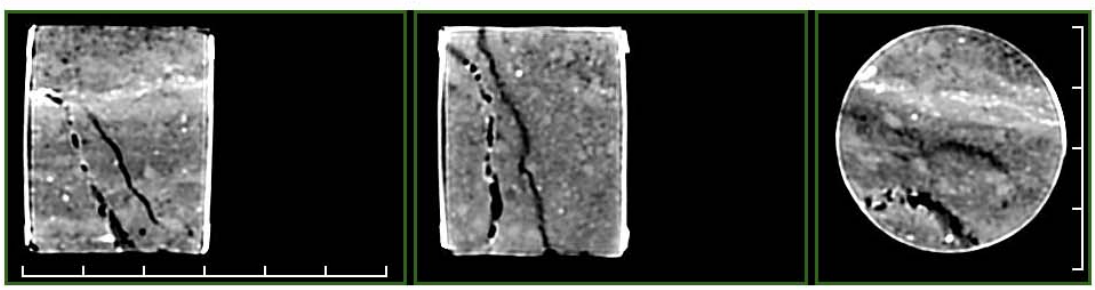

SAMPLE : 48A
DEPTH (m): 1814.81

Ka (mD): -
Por (%): -
GD (g/cc): -

CT No.(HU): 1650

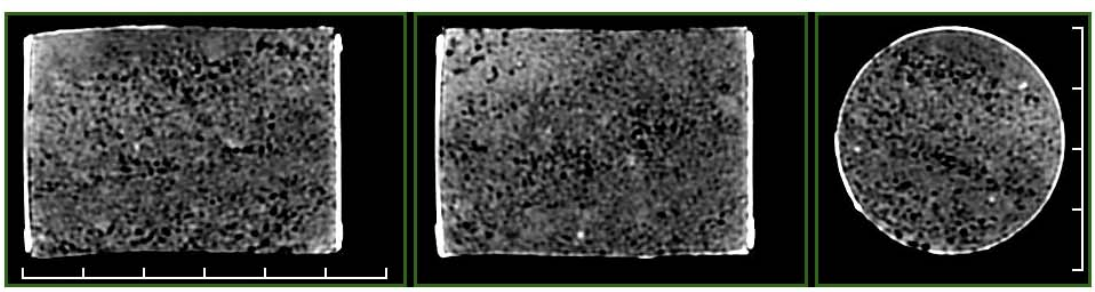

SAMPLE : 51A
DEPTH (m): 1815.73

Ka (mD): 8890
Por (%): 27.4
GD (g/cc): 2.648

CT No.(HU): 1340

scale in centimetres

Origin Energy Limited
Halladale - 1
X-ray CT Images and Base Data

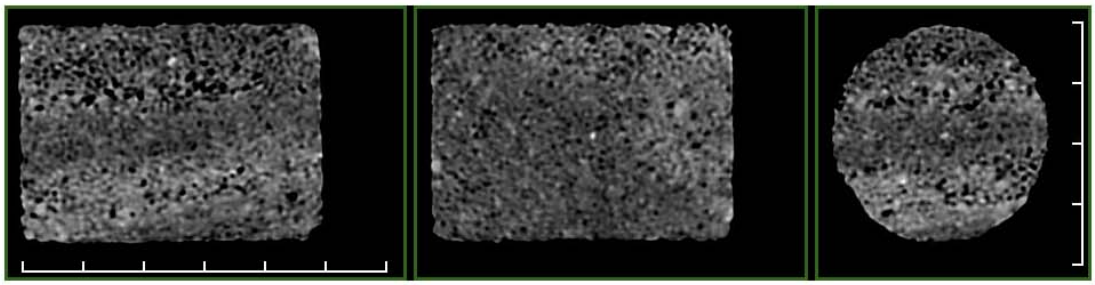

SAMPLE : 55
DEPTH (m): 1816.80

Ka (mD): 4220
Por (%): 24.3
GD (g/cc): 2.656

CT No.(HU): 1395

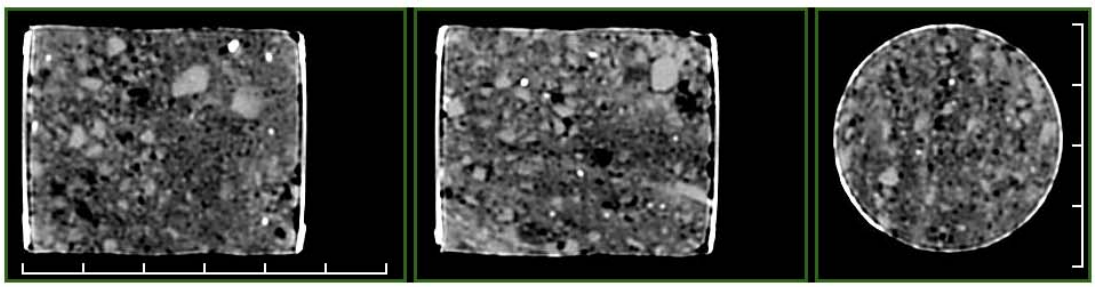

SAMPLE : 56A
DEPTH (m): 1817.04

Ka (mD): 3070
Por (%): 22.0
GD (g/cc): 2.652

CT No.(HU): 1444

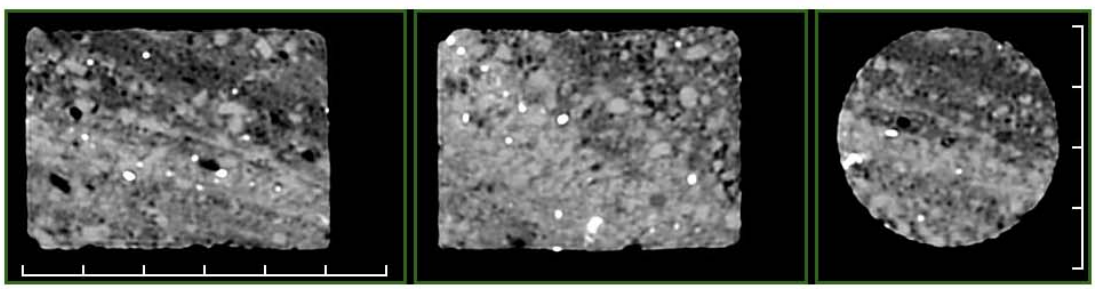

SAMPLE : 56
DEPTH (m): 1817.10

Ka (mD): 385
Por (%): 16.7
GD (g/cc): 2.654

CT No.(HU): 1547

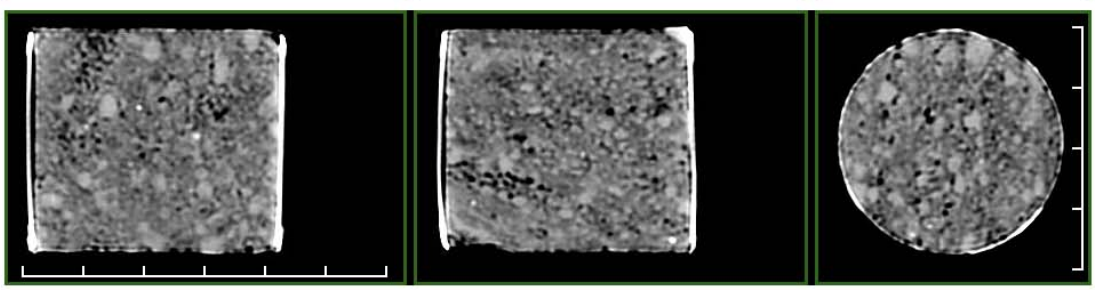

SAMPLE : 57A
DEPTH (m): 1817.50

Ka (mD): 5470
Por (%): 20.6
GD (g/cc): 2.656

CT No.(HU): 1582

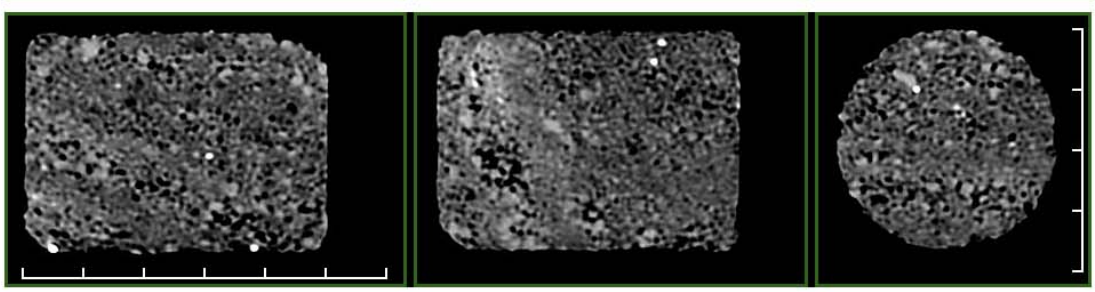

SAMPLE : 59
DEPTH (m): 1818.05

Ka (mD): >10000
Por (%): 23.8
GD (g/cc): 2.655

CT No.(HU): 1368

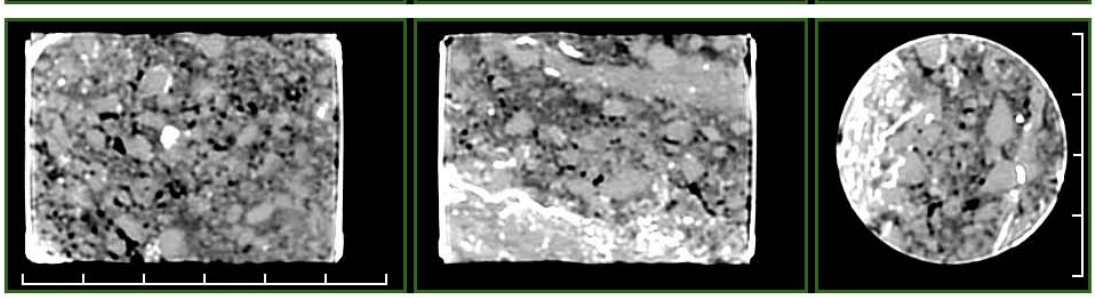

SAMPLE : 62B
DEPTH (m): 1818.84

Ka (mD): 416
Por (%): 13.6
GD (g/cc): 2.677

CT No.(HU): 1830

scale in centimetres

Origin Energy Limited
Halladale - 1
X-ray CT Images and Base Data

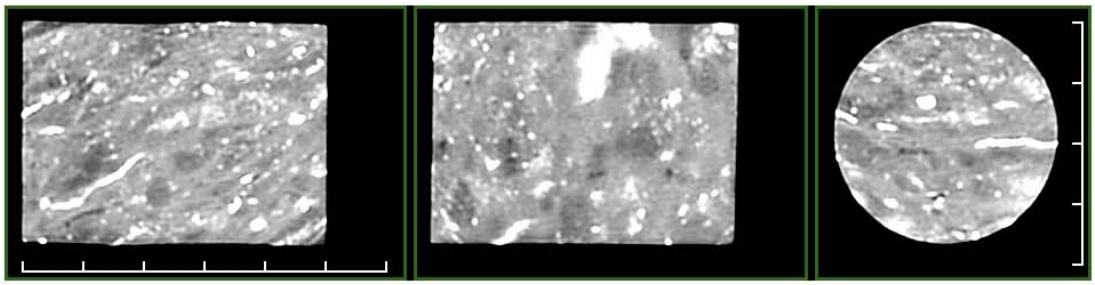

SAMPLE : 62A
DEPTH (m): 1818.95

Ka (mD): -
Por (%): -
GD (g/cc): -

CT No.(HU): 1959

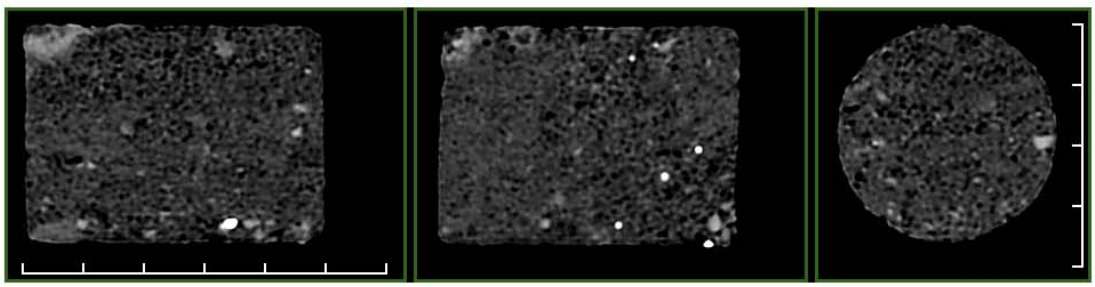

SAMPLE : 64
DEPTH (m): 1819.50

Ka (mD): 4140
Por (%): 26.7
GD (g/cc): 2.642

CT No.(HU): 1215

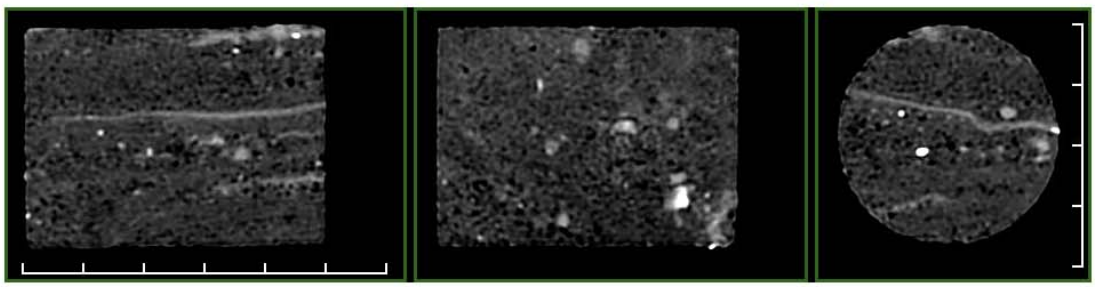

SAMPLE : 65
DEPTH (m): 1819.80

Ka (mD): 2800
Por (%): 26.3
GD (g/cc): 2.662

CT No.(HU): 1243

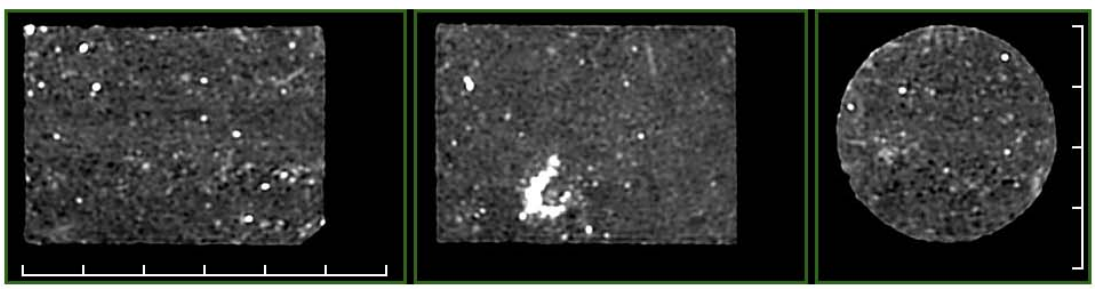

SAMPLE : 67A
DEPTH (m): 1820.49

Ka (mD): 2260
Por (%): 25.7
GD (g/cc): 2.672

CT No.(HU): 1336

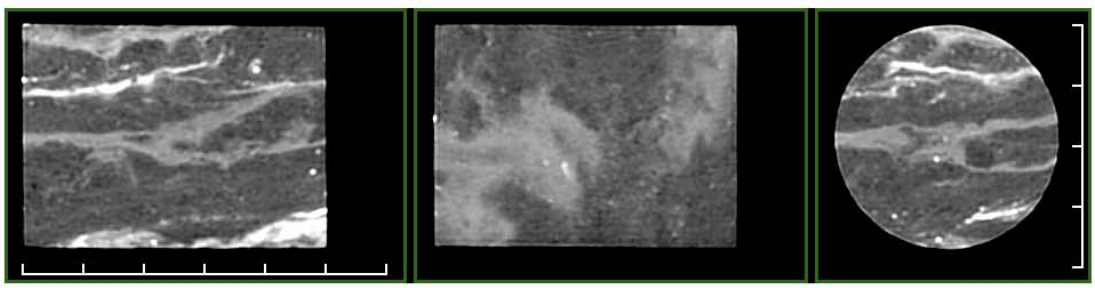

SAMPLE : 72
DEPTH (m): 1821.90

Ka (mD): 55.4
Por (%): 18.6
GD (g/cc): 2.673

CT No.(HU): 1570

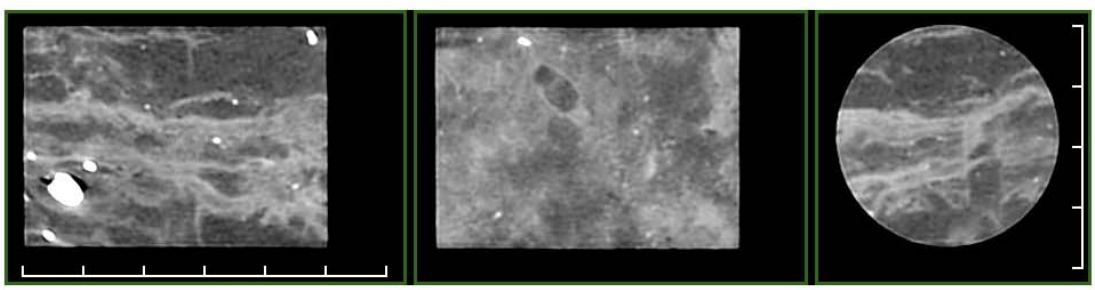

SAMPLE : 72A
DEPTH (m): 1821.98

Ka (mD): 13.7
Por (%): 16.6
GD (g/cc): 2.656

CT No.(HU): 1603

scale in centimetres

Origin Energy Limited
Halladale - 1
X-ray CT Images and Base Data

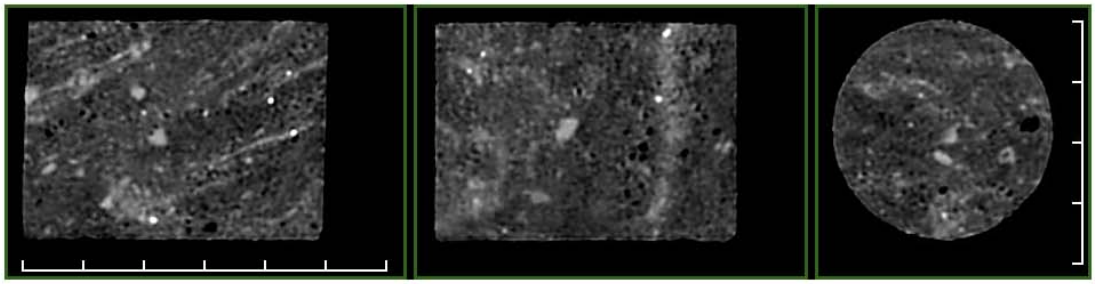

SAMPLE : 75A
DEPTH (m): 1822.83

Ka (mD): 706
Por (%): 25.7
GD (g/cc): 2.656

CT No.(HU): 1290

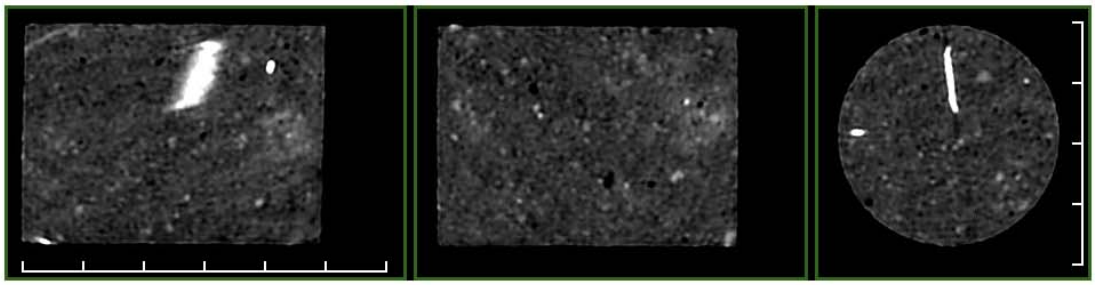

SAMPLE : 76
DEPTH (m): 1823.10

Ka (mD): 606
Por (%): 27.3
GD (g/cc): 2.665

CT No.(HU): 1249

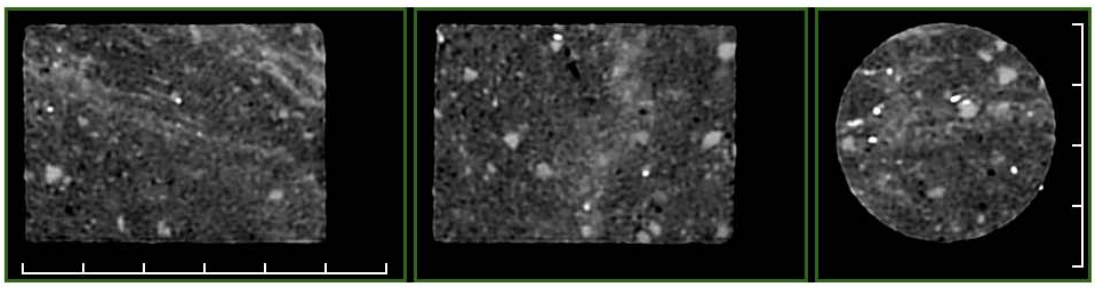

SAMPLE : 77A
DEPTH (m): 1823.36

Ka (mD): 392
Por (%): 24.9
GD (g/cc): 2.652

CT No.(HU): 1356

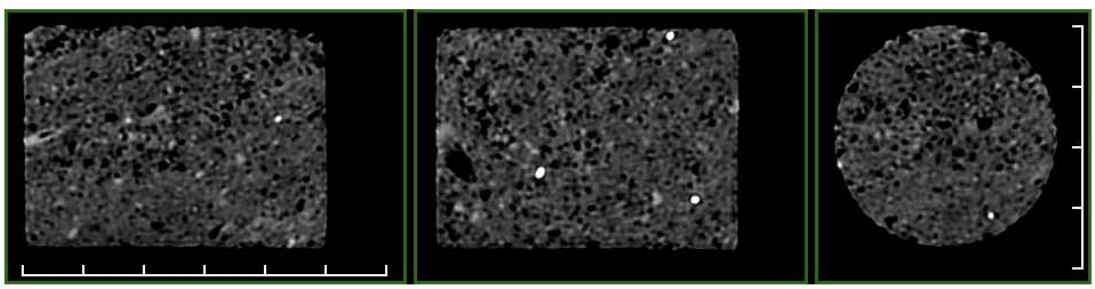

SAMPLE : 79
DEPTH (m): 1824.03

Ka (mD): 6430
Por (%): 25.5
GD (g/cc): 2.646

CT No.(HU): 1240

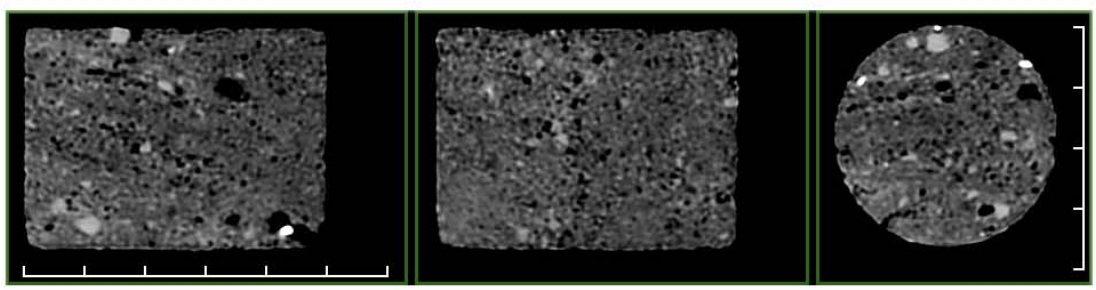

SAMPLE : 82
DEPTH (m): 1824.90

Ka (mD): 3380
Por (%): 23.4
GD (g/cc): 2.640

CT No.(HU): 1384

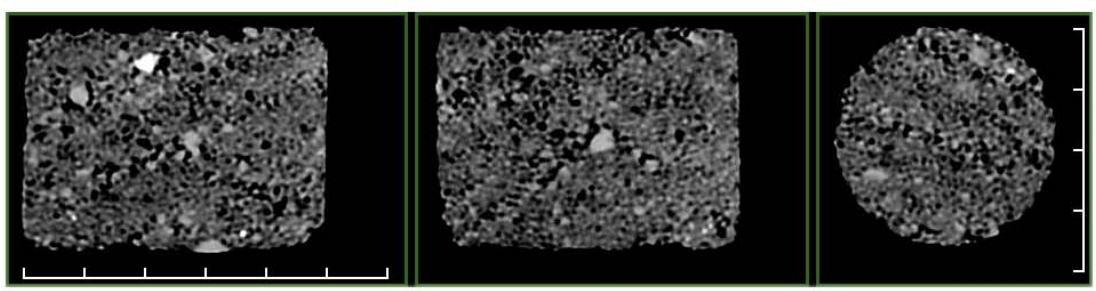

SAMPLE : 84
DEPTH (m): 1825.50

Ka (mD): >10000
Por (%): 23.7
GD (g/cc): 2.650

CT No.(HU): 1349

scale in centimetres

Origin Energy Limited
Halladale - 1
X-ray CT Images and Base Data

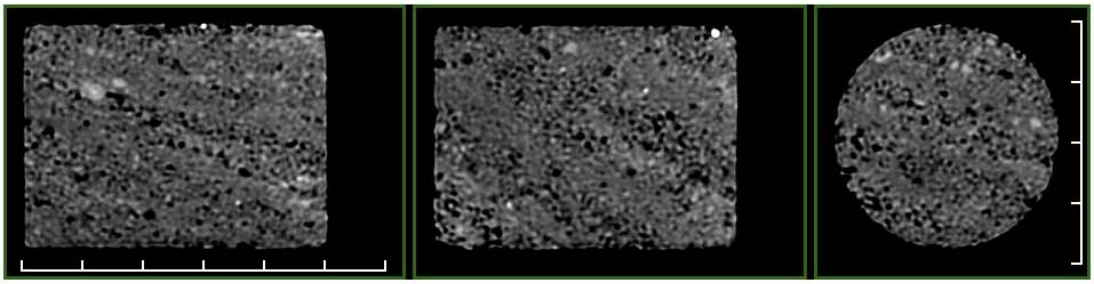

SAMPLE : 86
DEPTH (m): 1826.10

Ka (mD): 8140
Por (%): 22.9
GD (g/cc): 2.648

CT No.(HU): 1358

scale in centimetres

Origin Energy Limited
Halladale - 1
X-ray CT Images and Base Data

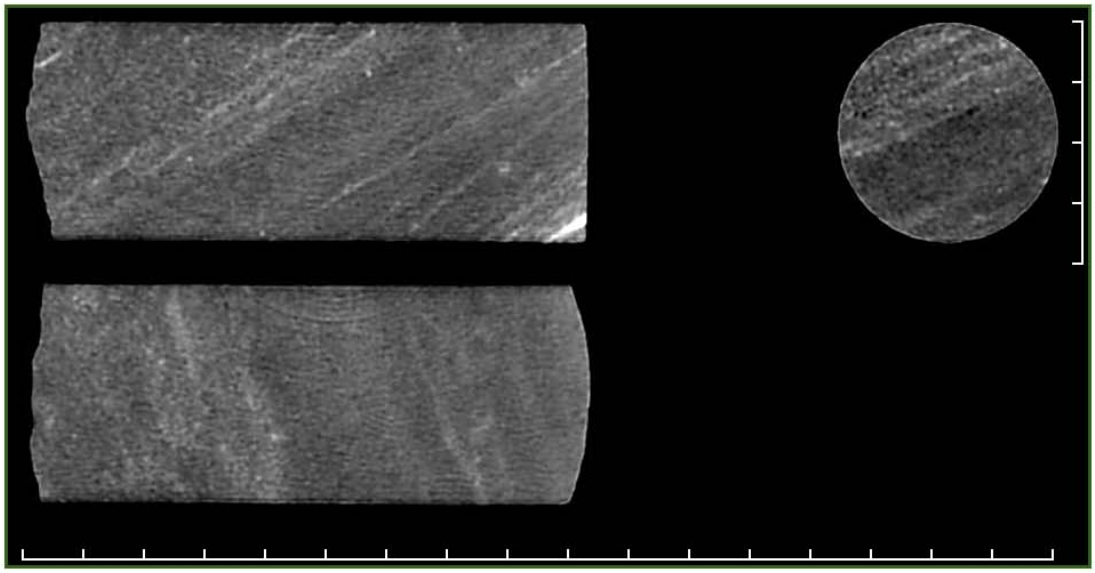

SAMPLE : A
DEPTH (m): 1809.45

CT No.(HU): 1485

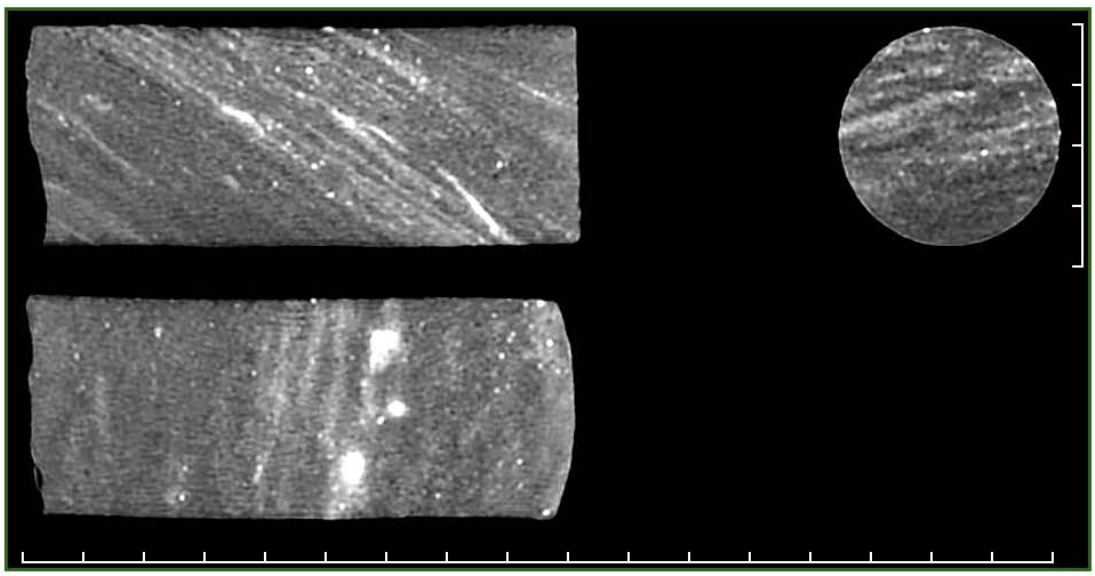

SAMPLE : B
DEPTH (m): 1809.50

CT No.(HU): 1663

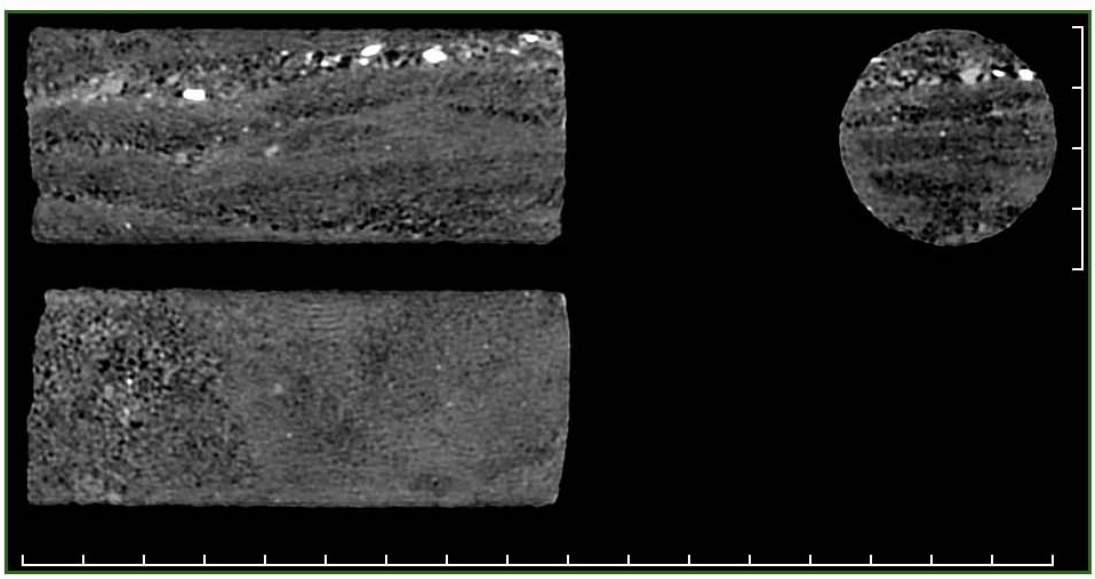

SAMPLE : C
DEPTH (m): 1812.40

CT No.(HU): 1415

scale in centimetres

Origin Energy Limited
Halladale - 1
X-ray CT Images and Base Data

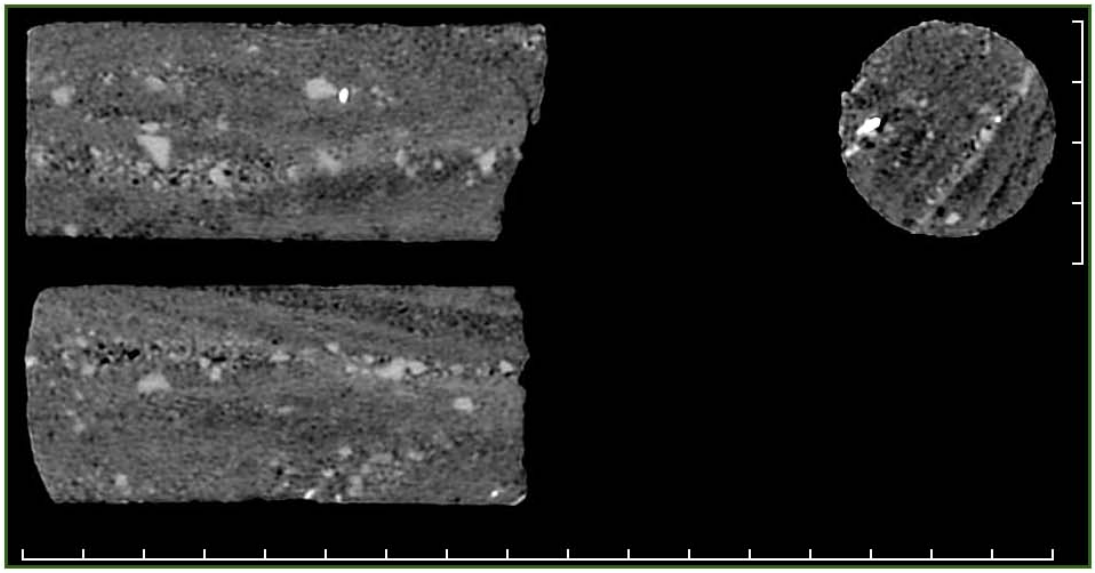

SAMPLE : D
DEPTH (m): 1812.45

CT No.(HU): 1464

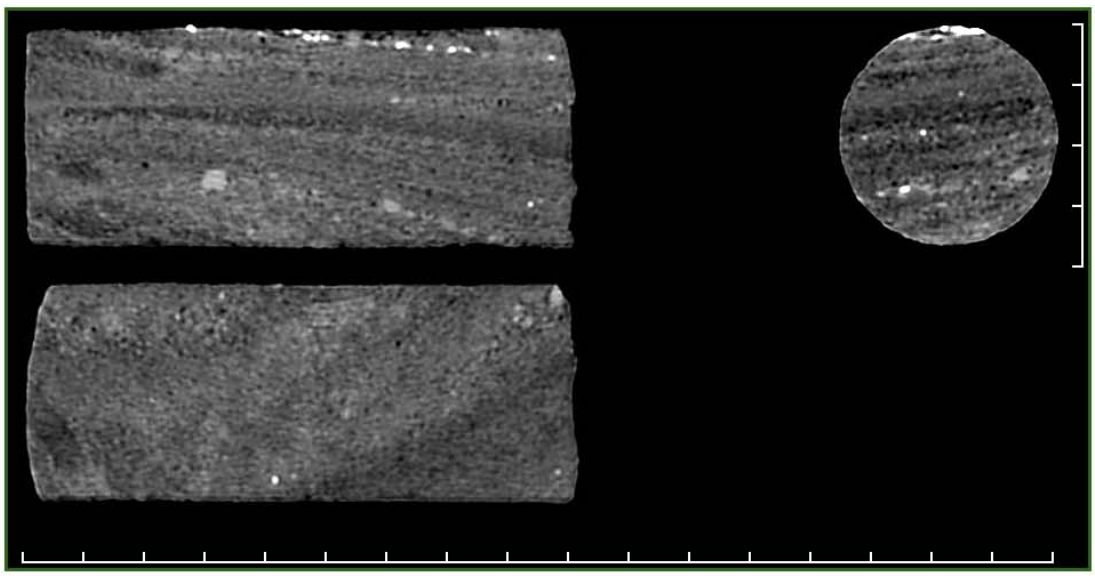

SAMPLE : E
DEPTH (m): 1812.50

CT No.(HU): 1481

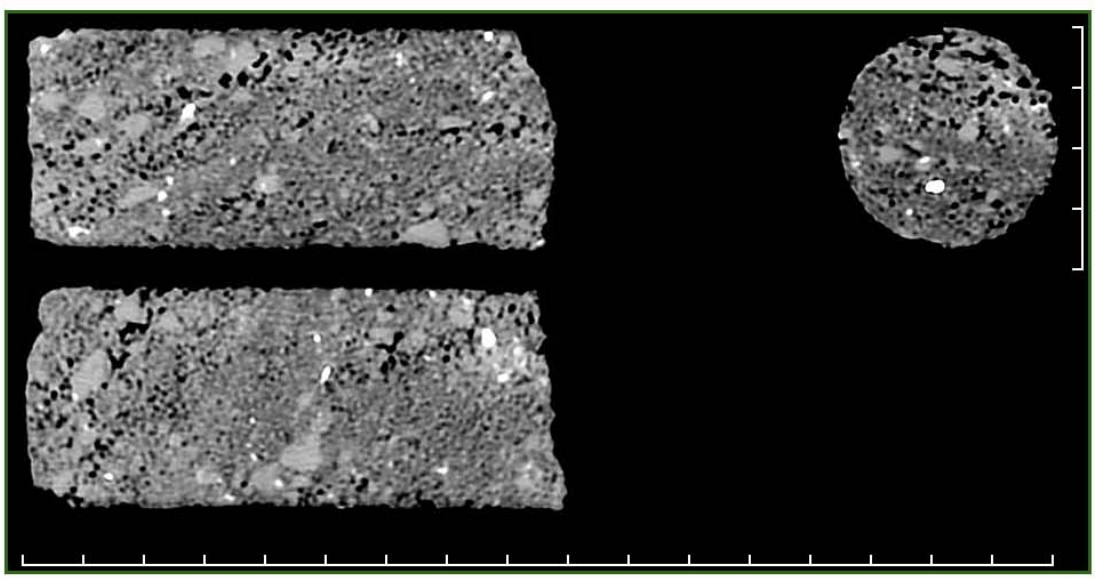

SAMPLE : F
DEPTH (m): 1817.77

CT No.(HU): 1619

scale in centimetres

Origin Energy Limited
Halladale - 1
X-ray CT Images and Base Data

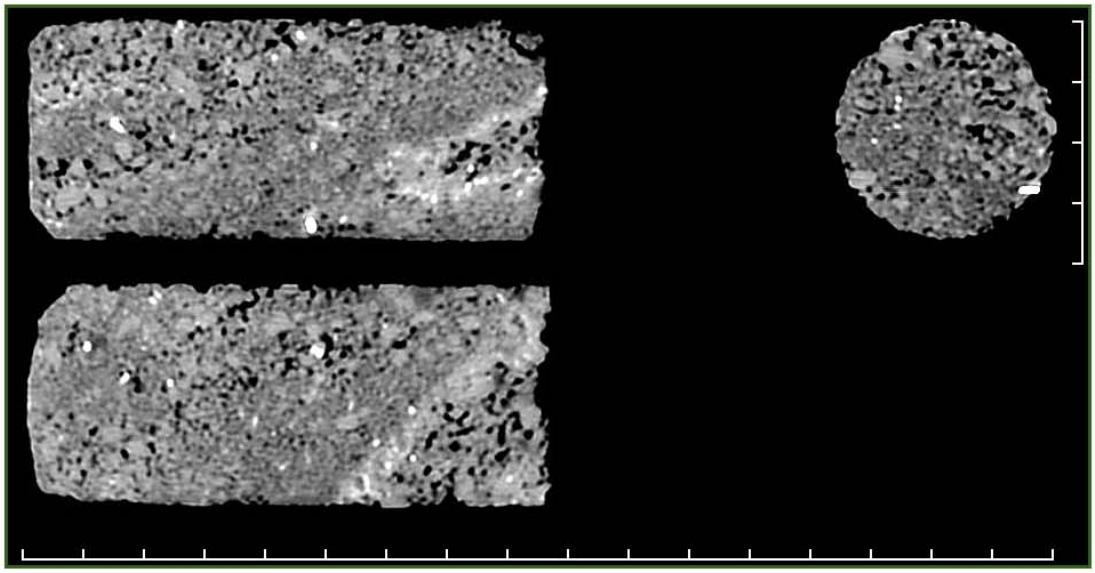

SAMPLE : G
DEPTH (m): 1817.83

CT No.(HU): 1626

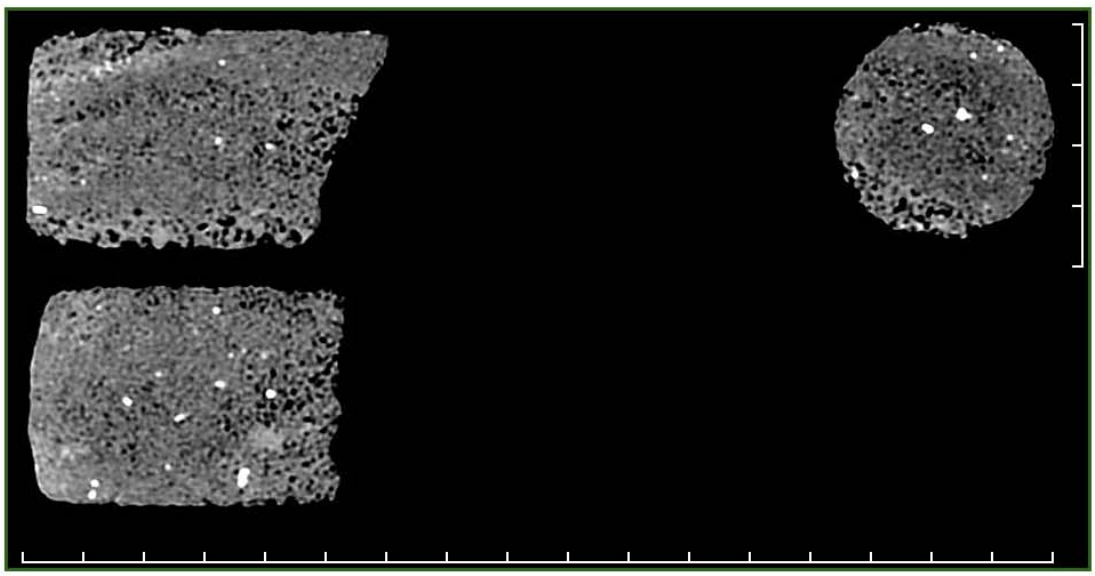

SAMPLE : H
DEPTH (m): 1817.88

CT No.(HU): 1559

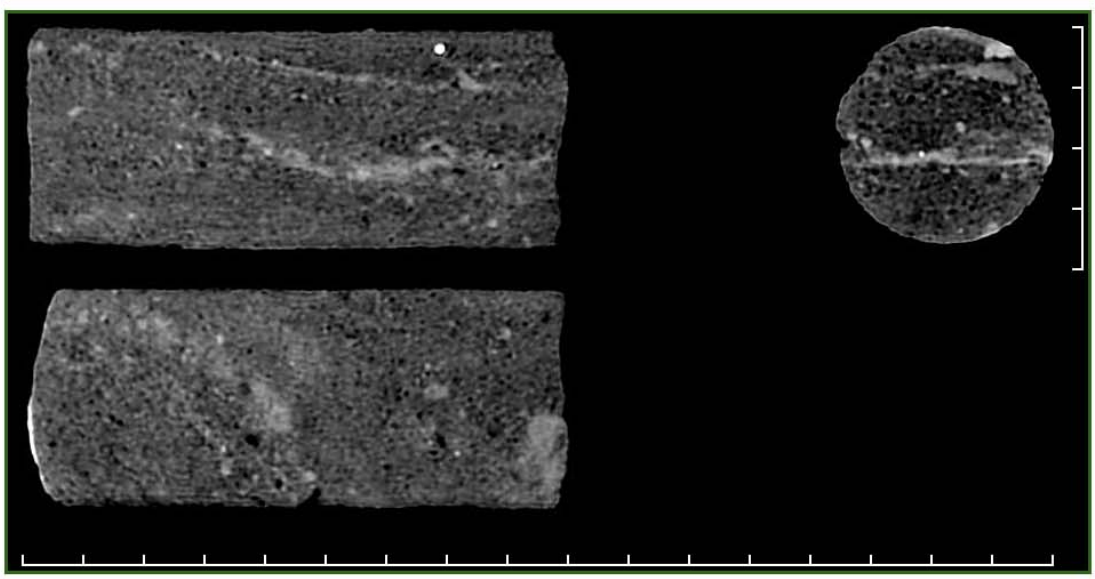

SAMPLE : I
DEPTH (m): 1819.62

CT No.(HU): 1396

scale in centimetres

Origin Energy Limited
Halladale - 1
X-ray CT Images and Base Data

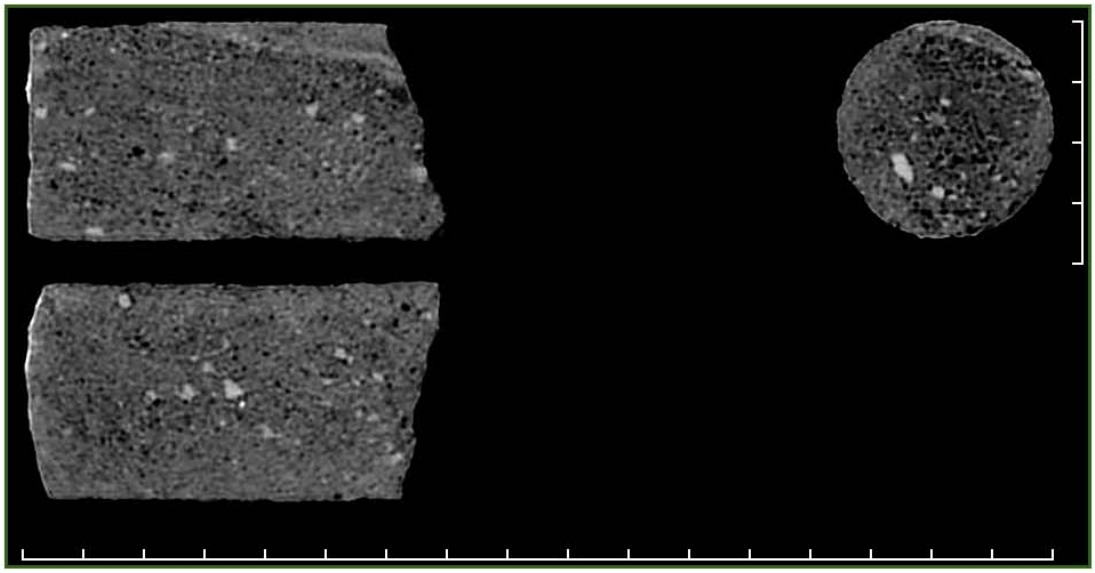

SAMPLE : J
DEPTH (m): 1819.67

CT No.(HU): 1420

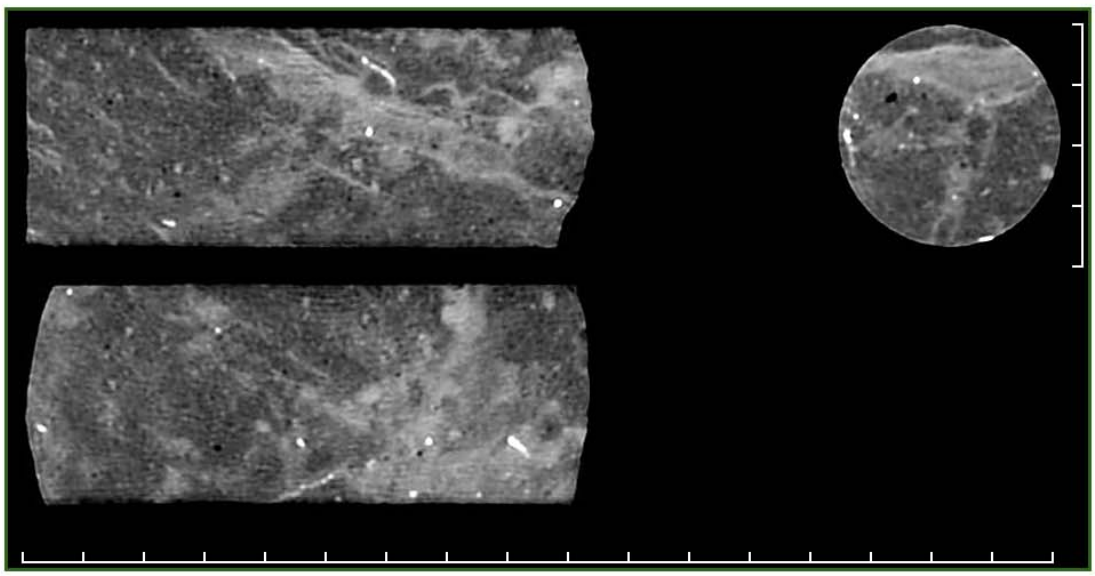

SAMPLE : K
DEPTH (m): 1822.91

CT No.(HU): 1504

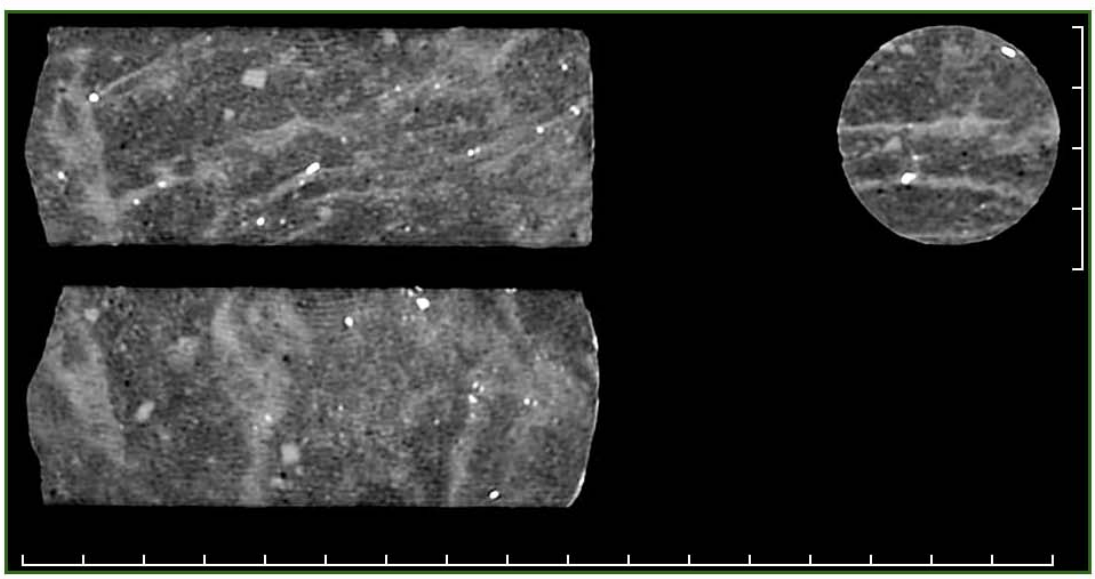

SAMPLE : L
DEPTH (m): 1822.95

CT No.(HU): 1473

scale in centimetres

Origin Energy Limited
Halladale - 1
X-ray CT Images and Base Data

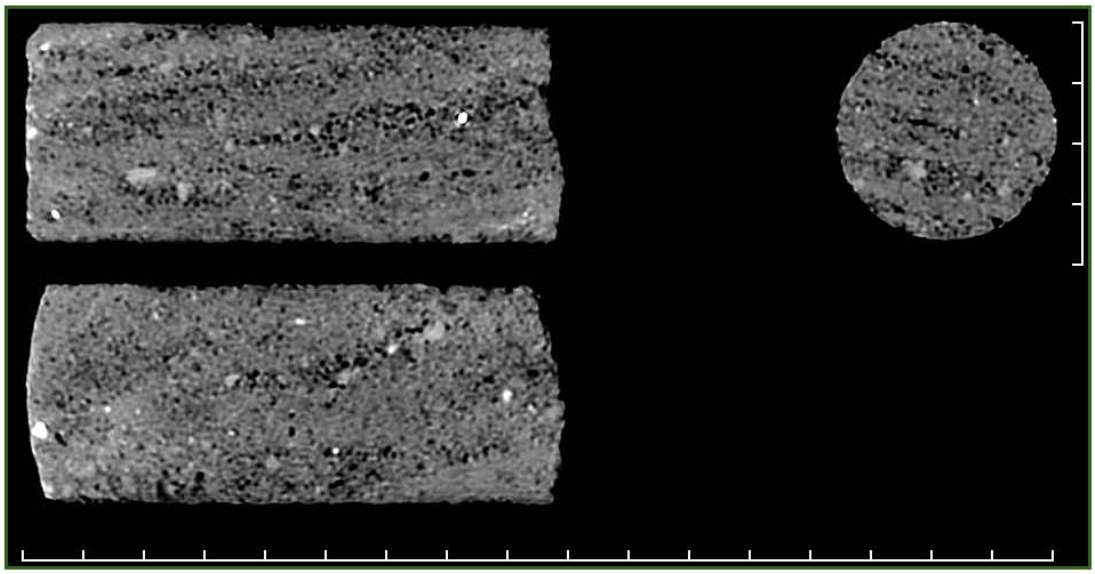

SAMPLE : M
DEPTH (m): 1826.27

CT No.(HU): 1465

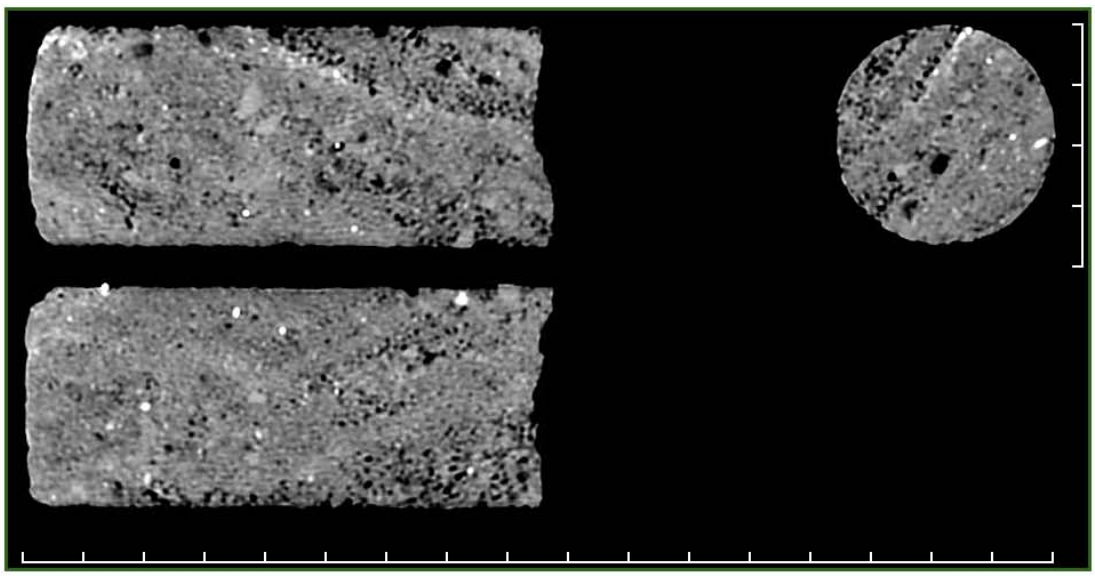

SAMPLE : N
DEPTH (m): 1826.23

CT No.(HU): 1585

scale in centimetres

Origin Energy Limited
Halladale - 1
X-ray CT Images and Base Data

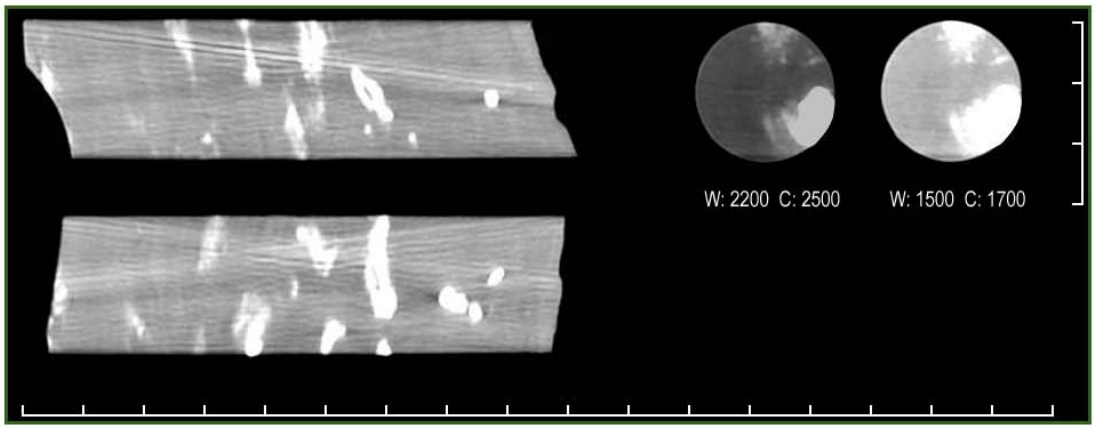

SAMPLE : W
DEPTH (m): 1831.21

CT No.(HU): 2226

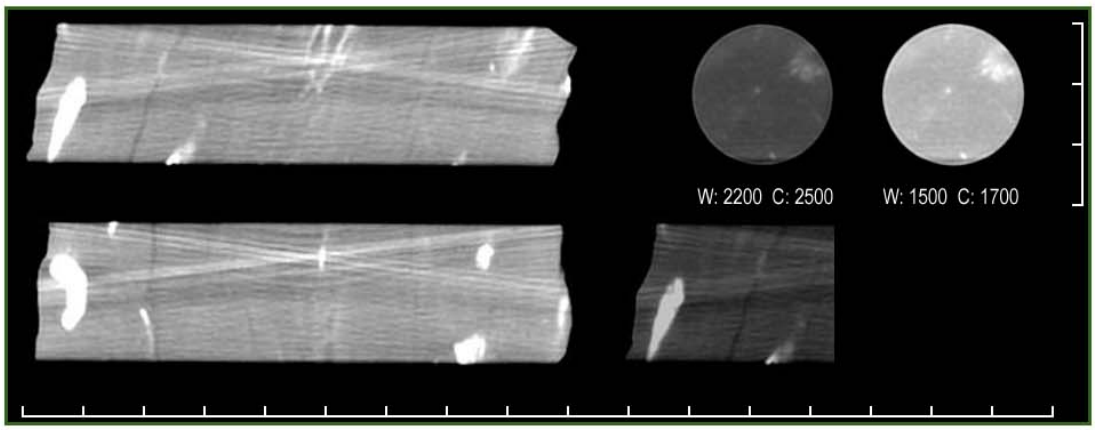

SAMPLE : X
DEPTH (m): 1831.21

CT No.(HU): 2046

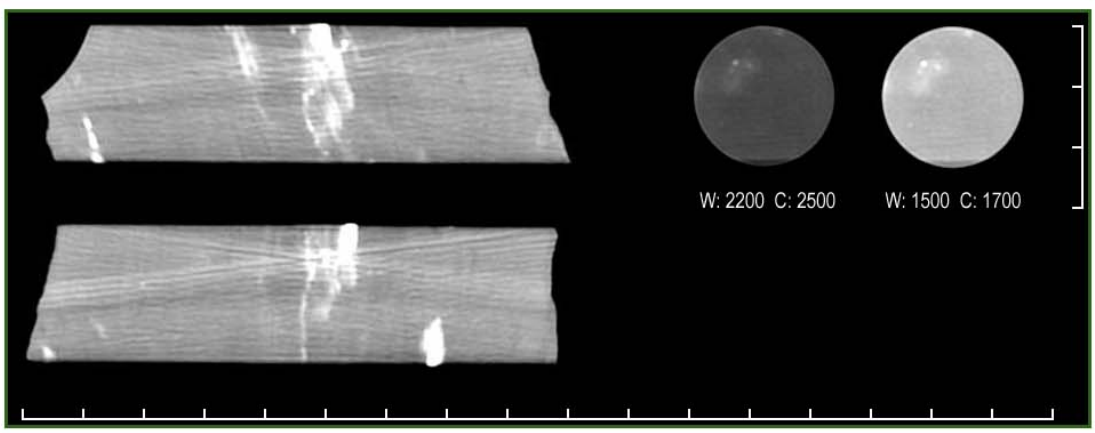

SAMPLE : Y
DEPTH (m): 1831.21

CT No.(HU): 2049

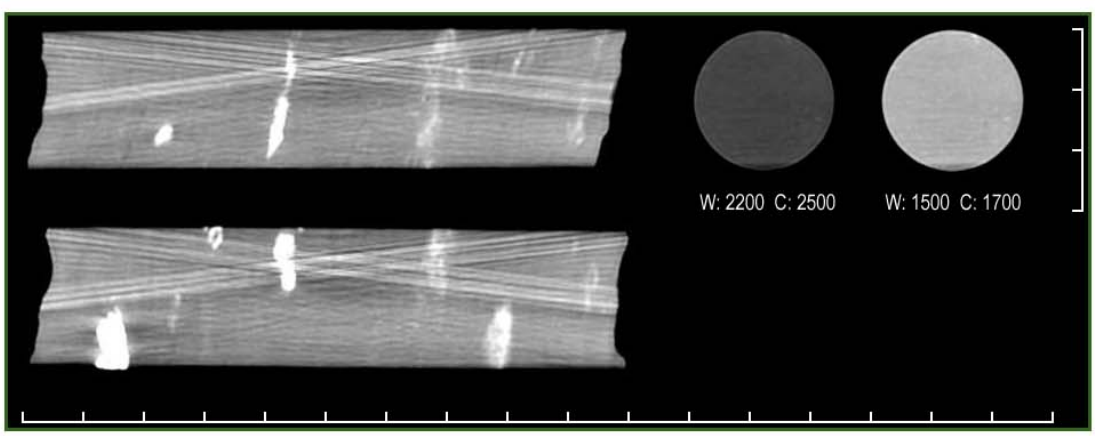

SAMPLE : Z
DEPTH (m): 1831.21

Ka (mD):
Por (%):
GD (g/cc):

CT No.(HU): 1996

scale in centimetres

Origin Energy Ltd
HALLADALE-1 DW1 & DW2

Plug Photography

No. 5A
Depth: 1792.55 m
Ka: 302 md
Por: 26.0 %
GD: 2.652 g/cc

No. 6A
Depth: 1792.60 m
Ka: 470 md
Por: 25.0 %
GD: 2.661 g/cc

No. 7
Depth: 1793.00 m
Ka: 958 md
Por: 26.6 %
GD: 2.648 g/cc

No. 28
Depth: 1808.70 m
Ka: 2110 md
Por: 20.9 %
GD: 2.662 g/cc

No. 29
Depth: 1809.05 m
Ka: 699 md
Por: 22.9 %
GD: 2.670 g/cc

No. 40
Depth: 1812.30 m
Ka: 4060 md
Por: 25.0 %
GD: 2.653 g/cc

Origin Energy Ltd
HALLADALE-1 DW1 & DW2

Plug Photography

No. 42
Depth: 1812.90 m
Ka: 3740 md
Por: 26.6 %
GD: 2.659 g/cc

No. 44
Depth: 1813.45 m
Ka: 3180 md
Por: 22.1 %
GD: 2.625 g/cc

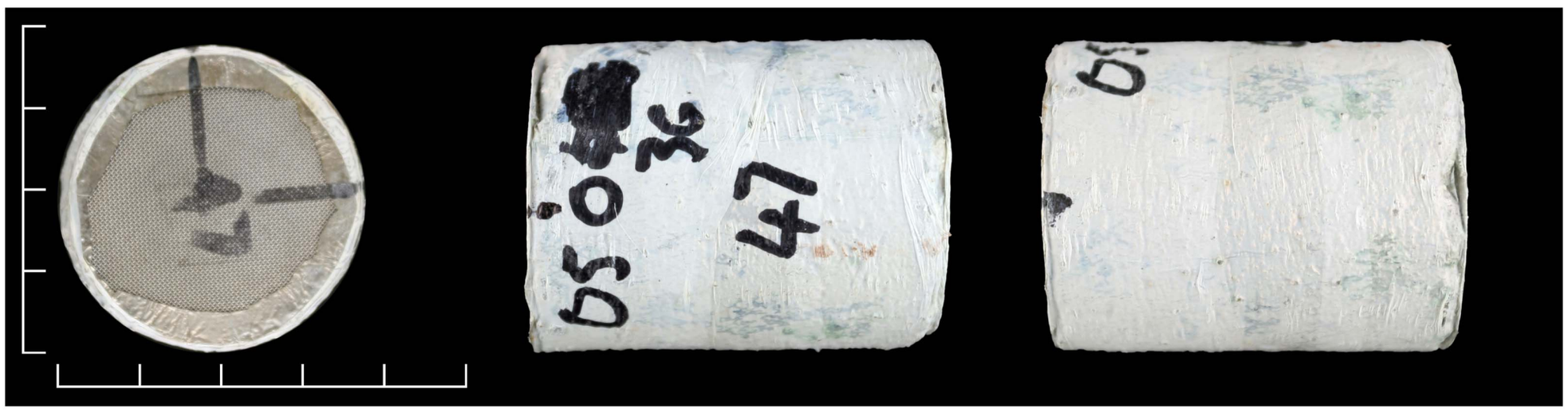

No. 47
Depth: 1814.42 m
Ka: 501 md
Por: 18.6 %
GD: 2.651 g/cc

No. 51A
Depth: 1815.73 m
Ka: 8890 md
Por: 27.4 %
GD: 2.648 g/cc

No. 55
Depth: 1816.80 m
Ka: 4220 md
Por: 24.3 %
GD: 2.656 g/cc

No. 56A
Depth: 1817.04 m
Ka: 3070 md
Por: 22.0 %
GD: 2.652 g/cc

Origin Energy Ltd
HALLADALE-1 DW1 & DW2

Plug Photography

No. 56
Depth: 1817.10 m
Ka: 385 md
Por: 16.7 %
GD: 2.654 g/cc

No. 57A
Depth: 1817.50 m
Ka: 5470 md
Por: 20.6 %
GD: 2.656 g/cc

No. 59
Depth: 1818.05 m
Ka: >10000 md
Por: 23.8 %
GD: 2.655 g/cc

No. 62B
Depth: 1818.84 m
Ka: 416 md
Por: 13.6 %
GD: 2.677 g/cc

No. 64
Depth: 1819.50 m
Ka: 4140 md
Por: 26.7 %
GD: 2.642 g/cc

No. 65
Depth: 1819.80 m
Ka: 2800 md
Por: 26.3 %
GD: 2.662 g/cc

Origin Energy Ltd
HALLADALE-1 DW1 & DW2

Plug Photography

No. 67A
Depth: 1820.49 m
Ka: 2260 md
Por: 25.7 %
GD: 2.672 g/cc

No. 72
Depth: 1821.90 m
Ka: 55.4 md
Por: 18.6 %
GD: 2.673 g/cc

No. 72A
Depth: 1821.98 m
Ka: 13.7 md
Por: 16.6 %
GD: 2.656 g/cc

No. 75A
Depth: 1822.83 m
Ka: 706 md
Por: 25.7 %
GD: 2.656 g/cc

No. 76
Depth: 1823.10 m
Ka: 606 md
Por: 27.3 %
GD: 2.665 g/cc

No. 77A
Depth: 1823.36 m
Ka: 392 md
Por: 24.9 %
GD: 2.652 g/cc

Origin Energy Ltd
HALLADALE-1 DW1 & DW2

Plug Photography

No. 79
Depth: 1824.03 m
Ka: 6430 md
Por: 25.5 %
GD: 2.646 g/cc

No. 82
Depth: 1824.90 m
Ka: 3380 md
Por: 23.4 %
GD: 2.640 g/cc

No. 84
Depth: 1825.50 m
Ka: >10000 md
Por: 23.7 %
GD: 2.650 g/cc

No. 86
Depth: 1826.10 m
Ka: 8140 md
Por: 22.9 %
GD: 2.648 g/cc